Fibroblast Growth Factors, A potential game plan for regeneration of skeletal muscle.

by
Kirankumar Gudagudi

Dissertation presented for the degree of Doctor of Physiological Science in the Faculty of Natural Science at Stellenbosch University

Supervisor: Prof. Kathryn H Myburgh

December 2019

Declaration

By submitting this thesis, I declare that the entirety of the work contained therein is my own, original work, that I am the sole author thereof (save to the extent explicitly otherwise stated), that reproduction and publication thereof by Stellenbosch University will not infringe any third party rights and that I have not previously in its entirety or in part submitted it for obtaining any qualification.

Date: December 2019

Abstract

Introduction: Adult mammalian tissue regeneration recruits progenitor stem cells. In skeletal muscle, these are primary satellite cells. Primary satellite cells can be harvested from muscle tissue to investigate or even use as potential therapeutic application. Satellite cells exist in quiescence in the muscle tissue and only become activated following an insult. Most studies investigating satellite cells *in vitro* use already activated satellite cells, called myoblasts. Fibroblast Growth Factors (FGFs) are fundamental in embryonic development but also in adult skeletal muscle regeneration from injury or pathology. Understanding the role of specific members of this growth factor family could assist in improving the understanding of their influence on the regeneration sequence in skeletal muscle.

Methods: Isolated satellite cells from human muscle biopsies were expanded *in vitro* creating primary human myoblast (PHM) clones. In order to distinguish the rate of proliferation between different PHM clones, a comparative index (CI) was established using the cell cycle and total RNA data of the two PHM clones. Two distinct index calculation models were also presented to determine if these may distinguish between the two clones with greater sensitivity. Secondly, the quiescent state is an integral part of stem cell regulation, therefore choosing the right protocol for inducing quiescence is important. In this study, two developed protocols were assessed, and a new blended protocol addressing the limitations of both protocols was established. This method involved the use of suspension culture (SuCu) with knock out serum replacement (KOSR). Finally, FGF6 and FGF2, both individually and sequentially, were used to treat quiescent myoblasts to determine their involvement in activation and proliferation with the use of cell cycle analysis and mRNA assessment of ki67, p21, myf5, and MyoD.

Results and conclusion: The development of the CI was successful in determining the difference in proliferation rate for the different clones. Suspension culture with KOSR, the blended protocol method, resulted in reduced ki67 expression and improved quiescence compared to both the SuCu or KOSR alone. Unlike FGF2, individual treatment with FGF6 was adequate to activate the quiescent PHMs and aid their re-entry into cell cycle with consistency in all three PHM clones by upregulating ki67

expression. However, FGF2 did impede the cell cycle inhibition factor p21, indirectly influencing proliferation. Sequential treatment of FGF6 and FGF2 allowed to determine whether the sequence of treatment would be important. The potential for significantly improving proliferation was found for the sequence: FGF6 followed by FGF2. The inverse sequential treatment order did not demonstrate any significant effect on both activation and proliferation of the quiescent cells.

In conclusion, using clones that were distinctly different as assessed by the comparative index, this thesis illuminates that the two FGF family members investigated, act on cell cycle in different ways, thus would influence their utilization in experimental or therapeutic applications.

Opsomming

Inleiding: Regenerasie van volwasse weefsel behels die werwing van voorloper stamselle. In skeletspier is hierdie primêre satellietselle. Dit kan vanuit spierweefsel versamel word vir ondersoeke of selfs as potensiële terapeutiese aanwending. Satellietselle bestaan in 'n rustoestand in die spierweefsel en word slegs na 'n aanslag geaktiveer. Meeste studies wat satellietselle *in vitro* ondersoek, maak van reeds-geaktiveerde satellietselle gebruik, naamlik mioblaste. Fibroblastgroeifaktore (FGFe) is noodsaaklik vir embrioniese ontwikkeling, maar ook vir skeletspierregenerasie na besering of patologie. Om die rol van spesifieke lede van hierdie groei faktor familie te verstaan, kan tot verbeterde begrip van hul invloed op die regenerasie proses in skeletspier lei.

Metodes: Geïsoleerde satellietselle vanaf menslike spierbiopsies is *in vitro* gegroei om primêre menslike mioblast (PMM) klone te genereer. Om die tempo van proliferasie tussen verskillende PMM klone te onderskei, is 'n vergelykende indeks (VI) opgestel met die selsiklus- en totale RNS data van twee PMM klone. Twee afsonderlike indeks berekeningsmodelle is ook voorgestel om te ondersoek watter van hierdie twee modelle met groter sensitiwiteit tussen die twee klone kan onderskei. Tweedens is die metode waarmee die rustoestand_geïnduseer word 'n integrale deel van die rustoestand/aktivering, dus is die keuse van protokol om die rustoestand te induseer, belangrik. In hierdie studie was twee ontwikkelde protokolle ondersoek, asook 'n nuwe verbonde protokol wat die tekortkominge van die ander twee protokolle bespreek, was gevestig. In hierdie metode is 'n suspensie kultuur met uitslaan serum vervanging (USV) gebruik. Laastens is FGF6 en FGF2 beide individueel en opeenvolgend, gebruik om rustende selle te behandel om hul betrokkenheid in aktivering en proliferasie te ondersoek met behulp van selsiklus analise en assessering van mRNS-vlakke van ki67, p21, myf5 en MyoD.

Resultate en gevolgtrekking: Die ontwikkeling van die VI om die verskille in proliferasie tempo tussen die verskillende klone vas te stel, was suksesvol. Suspensie kultuur met USV, die gemengde protokol metode, het gelei tot verlaagde ki67 uitdrukking en verbeterde rustende toestand in vergelyking met beide die (SuCu) of USV alleen ($p<0.05$). Anders as FGF2 was individuele behandeling met FGF6 genoeg om rustende PMMe te aktiveer en om hul hertoetrede tot die selsiklus te ondersteun met

konsekwentheid tussen al drie PMM klone deur opgereguleerde ki67 uitdrukking. FGF2 het egter die selsiklus inhibisie faktor p21 belemmer en so indirek proliferasie beïnvloed. Opeenvolgende behandeling met FGF6 en FGF2 het toegelaat dat daar bepaal kan word of die volgorde van behandeling belangrik is. Die potensiaal vir beduidende verbetering van proliferasie is gevind vir die behandelingsvolgorde: FGF6 gevolg deur FGF2. Die omgekeerde opeenvolgende behandelingsorde het nie enige beduidende effek op beide aktivering of proliferasie van rustende mioblaste getoon nie.

In opsomming, deur die gebruik van klone wat uitdruklik verskillend was, soos gemeet deur die vergelykende indeks, illumineer hierdie tesis dat die twee FGF familie lede wat ondersoek was, op verskillende maniere die selsiklus beïnvloed. Dit sal hul gebruik in eksperimentele of terapeutiese aanwending beïnvloed.

Dedicated to,

My beloved parents,

Dr. B. R. Gudagudi & Smt. G. B. Poornima

Acknowledgements

Throughout the project and writing of this dissertation, I have received a great deal of support and assistance from so many people that I wouldn't be able to list them all. However, there are a few key members who absolutely deserve the recognition.

I thank my supervisor, Dist. Prof. Kathryn H Myburgh, whose expertise was invaluable in formulation of the research topic, methodology and critical investigation inputs. I thank you for your excellent support and for all of the opportunities I was given to conduct my research and most importantly transforming a person who had some knowledge to a scientist who can think. THANK YOU.

I acknowledge all my colleagues from the MRG and the department of physiological sciences, specially Miss.Tracey Ollewagen for the immense support throughout the last 3 years. They not only are part of the department but also are very good friends. I couldn't have done it without your help. I also acknowledge Nicholas Woudberg and Veronique Human for proofreading the thesis and translating the abstract to Afrikaans.

I thank members of CAF Mrs. Lize Engelbrecht, Miss. Rozanne Adams and Ms. Dumisile Lumkwana for the constant support and expertise they have provided throughout the time.

I thank my parents Late Dr.B.R.Gudagudi and Late Smt.G.B.Poornima for their wise guidance given all through my life and pushing me to become what I am. I immensely thank my brother Vinodkumar Gudagudi, my sister in law Vijayalaxmi Gudagudi, importantly my nephew Vedanth Gudagudi and my niece Vedashri Gudagudi for all the support, sympathetic ear and guidance. Talking to you guys made me re-assure that there is a family waiting for me when I complete the work.

I immensely thank my wife Shaveta Gudagudi for being so patient with me, encouraging me to think and try again for every obstacle I faced, without ever allowing me to give up. Without her support it would have been extremely difficult if not impossible.

I also thank Dr.Ashwin Isaacs, Dr.Danzil Joseph, Dr.Theo Nell, Dr.Balindiwe Sishi and soon to be doctor Marthinus Janse van Vuuren for all the support they have provided me, which played a significant role not only in producing this thesis but also providing me with happy distractions.

Finally, there are my friends of Stellenbosch, who were of great support in deliberating over problems and findings, as well as providing happy distractions to rest my mind outside of my research.

"Everyone has the right to their own happiness"

-Kirankumar Gudagudi-

Conferences attended:

- International conference on Tissue Engineering and Regenerative Medicine (ICTERM), van der byl park, South Africa 2016. Podium presentation, titled *"An approach to establishing a comparative index by comparing primary myoblasts of two subjects in vitro"*. 2nd prize for best oral presentation.
- Tissue Engineering and Regenerative Medicine International Society (TERMIS) World Congress, Kyoto, Japan 2018. Poster presentation, titled "*Fibroblast Growth Factor, Potential Game Plan for Regeneration of Skeletal Muscle*".
- Tissue Engineering and Regenerative Medicine International Society (TERMIS) – EU chapter, Rhodes, Greece 2019. Podium presentation, titled *"Hybrid protocol to induce quiescence in vitro in Primary Human Myoblasts"*
- 5th National Stem cell and Gene therapy Conference, Pretoria, South Africa 2019. Podium presentation, titled *"Comparative index, A novel model to compare primary myoblasts in vitro"*.

Publications:

- Validation of in vitro induction of quiescence in isolated primary human myoblasts (*submitted to journal Cytotechnology*).

Table of contents

List of Figures:

List of tables

List of abbreviations

APC	Allophycocyanin
BSA	Bovine Serum Albumin
BSL2	Biosafety level 2
CDK	Cyclin dependent kinase
Cks1	Cyclin-dependent kinase 1
DM	Differentiation media
DMSO	Dimethyl sulfoxide
ECL	Entactin-collagen IV-Laminin
FBS	Foetal bovine serum
FGF	Fibroblast growth factor
FGF2	Fibroblast growth factor 2
FGF6	Fibroblast growth factor 6
FGFR	Fibroblast growth factor receptor
FM	Freezing media
FRS2:	Fibroblast growth factor receptor substrate 2
FSC	Forward scatter
G_1 (phase)	Gap 1 phase
G_2 (phase)	Gap 2 phase
HEPES	4-(2-hydroxyethyl)-1-piperazineethanesulfonic acid.
HGF	Hepatocyte growth factor
HpRb	Hyperphosphorylated retinoblastoma
KOSR	Knock-out serum replacement
M (phase)	Mitosis phase
MAPk	Mitogen-activated protein kinase

MRF	Myogenic regulatory factor
MTT	3-(4,5-dimethylthiazol-2-yl)-2,5-diphenyl tetrazolium bromide
PDGF	Platelet derived growth factor
PHM	Primary Human Myoblast
PI	Propidium iodide
PM	Proliferation media
PMT	Photomultiplier tube
pPHM	Proliferative primary human myoblast
QM	Quiescence media
qPHM	Quiescent primary human myoblast
Rb	Retinoblastoma
rhFGF2	recombinant human fibroblast growth factor 2
rhFGF6	recombinant human fibroblast growth factor 6
RT	Room temperature
S (phase)	Synthesis phase
SC	Satellite cells
SP1	Specificity protein 1
SSC	Side scatter
SuCu	Suspension culture
WST-1	2-(4-iodophenyl)-3-(4-nitrophenyl)-5-(2,4-disulfophenyl)-2H-tetrazolium

Chapter 1: Introduction and literature review.

1.1 Basic introduction to skeletal muscle and satellite cells.

1.1.1 Skeletal muscle, physiological function and structure.

Skeletal muscle is one of the most important structural and functional parts of the body [1-4]. Located throughout the body, bundles of fibres make up the muscle tissue. Skeletal muscle is comprised of long muscle fibres which are generally consistent in shape although they may differ in diameter depending on the typical function [5]. Typically, muscle fibres contain multiple elliptical nuclei in each cell and a homogeneous cytoplasm deriving from up to hundreds of muscle progenitor cells.

Skeletal muscle is one of the three major muscle types in the human body [6]. Skeletal muscle, cardiac muscle and smooth muscle. Physiological functions of skeletal muscle include, differs in that it is used for voluntary movement and plays an important role in energy metabolism and storage. Cardiac muscle helps the heart move the blood from the heart to the vascular system aiding in proper oxygenation of all the cells in the body. Smooth muscle on the other hand is involved in multiple organ systems in an involuntary fashion, shortening in order to either propel various contents in the lumen of the organs or to keep an opening closed [6]. Skeletal muscle cells (fibres) create the most force. A single skeletal muscle can contain hundreds of individual muscle fibres bundled together within connective tissue called epimysium. Skeletal muscle varies in size, shape and arrangement of fibres depending on localization. For example, individual muscle fibres can be thin but total muscle mass can be large as seen in the *gastrocnemius* muscle. Skeletal muscle fibres are fragile when exposed to high contractile forces. In particular, skeletal muscles are attached via tendons at both proximal and distal tips to bones, the contractions allow for movement of attached bone elements and which increases the inherent risk of damage but also damage can occur from trauma or disease. They are prone to constant damage and regular regeneration. Figure 1.1 illustrates the structure of skeletal muscle *in vivo* and the various components each of which is generated from different progenitor cell types. The muscle is encapsulated in a connective tissue sheath called as epimysium. The bundle of each muscle fibre is called as a fasciculus and is covered by another connective tissue known as perimysium. Furthermore, each individual muscle cell within the fasciculus called as a muscle fibre is surrounded by endomysium. Together

the bundle of muscle cells within epimysium is connect to the bone by a connective tissue called as tendon.

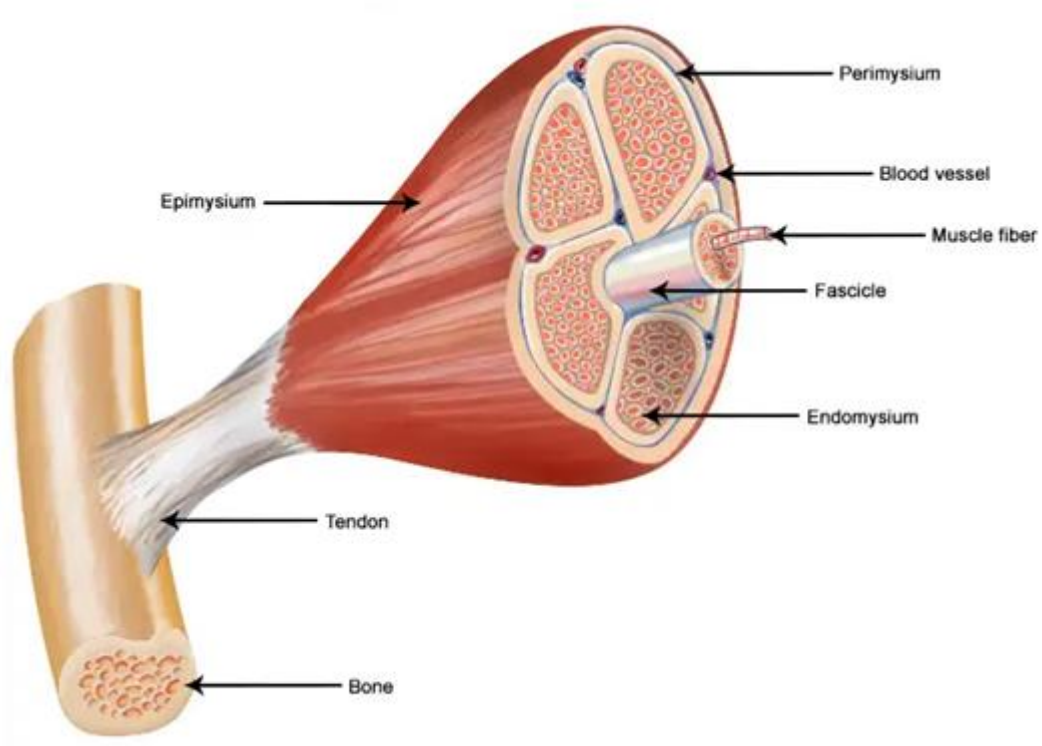

Figure 1.1 Structure of Skeletal Muscle *in vivo* [7]

1.1.2 Satellite cells: their quiescence and activation

The study of satellite cells or muscle stem cells can be dated back to 1961 when they were identified by Alex Mauro [8] using electron microscopy. Satellite cell numbers peak at about 30-35% of total muscle cells during the neonatal stage [9-13]. Satellite cells are highly active during this early stage of development to facilitate the rapid gain in muscle mass [9, 14-16]. In adulthood they stabilise at approximately 2-7% of the total muscle cells [10-13, 17]. These cells reside in a quiescent state, between the basal lamina and sarcolemma of the muscle fibre and express specific genes resulting in identifiable mRNA and protein markers such as Pax7, Pax3, CD34, M-cadherin, syndecan-4 and CXCR4 [18-20].

In adults, muscle regeneration is a complex and time-consuming process involving numerous stages [21-24]. Starting with the activation of individual skeletal muscle progenitor cells (also called satellite cells), followed by their proliferation, differentiation and fusion to form myotubes. There are a number of additional cell types that are

activated by damage and participate in regeneration, including fibroblasts. However, satellite cells are the main contributors [17, 25].

Quiescent satellite cells are multipotent cells with a high nucleus to cytoplasm ratio and a large quantity of heterochromatin [26]. Satellite cells are proficient and essential stem cells for skeletal muscle regeneration, which has been demonstrated by lineage-tracing, cell ablation and cell transplantation studies [27-33]. Upon activation, they re-enter the cell cycle and have the potential to fuse to their adjacent myofibre thus providing additional nuclei to the myofiber, or else return to the quiescent state in which they maintain their stem cell characteristics. Following activation, the satellite cells become spindle-shaped and have decreased levels of heterochromatin and an increased number of cytoplasmic organelles. Due to their usual quiescent nature, satellite cell activation is a crucial step in skeletal muscle regeneration [34].

Entry into the cell cycle, in response to tissue damage, occurs under the influence of several activation factors including hepatocyte growth factor (HGF) [35], fibroblast growth factors (FGF) [36] and platelet derived growth factor (PDGF) [37, 38]. The damage may be acute or chronic. For example, following acute injury of muscle tissue, HGF is typically highly elevated, whilst with chronic damage leading to necrosis of muscle tissue, FGF6 is upregulated [39]. These factors have been added to satellite cells cultures to determine their effects on proliferation and differentiation, however, satellite cells in culture are typically already activated, which is not the case *in vivo*.

Before undergoing myogenic differentiation, activated satellite cells proliferate and begin to express low levels of myogenic regulatory factors (MRFs), at which time they are called myoblasts. The earliest markers associated with satellite cell activation are phosphorylated-p38 mitogen-activated protein kinase (p38 MAPK) followed by MyoD [39-41]. The earliest markers indicating a switch to a more differentiation-prone phenotype is higher MyoD expression and the expression of the MRF, myogenin, and the cytoskeletal protein, desmin [8] . This myogenic differentiation step preceeds fusion whereby satellite cells provide additional nuclei to the existing myofibers [42] (Fig 1.2).

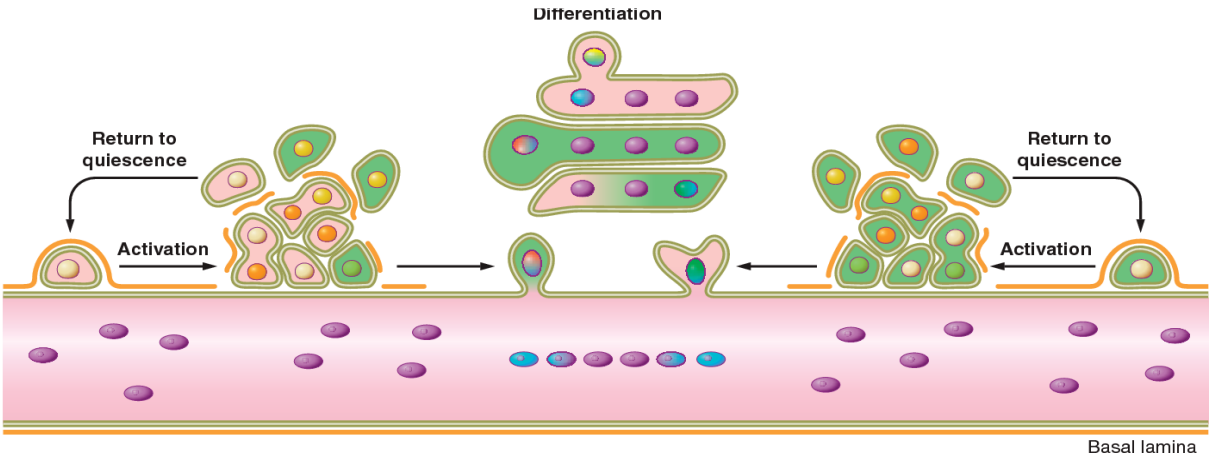

Figure 1.2 Illustration of Skeletal muscle satellite cells and its function originally published by Yin H (2013) [26]

1.1.3 Primary satellite cells

Although skeletal muscle regeneration has been extensively studied both *in vitro* and *in vivo*, a main focus was on factors promoting proliferation (*in vitro*) and the post-fusion myonuclear counts (*in vivo*). Also, the overwhelming majority of research was completed using an immortalised cell line (the C2C12 cells) and although the data generated advanced understanding in this field, it does not adequately represent primary satellite cells harvested directly from excised adult tissue.

Primary cells are derived from tissue samples from living donors. Since donors have different genetic variability, physiological states and may have adapted distinctly to living conditions prior to tissue harvesting, there is a significant heterogeneity in the primary cells isolated from different individuals. This heterogeneity could be further exacerbated by varying abilities to adapt to cell culture conditions. This complicates the use of primary myoblasts in the research setting and hence requires protocols to establish a more uniform baseline. Establishing uniform baseline conditions is important for at least two reasons: to assess inherent individual variability that is not simply due to harvesting protocols, and to more effectively evaluate the effects of a subsequent experimental intervention.

Taking into account the arguments set out above and recent advances in techniques, this thesis addresses both of these issues in the following ways: the study of primary myoblast proliferation *in vitro* and their activation after first inducing quiescence.

Specifically, this thesis developed a novel protocol to compare the proliferative capacity of primary human myoblasts from different donors (comparative index). Further, compared two distinct *in vitro* protocols to induce quiescence. Thereafter, a blended protocol of both was designed and tested. Finally, the influence of FGFs on activation of satellite cells following induced quiescence was studied, specifically focusing on FGF6 and FGF2. The following sections in this chapter (1.2 to 1.4) gives the brief explanations of what the experimental chapters contain.

1.2 Comparative index of isolated PHMs

As previously discussed, primary cells are derived from tissue samples from living donors, who may have adapted distinctly to living conditions prior to tissue harvesting. Since there is significant heterogeneity in the primary cells isolated from different individuals prior to experimental intervention, it is important to understand and quantify individual variability. Surprisingly, there are no clearly defined protocols currently available to assess the characteristics of primary cells *in vitro* in a comparative manner. Also, when performing *in vitro* experiments during which cells are exposed to treatments that affect cellular and molecular function, a key aspect would be to establish a baseline characteristic which could then be used to compare the responses to the various treatments or interventions in the future. This part of the thesis aimed to establish a baseline index with which primary human myoblasts can be compared to each other.

1.3 Comparison of two distinct in vitro quiescence protocols and induction of novel blended protocol.

Transforming cells *in vitro* into a state of quiescence is a relatively new technique and allows the progression from quiescence to activation to be studied in greater detail. In chapter 4, two established protocols to promote cellular quiescence were compared in order to select the suitable protocol for the remainder of the study.

1.3.1 In vitro quiescence using suspension culture

In order for primary human skeletal muscle cells (PHMs) to proliferate and differentiate *in vitro*, they require some cell to cell contact for certain types of intracellular communication and cell to surface contact for anchoring. Depriving immature cells of these two factors tend to guide them towards reversible cell cycle exit and this can be achieved by individual cell suspension in a semi-solid medium (2% methyl cellulose) [43]. For example, methyl cellulose suspension of PHMs has been shown to permit cell separation and reduce aggregation or the settling of cells to the bottom of the media.

1.3.2 In vitro quiescence using knock-out serum replacement (KOSR)

Foetal bovine serum (FBS) is a well-known media supplement for cell culture. FBS is composed of a heterogenous mixture of proteins, hormones, macromolecules and other chemical components which promote cell survival and proliferation.

KOSR however, is a synthetic serum replacement cocktail that supports growth of pluripotent stem cells but lacks components that stimulate proliferation. Previous work in our group found that culturing of PHMs in Ham's F10 nutrient media with KOSR for 10 days without any additional supplementation, stimulated cells to reversibly exit the cell cycle [44].

1.3.3 Development of a novel blended protocol to achieve improved quiescence.

Given that suspension culture provides quiescence and KOSR replacement cocktail also promotes quiescence, replacing FBS with KOSR in the suspension culture could potentially provide an improved state of reversible quiescence in PHMs, compared to either method or alone.

1.4 Fibroblast growth factors (FGFs).

FGFs are a family of cell signalling proteins that bind to heparin or heparin sulphate and regulate a broad spectrum of biological functions, including cellular proliferation, survival, migration and differentiation [45]. Any defect in their function

leads to developmental defects. In humans, FGF is a 22-member family signalling through four FGF receptors (FGFR-1 to FGFR-4) [46-48]. The canonical FGFs are secreted proteins and the receptors are located on the surfaces of the cell. The receptors contain three extracellular immunoglobulin-type domains (D1-D3) and a single intracellular tyrosine kinase domain for activating downstream cascades such as PI3K/AKT, MAPK and STAT. Phylogenetic analysis of the FGFs suggests that the 22-member family can be classified into seven smaller sub-families of two to four members each. The analysis of the FGFs also suggests that the sub-families FGF1,4,7,8 and 9 are involved in encoding secreted canonical FGFs which function by binding and activating FGFRs with heparin or heparin sulfate as a cofactor [49]. Within the sub-families, the individual FGFs were numbered according to their discovery. Importantly, satellite cells /myoblasts have been shown to have high affinity to heparin sulfate proteoglycan receptors of FGF [50]. During muscle regeneration, increase in heparin sulfate proteoglycans and the requirement of syndecan-3 for successful fibre formation has been established [51].

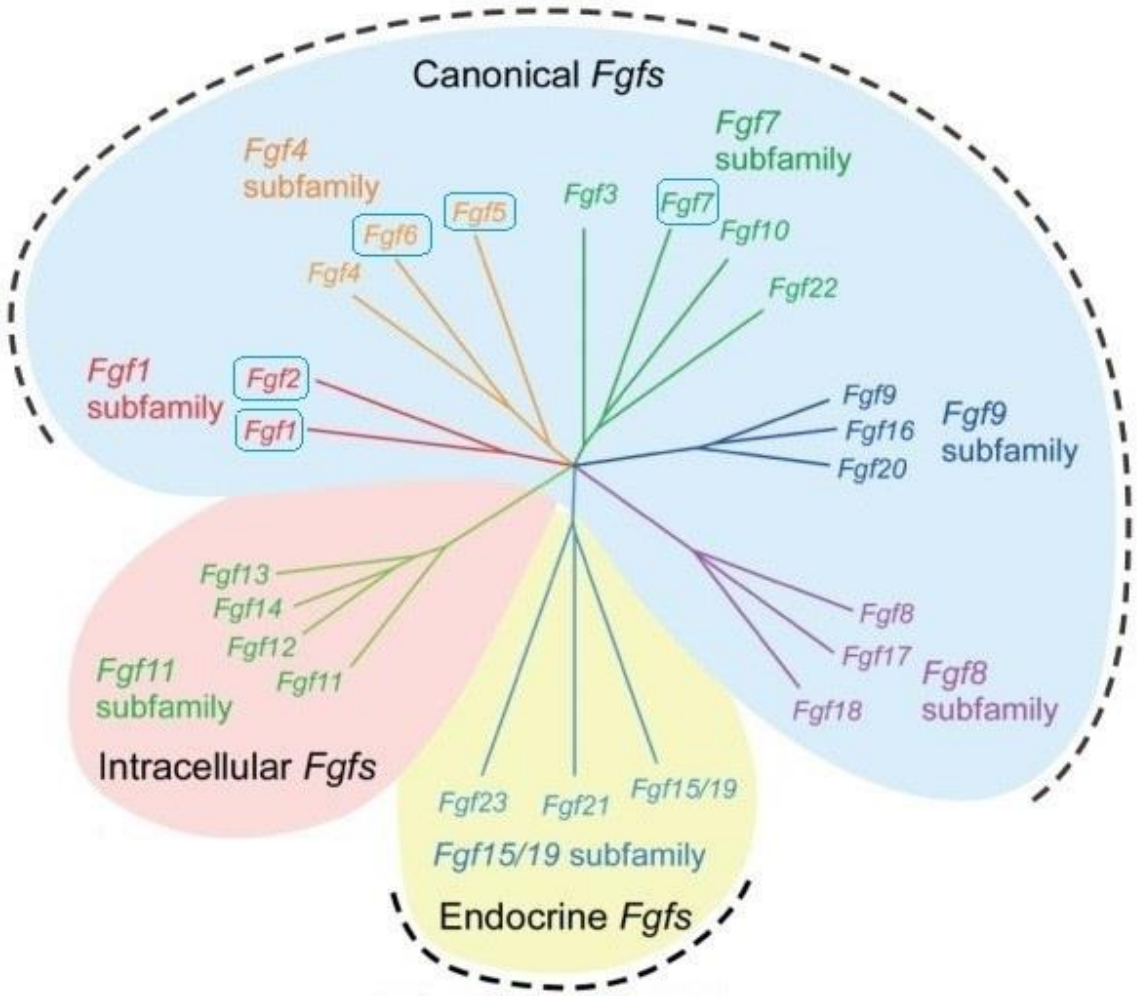

Figure 1.3 The FGF superfamily and subclassifications of Fibroblast Growth Factors. Boxes around FGF indicate importance for myoblast biology. [Modified from [49]]

1.4.1 Introduction to Fibroblast growth factor 2

FGF 2 also known as bFGF or basicFGF, is a signalling protein first purified in 1975 [52]. It is a critical growth factor for embryonic stem cells to remain in an undifferentiated state in culture [53]. In humans, FGF2 has a protein weight of 18 kDa. It is a 155 amino acid polypeptide that binds to fibroblast growth factor receptors. Like other members of the FGF family, FGF2 has broad mitogenic properties and influences many biological processes like embryonic development, cellular proliferation and tissue repair .

Normally, FGF2 is located in basement membranes and in the subendothelial extracellular matrix of blood vessels [54]. Following activation of the wound healing cascade, heparin sulfate degrading enzymes activate FGF2. This early endogenous

response to injury suggests that FGF2 has an important role to play in processes occurring specifically in the early phases [45].

FGF2 is widely used in regeneration of soft tissue [45, 54, 55]. PI3k/Akt is an intracellular signalling pathway important for cell cycle progression. A recent study involving bovine endometrial cells reported that FGF2 induces proliferation and distribution of cells in the G_2 /M phase and that activation of PI3K/Akt cell signalling occurs [48]. Thereafter some regulation of cyclin D1 is by miR-1 and miR-133 which are primarily tumour suppressors. However, miR-133 in specific has been reported to play a feedback mechanism using ERK1/2 pathways regulating myoblast proliferation and differentiation [56].

Cyclin D1 expression is essential for cell cycle progression. Elevated FGF2 has been shown to attenuate p38 mediated miR-1/133 expression and subsequent upregulation of Sp1 (specificity protein 1)/Cyclin D1 which increases myoblast proliferation during early stage of muscle regeneration [57]. Similarly, in a study performed *in vivo* (murine model) as well as *in vitro* on Sca-1+ cardiac muscle stem cells revealed FGF2 as an essential molecule in cell migration. However, endogenous FGF2 levels observed in the *in vitro* model were not adequate to be effective for aiding regeneration of the tissue in the case of myocardial infarction. When provided with exogenous FGF2, the cardiac muscle cell migration was greatly improved through activation of the PI3K/Akt pathway [58].

In an *in vivo* study that aimed to evaluate the role of myoblasts in recovery and regeneration of injured muscle tissue, Sprague-Dawley rats with thigh muscle injury were transplanted with GFP-positive myoblasts. Four weeks after the transplant the GFP-positive cells were found to be integrated into the damaged area. Their contribution to the regeneration of the tissue was shown by Hagiwara *et al (2016)* [59]. Thereafter, the efficacy of myoblast transplantation in combination with controlled and sustained delivery of FGF2 was investigated. This strategy resulted in promotion of muscle regeneration [59].

In agreement with the literature [60] the preliminary work on primary human myoblasts with FGF2 indicated an increase in the rate of proliferation. Active myoblasts treated with FGF2 progressed through cell cycle phases quicker compared to no

supplementation. This work on myoblasts correlates with findings from other research suggesting FGF2 promotes proliferation of myoblasts [61-63].

1.4.2 Introduction to Fibroblast growth factor 6

FGF6 is one of the FGF family members predominantly found in cells of myogenic lineage suggesting a role in muscle development [64]. The FGF6 gene encoded in humans has comparable properties to FGF2 in terms of cell growth, tissue repair and embryonic development. However, subtle and less subtle differences have been shown with FGF6 being the key ligand for FGFR4 as well as being known to be important in initiation and regulation of osteoblasts [65]. Indeed, there is evidence that FGF6 has dual functions in muscle, influencing regeneration as well as differentiation/hypertrophy in a dose dependent manner using distinct pathways employing either FGFR1 or FGFR4 [66]. During muscle necrosis FGF6 was released from necrotic myofibers and then sequestered in the basal laminae [67]. Due to the position of satellite cells just under the basal lamina, this could be the mechanism that initiates the activation of quiescent satellite cells and to aid the rescue. One particular study looking at FGF2/FGF6/mdx triple mutant mice found that FGF6 mutant myoblasts did have reduced ability to migrate *in vivo* [68]. These studies support the initiation side of the FGF6 in regeneration [69, 70].

Compared to FGF2, studies investigating FGF6 are limited, therefore, understanding the relationship of FGF6 to skeletal muscle regeneration in the adult setting requires further investigation.

1.4.2.1 FGF6, debate on activation of quiescent cells.

In a study published by Floss *et al* in 1997, the function of FGF6 in skeletal muscle regeneration was investigated using FGF6 (-/-) mice [69]. The global inactivation of the FGF6 gene severely impaired muscle regeneration, reducing MyoD+ and myogenin+ satellite cell number. The quiescent satellite cell pool was remained unaffected. Therefore, the activation or proliferation process was impaired. The authors concluded that FGF6 plays an integral role in the skeletal muscle regeneration process by facilitating activation of satellite cells.

On the contrary a similar study conducted by Fiore *et al* in 2000 suggested that "skeletal muscle regeneration is not impaired [70]" using FGF6 (-/-) mutant mice. The FGF6 inactivation was achieved by targeting the FGF6 gene by using a replacement vector [70]. Muscle degeneration was achieved by addition of notexin drug or crush injury, after which the defect in the gene did not seem to affect the muscle regeneration.

Comparing the two studies, one could see the similarity in the strategy employed in both investigations to achieve FGF6 (-/-). In the study conducted by Floss *et al*, homologous recombination was employed to inactivate the FGF6 gene in embryonic stem cells by utilising a vector to target the FGF6 gene and replace 3.8kb of genomic content. The inactivation resulted in complete inhibition of the gene. This resulted in MyoD- and myogenin- satellite cells resulting in incomplete regeneration.

Following the study by Fiore *et al,* a similar strategy was employed to target the FGF6 gene in the embryos by vector, and homozygous disruption of FGF6 gene was achieved. However, the regeneration of skeletal muscle was studied further by breeding with C57BL/6 females. Southern blot evaluation revealed FGF(+/-) heterozygous mice having apparent normal phenotype. Furthermore, the F2 generation was obtained by mating heterozygous males with heterozygous females and later southern blot analysis was found to follow mendelian distribution. Although further evaluation states FGF6's absence in regeneration, the complex study design does not clearly illustrate achieving FGF6 inhibition. With F1 and F2 generations both presenting FGF6(+/-) genes, it demonstrates that a single dominant allele with FGF6 could be sufficient to maintain normal muscle regeneration.

The *in vivo* studies are complicated and often regeneration could be assisted by other functions or role players. An advantage of *in vitro* work is that a single treatment can be applied directly. The *in vitro* treatment method allows a clear assessment of the treatments' individual specific action on the cells as there would be no additional processes involved compared to that demonstrated *in vivo*.

1.4.3 Introduction to FGF2 and FGF6 as treatments.

FGF2 has been applied in recent clinical trials investigating angiogenesis and tissue regeneration in various adult tissues [71] (Table 1) . Owing to the pro-proliferative effect of FGF2, it has been used to enhance the precursor cell population numbers. *In vivo* skeletal muscle regeneration begins with the activation of quiescent satellite cells. Although it has been suggested that FGF2 might help in activating quiescent satellite cells in rodent models [72], this has been eclipsed by focus on proliferation.

Table 1.1 Selected list of clinical trials involving FGF2 as an individual or combined treatment. [73]

Sl No	Clinical trial registration number	Current status	Description	Requirement	Date
1	NCT01663298	Recruiting	Gene Expression Variation and Implant Wound Healing Among Smokers and Diabetics	Smoking; Diabetes	February 5, 2019
2	NCT02307916	Active, not recruiting	Fibroblast Growth Factor Regeneration of Tympanic Membrane Perforations	Tympanic Membrane Perforation	March 2, 2019
3	NCT00514657	Completed	Trial in Periodontal Tissue Regeneration Using Fibroblast Growth Factor-2	Periodontitis	August 9, 2007
4	NCT00734708	Completed	Phase 3 Clinical Trial of Periodontal Tissue Regeneration Using Fibroblast Growth Factor-2(Trafermin)	Periodontitis; Alveolar Bone Loss; Periodontal Attachment Loss	June 14, 2012
5	NCT03303885	Recruiting	The FGF/FGFR Signalling Pathway:	Liposarcoma	November 20, 2018

FGF6 has been linked predominantly to the myogenic lineage during development suggesting that FGF6 might hold significant value in the regeneration sequence which replicates the development process. With limited information available about the effects of FGF6 on activation of quiescent skeletal muscle cells, the subsequent study

combined both growth factors to determine whether activation / proliferation could be improved if used in combination.

The experimental plan involved applying a treatment regimen of FGF6 and FGF2 in sequence to actively proliferating PHMs as well as to KOSR-treated quiescent PHMs. Assessment involved cell cycle analysis concentrating on the G_0/G_1 phase to S phase transition and qPCR analysis of key markers genes of activation and proliferation, i.e. ki67, p21, myf5 and MyoD.

1.4.4 Significance of ki67, p21, myf-5 and MyoD.

ki67 also known as MKI67 is a protein encoded by the MKI67 gene in humans found on chromosome 10 [74]. It is a nuclear protein that is associated with cellular proliferation and ribosomal RNA transcription and is present in each phase of the cell cycle (G_1, S, G_2 and M). During interphase, the ki67 antigen is located exclusively inside the cell nucleus, while during mitosis the protein is located on the surface. This suggests that the main role is during cellular proliferation and it can therefore be used as a marker for proliferation [75].

Cyclin-dependent kinase inhibitor 1, also known as p21 is an important regulating factor in the cell cycle. It is encoded by the CDKN1A gene found on chromosome 6 in humans [76]. The regulation of cell cycle progression involves inhibiting the CDK2 complex at G_1 and S phase [77]. Studies investigating CDK2 activity have shown that the expression level of p21 in the cell could be responsible for the bifurcation in CDK2 which in turn could be involved in regulating proliferation or attaining G_0/quiescent state [78].

The myf5 protein is encoded by MYF5 gene in humans with the key role associated with myogenesis and regeneration. Located on chromosome 12, myf5 belongs to the group of myogenic regulatory factors (MRFs. The loss of MyoD and myf5 has been shown to result in altered skeletal muscle programming and failed regeneration [79]. The muscle-specific gene myf5 plays a critical role in embryonic and foetal myogenesis. Expression of myf5 has been studied and linked to ultimately giving rise to adult satellite cells [80].

Myoblast determination protein 1, more commonly known as MyoD, is a transcription factor of the MRF family. Discovered and characterised by Weintraub's lab, MyoD is well known to be associated with myogenesis [81]. Since the discovery, MyoD has been the gold standard identification marker for myoblasts. The potency of MyoD was well recognized when it was proved that MyoD could convert fibroblasts to myoblasts [81, 82]. Both MyoD and myogenin are seen co-expressed in differentiating myoblasts in regeneration of injured skeletal muscle tissue [83] and its expression is absent from quiescent satellite cells. In contrast, myf5 discussed above is expressed in quiescent cells (Partridge T) and hence these two MRFs can be used as markers distinguishing how far myoblasts are in the path from quiescence to differentiation.

1.4.5 Aims and objectives

The background information regarding the gaps in the published research discussed above brings us to the aims and objectives of the research.

Aim 1: Establish a comparative index.

Objectives:

1. Establish a new protocol to compare primary human myoblasts *in vitro*.
2. The protocol should use the rate of proliferation and at least one other phenotypic characteristic that is likely to be adaptable to treatments.
3. Establish a mathematical model which can be used to explain the difference between cells derived from different donors.

Aim 2: Comparison of two *in vitro* quiescence protocols to choose the right quiescent method for future experiments and to determine if a blended protocol would differ from either or both of the specific protocols.

Objectives:

1. Compare induction of quiescence using SuCu and KOSR by assessing effects on cell cycle genes.
2. Using cell cycle analysis, assess the induction of quiescence in KOSR method.

3. Replace FBS in SuCu with KOSR to investigate if this changes the induction of quiescence.

Aim 3: Understanding the role of FGF6 and FGF2 in activation and proliferation of PHMs.

Objectives:

1. Establish quiescence in all the PHM clones to be used.
2. Assess the activation potential of FGF6 in quiescent PHMs
3. Assess the activation potential of FGF2 in quiescent PHMs
4. Assess activation and proliferation of quiescent PHMs using sequential treatment of FGF6 followed by FGF2
5. Assess activation and proliferation of quiescent PHMs using inverse sequential treatment of FGF2 followed by FGF6.

Chapter 2: Materials and methods

All chemicals used were of analytical grade.

2.0 Materials:

Description	Catalogue number	Company
Bovine Serum Albumin (BSA)	10735086001	Roche Holding AG, Basel, Switzerland
Cell counter counting chamber slides	C10228	Thermo Fisher Scientific, Massachusetts, USA
Cell culture Flask, 175m^2	709003	Nest Biotechnology Co.,Ltd, Jiangsu, China
Cell culture Flask, 75m^2	708003	Nest Biotechnology Co.,Ltd, Jiangsu, China
Cell culture Flask, 25m^2	707003	Nest Biotechnology Co.,Ltd, Jiangsu, China
Cell culture Plate 6- well	703001	Nest Biotechnology Co.,Ltd, Jiangsu, China
Cell cycle kit BD	BD/340242	Becton Dickinson, New Jersey, USA
Cell tracker	C2925	Thermo Fisher Scientific, Massachusetts, USA
Chloroform	C2432	Sigma-Aldrich (Pty) Ltd, Missouri, USA
Dimethyl Sulfoxide	C6164	Sigma-Aldrich (Pty) Ltd, Missouri, USA
DMEM	11965092	Thermo Fisher Scientific, Massachusetts, USA.
E-C-L cell attachment matrix (Entactin- collagen IV-laminin)	11965092	MilliporeSigma, Massachusetts, USA.
Equine serum	16050122	Thermo Fisher Scientific, Massachusetts, USA

Ethyl alcohol	E7023	Sigma-Aldrich (Pty) Ltd, Missouri, USA
Fetal Bovine Serum	10438026	Thermo Fisher Scientific, Massachusetts, USA
Glutamax	35050061	Thermo Fisher Scientific, Massachusetts, USA
Ham's F10	N6908	Sigma-Aldrich (Pty) Ltd, Missouri, USA
HEPES	7365-45-9 H4034	Sigma-Aldrich (Pty) Ltd, Missouri, USA.
Hoescht	62249	Thermo Fisher Scientific, Massachusetts, USA
Isopropanol	I9516	Sigma-Aldrich (Pty) Ltd, Missouri, USA
KOSR (KnockOut™ Serum Replacement)	10828010	Gibco™, Thermo Fisher Scientific, Massachusetts, USA
Methyl Cellulose	M0512	Sigma-Aldrich (Pty) Ltd, Missouri, USA
PenStrep (Penicillin-Streptomycin)	15070063	Gibco™, Thermo Fisher Scientific, Massachusetts, USA
Phosphate Buffered Saline tablets	P4417	Sigma-Aldrich (Pty) Ltd, Missouri, USA
qPCR Gene primers		Integrated DNA Technologies - Iowa, USA.
rh-FGF2 protein	PHG0266	Gibco™, Thermo Fisher Scientific, Massachusetts, USA
rh-FGF6 protein	PHG0174	Gibco™, Thermo Fisher Scientific, Massachusetts, USA
SYBR™ Select Master Mix	4472908	Thermo Fisher Scientific, Massachusetts, USA
Tripure	11667157001	Sigma-Aldrich (Pty) Ltd, Missouri, USA

Trypan blue 0.4%	15250061	Thermo Fisher Scientific, Massachusetts, USA
Trypsin 0.25% EDTA	25200072	Thermo Fisher Scientific, Massachusetts, USA
0.22 µm filter syringe		MilliporeSigma, Massachusetts, USA.

Methods:

All *in vitro* experimentation was performed under sterile conditions in a BSL2 laminar flow hood, unless otherwise stated. In Chapter 2, general methods used to set up the subsequent experiments are described. Specific methods are discussed in the relevant chapters (3, 4, 5) along with a brief introduction and the results.

2.1 Media and buffer preparation

2.1.1 Preparation of Phosphate Buffered Saline 1x (PBS)

PBS tablets (cat # P4417, Sigma-Aldrich (Pty) Ltd, Missouri, USA) were used to prepare 1xPBS solution in deionized water. According to the manufacturer 1 PBS tablet provides 200 ml of 1x PBS. 1 Tablet was placed in a clean glass bottle with 50 ml of deionized water and swirled until the tablet completely dissolved, dH_2O was added to make the final volume 200 ml. The solution was then autoclaved at 121˚C for 30 min to obtain sterilized 1x PBS for cell culture use.

2.1.2 Proliferation Media (PM)

Proliferation media was prepared using Ham's F10 (cat # N6908, Sigma-Aldrich (Pty) Ltd, Missouri, USA) nutrient mixture, containing high glucose and L-Glutamine. Ham's F10 was supplemented with 20% FBS (cat # 10438026, Thermo Fisher Scientific, Massachusetts, USA) and 1% penicillin/streptomycin (PenStrep) (cat # 15070063, Gibco™, Thermo Fisher Scientific, Massachusetts, USA). The mixture was then filtered through 0.22µm filter using a syringe (cat # SOGV033RS , MilliporeSigma, Massachusetts, USA). aliquoted into 50 ml tubes and stored at 4˚C. Media was stored maximum for 4 weeks. Prior to use, 10 ng/ml of rh-FGF2 was freshly added.

2.1.3 Quiescence Media (QM)

Quiescence media was prepared using Ham's F10 nutrient mixture supplemented with 20% knockout serum replacement (KOSR) (cat # 10828010, Gibco™, Thermo Fisher Scientific, Massachusetts, USA) and 1% PenStrep. KOSR is a defined FBS-free medium supplement that supports growth of stem cells. The mixture was aliquoted into 50 ml tubes and stored at 4˚C. Media was stored for a maximum of 4 weeks. This mixture will henceforth be called as Quiescent media (QM).

2.1.4 Suspension culture media (SuCu)

The suspension culture media (SuCu) consisted of 2% sterilized methyl cellulose (cat # M0512, Sigma-Aldrich (Pty) Ltd, Missouri, USA) in Dulbecco's modified eagle medium (DMEM) (cat # 11965092, Thermo Fisher Scientific, Massachusetts, USA). The solution was heated to 50 ˚C and stirred overnight prior to storage at 4˚C.

2.1.5 Differentiation Media (DM)

Differentiation media was prepared with DMEM containing high glucose with L-Glutamine supplemented with 1% Equine serum (cat # 16050122, Thermo Fisher Scientific, Massachusetts, USA) and 1% PenStrep. The mixture was then filtered through 0.22 µm filter using a 50 ml syringe. aliquoted into 50 ml tubes and stored at 4˚C. The solution was stored maximum for 4 weeks.

2.1.6 Freezing Media (FM)

Freezing media was prepared using 10% DMSO (cat # C6164, Merck, New Jersy, USA) and 90% FBS. The solution was prepared when required just before freezing the cells and not stored. The volume of freezing media was prepared according to the number of cells being frozen. A concentration of 1x10^6 /ml was maintained for cryopreservation.

2.1.7 Entactin-collagen IV-laminin (ECL) preparation.

Entactin-collagen IV-laminin (cat # 11965092, MilliporeSigma, Massachusetts, USA) solution with the final concentration of 20 µg/ml was prepared in PBS.

2.1.8 Preparation of 0.1% Bovine Serum Albumin (BSA)

10 mg of BSA fraction (cat # 10735086001, Roche Holding AG, Basel, Switzerland) was dissolved in 5 ml PBS, once completely dissolved PBS was added to make the final volume 10 ml to obtain a final concentration of 0.1%. The solution was then sterile filtered using 0.22 µl syringe filter inside laminar airflow. The BSA solution was prepared just before preparing stock solutions.

2.1.9 Preparation of recombinant human Fibroblast Growth Factor 2 (rh-FGF2) Stock solution

Lyophilized rh-FGF2 vial (25 µg) (cat # PHG0266, Gibco™, Thermo Fisher Scientific, Massachusetts, USA) was briefly centrifuged before opening. 25 µg of rh-FGF2 was dissolved in 2.5 ml of 1x PBS. As per manufacturers recommendations, rh-FGF2 was reconstituted at a stock concentration of 10 ng/µl in 1x PBS, 50 µl aliquots were prepared and stored at -80˚C.

2.1.10 Preparation of recombinant human Fibroblast Growth Factor 2 (rh-FGF2) working solution.

Stock solution of FGF2 (10 ng/µl) was added to the required media (PM or QM) to obtain the final concentration of 10 ng/ml of media (1 µl of stock to 1 ml of media).

2.1.11 Preparation of recombinant human Fibroblast Growth Factor 6 (rh-FGF6) stock solution.

Lyophilized rh-FGF6 vial (25 µg) (cat # PHG0174, Gibco™, Thermo Fisher Scientific, Massachusetts, USA) was briefly centrifuged before opening. 25 µg of rh-FGF6 was dissolved in 2.5 ml of 0.1% BSA. As per manufacturers recommendation,

rh-FGF6 was reconstituted at a stock concentration of 10 ng/µl in 0.1% BSA, 10 µl aliquots were prepared and stored at -80˚C.

2.1.12 Preparation of recombinant human Fibroblast Growth Factor 6 (rh-FGF6) working solution.

Stock solution of rh-FGF6 (10 ng/µl) was added to the required media (PM or QM) to obtain the final concentration of 10 ng/ml of media (1 µl of stock to 1 ml of media)

2.2 Procedures and protocols

2.3.1 Coating of Culture Plates with ECL

ECL was brought to 37˚C in a water bath and enough solution was added to cover the culture area generously (consult table 2.1). The plate was then incubated either at 4˚C overnight or for 2 hours at 37˚C in the incubator. The excess ECL was either discarded or used immediately to coat another plate. The excess ECL was only removed just before plating of the cells. Reusing of the ECL was performed only once.

Table 2.1 ECL for coating culture dishes

Plate / Flask size	Volume of ECL
12 well plate – per well	500 µl
6 well plate – per well	1 ml
t25	2 ml
t75	3 ml
t175	7 ml

Note: All culture plates and culture flasks further described were observed under microscope every time they were taken out of incubator.

Media Change: After removing the previous media present in the flask and washing with 37˚C 1x PBS (2x), it was replaced with fresh media (the same that was

previously in the flask or the new required media) and placed in the incubator, unless otherwise stated. This procedure will further be referred to as changing media.

2.3.2 Procurement of PHMs

2.3.2.1 PHM isolation

Excess tissue from muscle biopsies from *Vastus Lateralis* of human subjects were generously provided by Greig Thomson, Jason Lovett (ethics number S17/03/061) and Cameron Sugden (ethics number S17/10/240) after these researchers had cut samples to a shape suitable for histology. The biopsies were about 100 mg and 3-5 mm in diameter before dividing according to purpose. The portions for isolation of satellite cells were transported from the clinical room to the culture laboratory in ice cold PBS with 10% PenStrep and 1% Gentamycin.

The tissues were dissected into about 3 mm^2 square pieces on a sterile glass slide inside a 10 cm sterile petri dish, repeatedly washed in fresh ice-cold PBS and plated on to a 12 well culture plate coated with ECL. Tissues were incubated with 300 µl proliferation media for 24 hours at 5% CO_2 and at 37˚C. After 24 hours, additional 1 ml of proliferation media was added gently to the wells without disturbing the tissues and incubated again for 24 hours. Media was then changed after a further 24 hours. On day 4, the tissue was aspirated and placed in a new well coated with ECL and 300 µl of media was added carefully. The culture was continued with media changes every 48 hours and the transfer of the tissue to a new coated well every 3-4 days for 18 days to selectively separate fibroblasts from late migrating myoblasts. As fibroblasts migrate from the tissue in the early stages, the period from 14-18 days represented the time when the majority of cells separated from the tissue samples were myoblasts. During this period (or at 18 days?), a small portion of each well containing almost exclusively myoblasts was demarcated using an insert and trypsinised. The cells harvested from this partial trypsinisation were replated and subjected to differentiation conditions to assess the successful formation of myotubes to verify the validity of the isolated myoblasts (see next section). Remaining adherent cells were trypsinsed with 0.5% EDTA trypsin (cat # 25200072, Thermo Fisher Scientific, Massachusetts, USA) and replated? Or just left to distribute themselves? in order to evenly distribute them. Once

actively proliferating and confluent, the cells were trypsinised and transferred to larger culture dishes for expansion.

2.3.2.2 Confirmation of myoblast phenotype

The partially trypsinised PHMs were proliferated to 90% confluency and the media was changed to DM. The culture was continued for 5 days. Cell tracker with nuclear staining was performed to identify multinucleated tubes. Hoescht (cat # 62249, Thermo Fisher Scientific, Massachusetts, USA) 1:200 dilution and cell tracker (cat # C2925, Thermo Fisher Scientific, Massachusetts, USA) 1:1000 dilution in proliferation media was used to prepare the staining solution with final volume of 3ml. 5 min before the imaging, the staining solution was added to the well inside the hood and incubated at 37˚C and imaging was performed on Nikon ECLIPSE E400 microscope. The same differentiation was confirmed with all the PHM clones used in the studies.

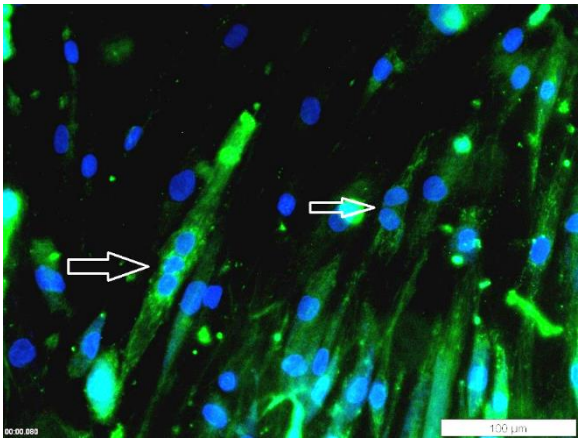

Figure 2.1 Representative image of multinucleated myotubes. White arrow indicating multinucleated myotubes.

2.4.1 Suspension culture protocol

The suspension culture was prepared by combining the SuCu with 20% FBS, 4 mM Glutamax (cat # 35050061, Thermo Fisher Scientific, Massachusetts, USA), 0.1% PenStrep and 1M HEPES (cat # 7365-45-9 H4034, Sigma-Aldrich (Pty) Ltd, Missouri, USA). All components were pre-warmed to 37˚C whilst the latter components were prepared and filtered separately from the SuCu, prior to mixing. PHMs (1 million/ml)

were added to the suspension culture in a slanted tube and were mixed gently for 5-10 min by rotating the tube. Thereafter, the tube was incubated for 24 hrs at 37˚C with 5% Co_2 in an incubator and gently mixed again by rotating the tube and then incubated for 24 hrs more. The composition of the suspension culture is summarized below

10 ml Suspension culture.

2 % Methyl cellulose	-	6.70 ml
20 % FBS	-	2 ml
4 mM Glutamax	-	100 µl
PenStrep	-	100 ul
1M HEPES	-	100 ul
Cells 1 million /ml	-	1 ml

2.4.2 Cell culture and passaging

Cell culture was performed in a laminar flow with sterile techniques. All required media, PBS and Trypsin were brought to 37˚C before being used for cell culture. For culturing PHMs, the culture dish was coated with ECL as previously discussed. Passaging was performed when the cells proliferated to about 70% of the culture dish used. Media was removed followed by two washed with 1x PBS and subsequent trypsinization. Trypsin-EDTA (1X, T3924) was used to dislodge cells from the surface of the culture dish (*refer to table 2.2 for volume of trypsin used*). Preheated media was used to deactivate the trypsin and the cells were collected in a falcon tube. Centrifugation was performed at 325 g at 22˚C for 3 min. Supernatant was discarded. 1 ml of fresh media was added and triturated to get uniform single cell suspension. Additional fresh media was added to obtain the final volume and cell concentration for replating.

Table 2.2 Volume of trypsin for Trypsinization

Plate / Flask size	Volume of Trypsin
12 well plate – per well	125 µl
6 well plate – per well	250 µl
t25	500 µl
t75	1.5 ml
t175	3.5 ml

2.4.3 Partial trypsinisation (Trypsin inserts)

Inserts were prepared using a 25 ml serological pipette (Figure 2.2, 2.3). Approximately ½-1 cm was cut from both ends using microtome knife. The inserts were then cleaned under naked flame to burn any plastic residue. The inserts were sterilized in 70% ethanol overnight and washed serially in 1x PBS before use.

Figure 2.3 25 ml serological pipette marked for separation

Figure 2.3 Inserts separated from the pipette

The culture well was divided into 45˚ angles and marked underneath the plate. The area of trypsinization was chosen by observing under the microscope. In the laminar flow, the dish was washed twice with PBS and the inserts were placed in the region chosen. While holding the insert with sterile forceps, 50 µl of trypsin was added and incubated for 2-3 min (Figure 2.4, 2.5). Once cells began to lift from the culture surface, the trypsin (containing cells) was aspirated and placed in an 1.5 ml Eppendorf tube. 50 µl of media was then added inside the insert to collect the remaining dislodged cells.

2.4.4 Cell counting using automated cell counter (Countess II, Thermo Scientific™)

Using 1:1 mixture of 0.4% trypan blue (cat # 15250061, Thermo Fisher Scientific, Massachusetts, USA) and cell suspension, 10 µl was loaded onto disposable cell counter slides (cat # C10228, Thermo Fisher Scientific, Massachusetts, USA). The slide was then loaded on to the automated cell counter, focused using coarse and fine adjustments and cell were counted. Instrument reading of live cell, dead cell, total cell count and cell viability in % were noted.

2.4.5 Preparation of cells for cryopreservation

Culture flask was observed under phase contrast microscope to ensure live and healthy cells. After removing the media, the flask was washed twice with 37˚C PBS . An appropriate amount of trypsin was added depending on the size of the plate (Table 2.2) and incubated at 37˚C for 3 min. The flask was observed under the microscope to ensure all the cells have dislodged. Using 5 ml of PM the flask was washed, all the cells collected in a 15 ml tube for centrifugation. Centrifugation was performed at 115 g at RT for 5 min. The supernatant was discarded carefully, and 1 ml of proliferation

media was added and triturated for single cell suspension. The cells were counted using Automated cell counter (Countess II), as previously described. Freezing media (2.1.6) was added accordingly to obtain 1x10^6 /ml concentration. The cell suspension was then quickly transferred to cryovials and placed in Mr.Frosty (Freezing container, Thermo Scientific™) and placed in -80˚C overnight. The next day the vials were transferred to liquid nitrogen tank.

2.4.6 RNA isolation

Following removal of culture media, cells were lysed with 500 µl of Tripure (cat # 11667157001, Sigma-Aldrich (Pty) Ltd, Missouri, USA) and the lysate removed and stored at -20˚C prior to RNA isolation. The Eppendorf tube with lysed cells in Tripure was allowed to thaw completely on ice. 100 µl of chloroform (cat # C2432, Sigma-Aldrich (Pty) Ltd, Missouri, USA) was added to the lysate and mixed by inverting the tube for 15 sec and let it stand at RT for 5 min. Thereafter, the sample was centrifuged at 13,500 rpm for 15 min at 4˚C which formed 3 distinct layers. The clear supernatant was carefully transferred to a new Eppendorf tube prior to the addition of 250 µl of Isopropanol (cat # I9516, Sigma-Aldrich (Pty) Ltd, Missouri, USA). The sample was centrifuged again at 13,500 rpm for 15 min at 4˚C and the supernatant was discarded. The remaining pellet was resuspended in 500 µl of 70% Ethanol and centrifuged at 7,500 rpm for 7 min at RT. This step was repeated three times. The supernatant was discarded and the tube air dried for about 30 min (until ethanol was completely evaporated). The pellet was finally eluted with 20 µl of RNA/DNA free water and measured for RNA quantity and purity using Nanodrop lite

2.4.7 Measuring RNA using Nanodrop lite (Thermo Scientific™)

The Nanodrop lite is a compact microvolume spectrophotometer providing accurate and reproducible measurements without the need for dilutions. Nanodrop lite can be used to measure nucleic acid concentration at 260 nm and purity using 260/280 ratio. Purified protein can be measured at 280 nm.

To confirm purity and RNA concentration, the eluted samples were measured using the Nanodrop lite (Thermo Scientific™). The instrument contact point was cleaned with distilled water. The RNA/DNA free water used to elute the RNA was used as a

blank measurement. After setting blank twice, the contact point was blotted using lint free paper, 1 µl of sample was loaded and measured. The RNA concentration was quantified in ng/µl and purity was noted in ratio of 260nm/280nm wavelength.

Table 2.3 Representative table for RNA quantification.

Sample ID	**RNA concentration ng/µl Test 1 (260nm)**	**RNA concentration ng/µl Test 2 (260nm)**	**Mean RNA concentration ng/µl**	**Purity (260/280nm)**
KH 1.3 P	425.5	428.1	426.8	1.96
KH 1.3 Q	389.6	390.6	390.1	1.99
KH 1.3 PF2	574.9	589.6	582.25	1.94
KH 1.3 QF2	427.4	436.1	431.75	1.90

2.4.8 cDNA preparation with two different first strand cDNA kits

All procedures were performed on ice.

Prior to starting the procedure, a table was prepared with number of samples, concentrations of RNA, starting with least concentration of RNA, volume to RNA in µl and volume of dH_20 to pipette for each sample to obtain final volume of 11µl with equal concentration of RNA in each tube. Thermal cycler (Applied biosystems 2720) was used to synthesize the first strand cDNA.

Table 2.4 Representative table for cDNA preparation

Sample ID	**RNA concentration in ng/ul**	**Volume of RNA in µl**	**D/w in µl**	**Final volume**	**Final Concentration in ng/µl**
KH 1.3 P	426.8	10.05	0.95	11 ul	4291.1
KH 1.3 Q	390.1	11	0	11 ul	4291.1
KH 1.3 PF	582.25	7.37	3.63	11 ul	4291.1
KH 1.3 QF	431.75	9.94	1.06	11 ul	4291.1

2.4.8.1 Details about the instrument

Applied Biosystems 2720 thermal cycler is a standard PCR equipment with 96 well reaction plate area. Programable thermal block with heated lid allows to cycle through repeated temperatures required with 0.2 ml reaction tubes. Initial optimization was done using gradient temperatures.

Note: Two different cDNA synthesis kit were used, results were scrutinized, and the suitable kit was chosen for all further tests.

2.4.8.2 Revert Aid First strand cDNA Synthesis kit H minus

Required samples of template RNA were collected and allowed to thaw on ice. Table with the concentrations of RNA was consulted to pipette required amount of RNA to separate 200 µl RNAse free tube followed by required amount of dH_20. 1 µl of Random Hexamers was added and mixed by tapping the bottom of the tube gently. The mixture was incubated at 65˚C for 5 min followed by 1 min cooling on ice. 5x Reaction buffer (4 µl), Ribolock RNase inhibitor (1 µl), 10 mM dNTP mix (2 µl), and Revert Aid (1 µl) were added to each sample, mixed and centrifuged briefly. The tubes were then transferred to PCR thermal cycler and was run with the following protocol. 5 min @ 25˚C → 60 min @ 42˚C → 5 min @ 70˚C. The tubes were then preserved at -20˚C for short term, -80˚C for long term or used immediately for PCR reactions.

2.4.8.3 Superscript IV first strand kit

Using the Superscript IV first strand kit, the template RNA samples were collected and allowed to thaw on ice. The concentration table was consulted to pipette the required amount of RNA, 50 µM oligo dT and 10 mM dNTP were added to each tube and incubated @ 65˚C for 5 min followed by cooling on ice for 1 min. 10x RT Buffer 25 mM $MgCl_2$, 0.1 M DTT, RNase out and Superscript III were added to each tube. The mixture was then incubated in the PCR thermal cycler (Applied Biosystems, 2720) at 50˚C for 50 min.

Note: Superscript IV first strand kit was chosen for all further analysis due to the greater amount of cDNA produced.

2.5 Quantitative Polymerase Chain Reaction

2.5.1 qPCR Primers

Initial PCR runs were performed with gradient annealing temperature from 54.5˚C to 60.5˚C) in order to optimize conditions. 57.5˚C was chosen as the optimal temperature as all the primers annealed well and produced a single amplicon fragment indicated by uniform melt curve.

Table 2.5 qPCR primer sequence

Human Gene Primer Name	Orientation	Sequence
GAPDH	Forward Primer (5'- 3')	TGGTGCTGAGTATGTCGTGGAGT
	Reverse Primer (3'- 5')	AGTCTTCTGAGTGGCAGTGATGG
MYF5	Forward Primer (5'- 3')	AATTTGGGGACGAGTTTGTG
	Reverse Primer (3'- 5')	CATGGTGGTGGACTTCCTCT
MYOD1	Forward Primer (5'- 3')	TGCACGTCGAGCAATCCAAA
	Reverse Primer (3'- 5')	CCGCTGTAGTCCATCATGCC
PAX7	Forward Primer (5'- 3')	CCCCCGCACGGGATT
	Reverse Primer (3'- 5')	TATCTTGTGGCGGATGTGGTTA
MKI67 (Ki67)	Forward Primer (5'- 3')	TGACCCTGATGAGAAAGCTCAA
	Reverse Primer (3'- 5')	CCCTGAGCAACACTGTCTTTT
p21	Forward Primer (5'- 3')	TCTTGTACCCTTGTGCCTCG
	Reverse Primer (3'- 5')	ATCTGTCATGCTGGTCTGCC

2.5.2 qPCR primer concentration

Table 2.6 qPCR primer concentration

Primer Name	GC content in %	Molecular weight	Tm in ˚C
GAPDH F	52.2	7181.7	59.9
GAPDH R	52.2	7150.7	58.7
MYF5 F	45.0	6243.1	53.4
MYF5 R	55.0	6115.0	56.6
MYOD1 F	50.0	6095.0	57.6
MYOD1 R	60.0	6028.9	58.2
PAX7 F	73.3	4514.0	58.7
PAX7 R	45.5	6827.5	56.1
MKI67 F	45.5	6752.5	56.0
MKI67 R	47.6	6332.2	55.5
P21 F	55.0	6025.9	57.0
P21 R	55.0	6075.0	57.5

2.5.3 Reagents used for qPCR

qPCR was performed using SYBR Green dye (cat # 4472908, Thermo Fisher Scientific, Massachusetts, USA**)** . It is a commonly used fluorescent dye which binds to the double-stranded DNA by intercalating between the DNA bases. The fluorescence can be measured at the end of each amplification cycle to determine relative and absolute amplification of DNA.

2.5.4 qPCR plating

qPCR was similarly performed on the PCR Thermal cycler (Applied biosystems, 2720). 10 µl of each sample was loaded into each well in triplicate. One set of positive, negative and blank controls were used on every plate.

2.5.5 qPCR running protocol for Applied Biosystems instrument.

The StepOnePlus™ Real-Time PCR system was used to perform qPCR with temperature settings detailed in Table 2.6. This instrument is a 96 well instrument with 4 colour optical LED recording system connected to a Windows computer. The program temperature and time settings used for the qPCR run are described in Table 2.7. The SYBR green reporter dye was used.

Table 2.7 qPCR instrument protocol

Protocol	**Temp in ˚C**	**Time**	**Parameter**
UDG activation	50	2 Min	Hold
Dual lock	95	2 Min	Hold
Denature	95	15 Sec	40 Cycles
Anneal	57.5	15 Sec	
Extend	72	1 Min	

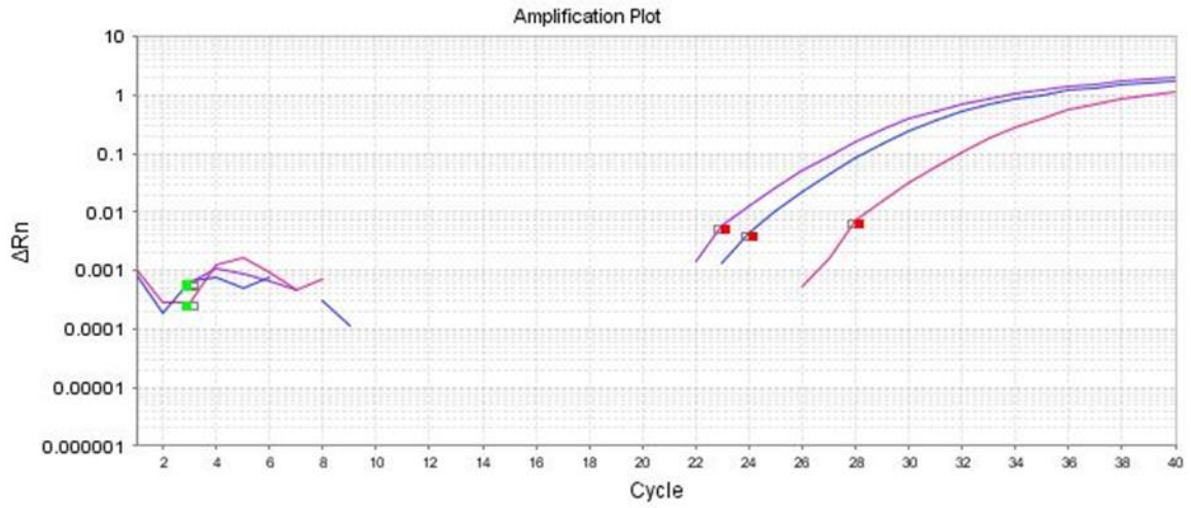

Figure 2.4 Representative qPCR reaction plot. X-axis representing the number of cycles and the fluorescence. The Y-axis represents the product amplification from the reaction minus the baseline.

The represented qPCR plot shows the number of cycles (X-axis) and fluorescence of the Sybr Green reporter dye minus the baseline (ΔRn). The Ct value is calculated from the plot and represents the target threshold (red) which is the number of cycles necessary for the fluorescent signal generated to rise above the background levels. The Ct value of the qPCR amplification graph is inversely proportional to the number of copies of the mRNA transcripts. The amount of doubling or amplification needed for the fluorescence signal to raise above the background noise represents the amount of mRNA transcript present in the sample. A lower Ct indicates higher mRNA transcripts as it does not need many amplification cycles. The trace on the farthest right on the plot would have a lower number of the mRNA transcript because its target threshold (red) is higher indicating an increased number of cycles required for the fluorescent signal to rise above background

2.5.6 qPCR data analysis.

qPCR data was analyzed using the *delta delta Ct method* (ΔΔct) to quantify fold change between control and test sample. The mean cycle threshold (Ct) of the triplicate, normalized against housekeeping gene GAPDH, as well as normalization against control sample of the same gene represented fold change in expression. The

formula to normalize against housekeeping gene (control) and normalizing against control sample gene used:

= mean of test Ct – mean of control Ct (ΔCt),

= ΔCt of test gene – ΔCt of control gene (ΔΔct).

= 2^-(ΔΔct)

= Fold change

2.6 Cell cycle measurements with flow cytometry

2.6.1 Preparing samples for cell cycle analysis.

The BD cell cycle analysis kit was used (cat # BD/340242, Becton Dickinson, New Jersey, USA). Post cell culture, cells were trypsinised, centrifuged and counted using automated cell counter. Cell concentration was maintained at 1 million cells /ml. 500 µl of cell cycle buffer was used to wash the cells twice followed by staining with Solution A, B and C according to manufacturer's guidelines.

Cells were pelleted down to the concentration of $1x10^6$ /ml. 250 µl of solution A (*trypsin in a spermine tetrahydrochloride detergent buffer*) was added and mixed gently and incubated for 10 min at RT. 200 µl of solution B (*trypsin inhibitor and ribonuclease A in citrate-stabilizing buffer with spermine tetrahydrochloride*) was added to the existing mix and incubated at RT for 10 min after gentle mixing. Finally, 200 µl of solution C (*Propidium Iodide (PI) and spermine tetrahydrochloride in citrate stabilizing buffer*) was added and incubated for 10 min at 4˚C in the dark. The sample was then used for analysis.

2.6.2 Description of instrumentation used for Flow cytometry.

The BD FACSAria II flow cytometer is a high-speed fixed-alignment benchtop cell sorter, equipped with 488 nm, 633 nm and 405 nm solid state lasers for fluorochrome excitation, for the simultaneous analysis of up to 9 fluorescent markers and two scatter parameters, forward scatter (FSC) and side scatter (SSC). Acquisition

and BD FACSAria II cytometer functions are performed and controlled by BD FACSDiva v8.1 software.

The cell sorter employs detector arrays with photomultiplier tubes (PMTs) and a photodiode detector to detect and amplify signal. An octagon detector array contains six PMTs that detect SSC and up to five fluorescence signals excited by the blue laser. The trigon arrays contain two PMTs to detect fluorescence signals excited by the red and violet lasers, respectively. The FSC signal is detected by the photodiode detector. The PMTs convert photons into electrical pulses, which are subsequently processed by the electronics system and converted into visual data.

The flow cytometric acquisition was performed at the Central Analytical Facilities (CAF) Fluorescent Imaging Unit, Stellenbosch University. Cell samples were analyzed on the BD FACSAria IIu flow cytometer (BD Biosciences, San Jose, USA) using BD FACSDiva™ version 8.1 software for data acquisition and analysis. The light path, filters, detectors for the instrument are detailed in Table 2.3. The propidium iodide (PI) dye was excited by the 488 nm laser and the fluorescence detected in the 595 long pass filter and 610/20 band pass filter. The sample tubes were resuspended by vortexing for 5 seconds before acquisition. . For data acquisition, a minimum of 50 000 gated, singlet events were collected for each sample tube. Data was further analysed using FlowJo™ v10.4.1

Table 2.8 Detectors, Parameters and Filters on BD FACSAria IIu

Laser	Detector	Parameter	Long Pass Filter	Band Pass Filter	Amplification type
	SSC	SSC	n/a	488/10	Linear
Blue	**488-C**	**PE-Texas Red**	**595**	**610/20**	**Log**
488nm	488-B	PerCP Cy5.5	655	695/40	Log
Red	633-B	APC-Cy7	755	780/60	Log
633nm	633-A	APC	n/a	660/20	Log
Violet	405-B	Brilliant Violet 421	502	450/40	Log
407nm	405-A	Alexa Fluor 430	n/a	530/30	Log

Legend:

SSC – Side Scatter

APC – Allophycocyanin

Log – Logarithmic

2.6.3 Gating strategy for Cell Cycle analysis

Figure 2.7 (Ungated), 2.8 (Live cell gating) and 2.9 (Gated) illustrates the gating strategy employed for cell cycle analysis of PHMs. A forward scatter (FSC) versus side scatter (SSC) dot plot distinguished cells from debris. Within the cell gate, singlets were gated using the fluorescent channel, PE-Texas Red, to detect PI staining. Thereafter, gates were created to identify the various stages of cell cycle, namely G_0/G_1, S-phase and G_2/M. To gate live cells separately from debris, proliferative control samples were employed as gating controls. To gate different phases of cell cycle, a quiescent sample was used as gating control to distinguish sub-populations. After bulk gating, the gates were checked and adjusted manually for each sample. All data was exported to Microsoft Excel 2016 for further analysis.

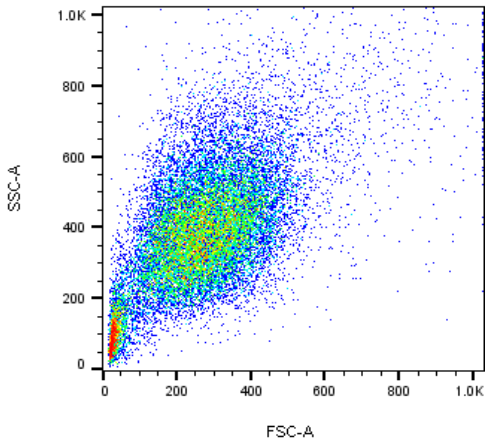

Figure 2.7 Representation of flow data before gating

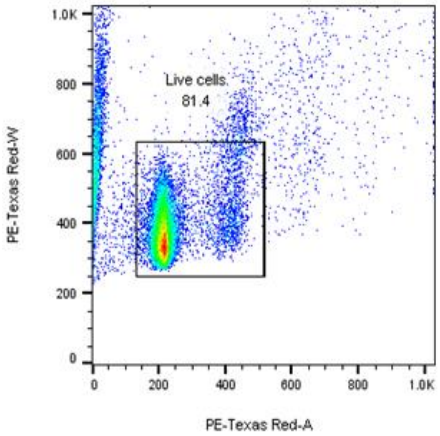

Figure 2.8 Representation of live cell gating

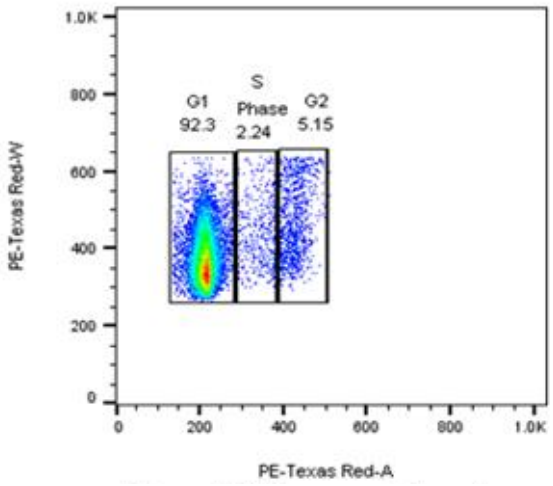

Figure 2.9 *Representation of gated image in G_1, S and G_2 phase*

Chapter 3: Establishing the Comparative Index.

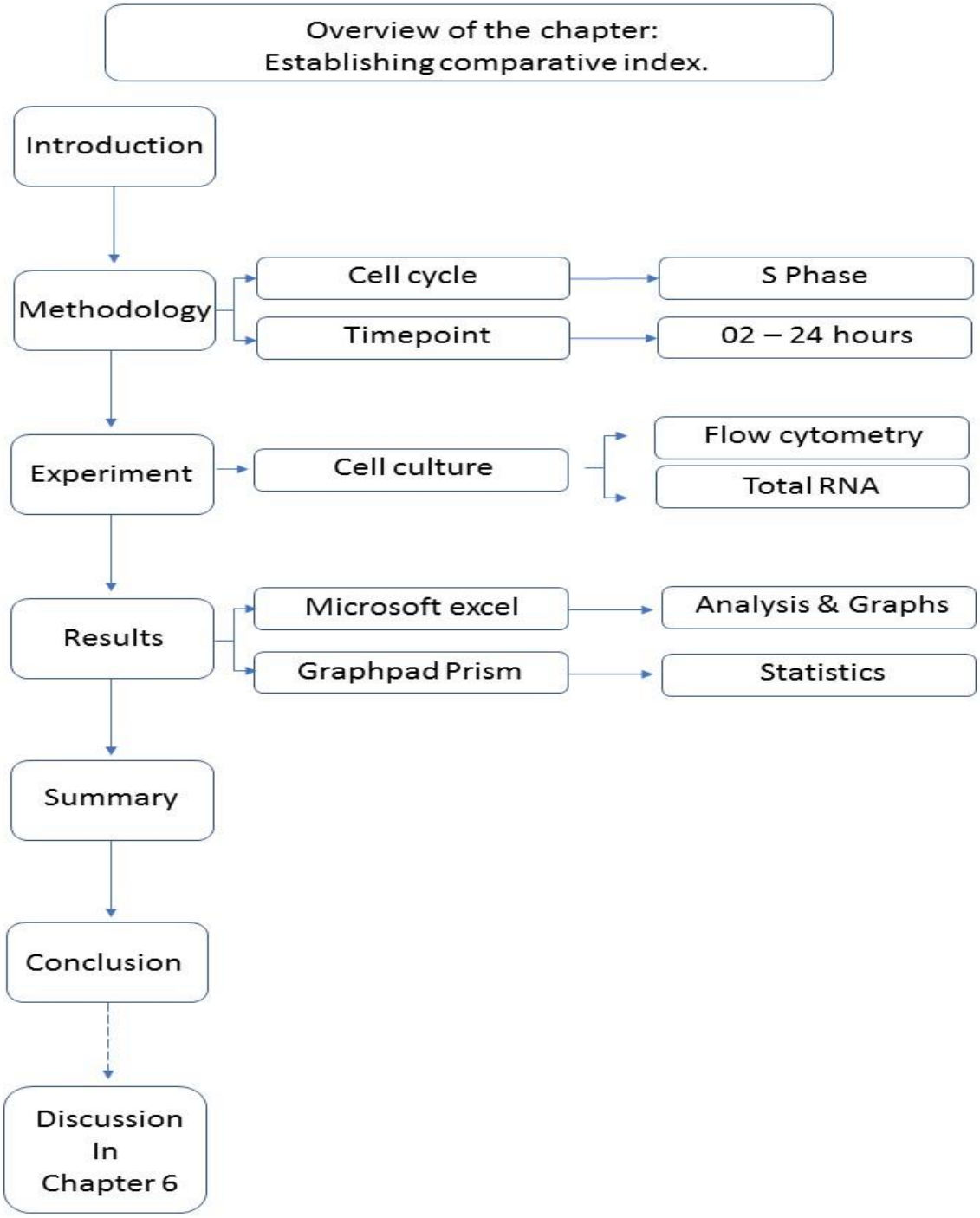

3.1 Introduction

The comparative index was established as a tool to compare primary cells' rate of proliferation. Primary cells are isolated from living donors. As previously discussed, conditions prior to tissue harvesting and cell isolation may cause variation in the behaviour of primary cells isolated from different individuals even with no experimental intervention. Therefore, comparison is essential when cells are harvested from multiple donors. Understanding the differences in cell characteristics would help to establish a baseline from which further evaluations can be assessed considering inherent variability. However, no clearly defined protocols exist to quantify primary cells' characteristic behaviour *in vitro.*

The eukaryotic cell cycle can be broadly divided into 4 distinct phases namely G_1 (Gap_1 phase), S phase (synthesis phase), G_2 (Gap_2 phase) and M phase (mitosis phase) [84]. Division of cells in culture can vary significantly depending on the type of cell. In the initial phase of G_1, activation of the Cdk complex initiates the accumulation of M-cyclin for mitosis [85]. Since the transition from G_1 to S phase represents a big change in transcription of genes. Therefore, the total RNA isolated at the corresponding timepoint can be used as a marker of the proliferative capacity of the cell.

Therefore, the comparative index was developed using cell cycle progression and total RNA quantification. Cell phase was used as a marker whilst the objectively quantifiable parameter, total RNA, was used as a comparison. Since large quantities of mRNA for downstream applications can be isolated after G_1, the "S" phase of the cell cycle was targeted as the marker.

When performing *in vitro* experiments, during which cells are exposed to treatments that affect the cellular function at the genomic and protein level, a key aspect influencing their responses could be the timing of treatment.

3.2 Hypothesis

Understanding that cells require generation of mRNA and progression through the cell cycle to proliferate, the hypothesis was: estimating the percentage of progression of cells from G_0/G_1 to S phase and quantifying the amount of RNA generated during the same period of time, could assist in comparing the rate of proliferation of the different PHM clones and establishing comparative index.

3.3 Methodology

Cell cycle progression is an integral part of any proliferating cell. A proliferating human cell with complete cell cycle time of about 24 hours spends roughly 11 hours in G1 phase followed by 8 hours of S phase and finally about 5 hours which includes G2 and M phase [84]. RNA synthesis varies during different phases.

3.3.1 PHM isolation and culture

PHMs isolated from skeletal muscle biopsies of two young (21,23 yrs) and healthy male subjects were compared: S6 and S9. PHMs were isolated from *vastus lateralis* tissue biopsy of the left thigh. Both samples were isolated separately with the same protocol as previously described (Chapter 2.3.2.1). PHMs were allowed to migrate off incubated explants of the biopsies for the initial harvesting after 5 days depending on the confluency. Incubation was done 3 times for S6, each time replating the same explant in a new well, resulting in a stock of PHMs called S6.3, whereas one incubation was sufficient to harvest PHMs from S9, resulting in a stock called S9.1.

Figure 3.1 A Representative image of cell migration from incubated explants, 3 days after plating.

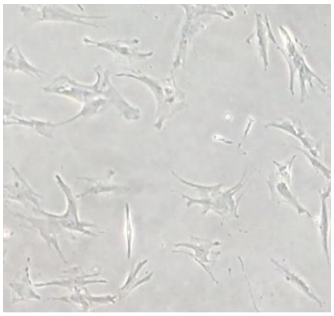

Figure 3.1 B Representative image of isolated primary cells, 10 days after plating.

The primary stock was frozen down in aliquots at passage 2. For experiments in this chapter, 1 aliquot was thawed and cells were plated in a T75 flask with proliferation media for expansion. Thereafter, 100,000 cells were plated in 12 individual T25 flasks coated with ECL. After about 4 days of culture with media change every 2 days, cells reached 70% confluency (~550,000 cells). The PHMs in each individual T25 flask were trypsinised, counted (using an automated cell counter) and 500 000 cells were replated into a new T25 flask. A 2-hour interval was left between each flask. The cells were left for 24 hours from the start of the replating of the first flask, resulting in 12 flasks where cells were plated for different lengths of time ranging from 2 – 24 hours. At the end of 2-24 hours of culture (12 flasks), cells from all flasks were harvested into separate tubes (15 ml falcon (Sigma Aldrich)), PHMs were counted using an automated cell counter (Thermo Fisher Scientific, USA).

3.3.2 Cell analysis

Total RNA was isolated from cell lysates of 250,000 cells (measured using an automated cell counter) using the Tripure Chloroform-isopropanol method (see chapter 2.4.4 for detailed method). The remainder of the cells were used for cell cycle analysis. PHMs were stained with PI (see chapter 2.6.1 for detailed method), prior to cell cycle analysis which was done using flow cytometry to distinguish different cell cycle phases.

3.3.3 Statistics and data representation

Statistical analysis was done on triplicates comparing all time points and included unpaired student's T-tests and two-way ANOVA where appropriate with Bonferroni post-hoc tests (GraphPad Prism 7).

3.4 Results

Data comparing the percentage of cells in S phase at different timepoints for S6.3 are presented in Figure 3.2 and total RNA for S6.3 in Figure 3.3. Similarly, for S9.1, data are presented in Figure 3.4 and 3.5 respectively.

PHMs from clone S6.3 had the peak number of cells in S phase (~23%) and total mRNA concentration (8933 ng) at 22 hours. In contrast, S9.1 had far fewer PHMs in transition to S phase between 2 and 22 hours (only 14%). Compared to S6.3, the total mRNA content was also lower (6418 ng) at 22 hours ($p<0.0005$ for S phase concentration) ($p<0.005$ for total RNA concentration).

Trendline analysis of both PHMs indicate that the proportion of cells in the S phase follows an exponential increase over time (Fig 3.2, 3.4). The r^2 values (adjusted to 4 decimals) of S phase data for S6.3 and S9.1 were 0.8702 and 0.9472 respectively. However, increases in total RNA, fit a linear trend for both (Fig 3.3, 3.5). The r^2 value (adjusted to 4 decimals) for total RNA were 0.872 and 0.9703 respectively.

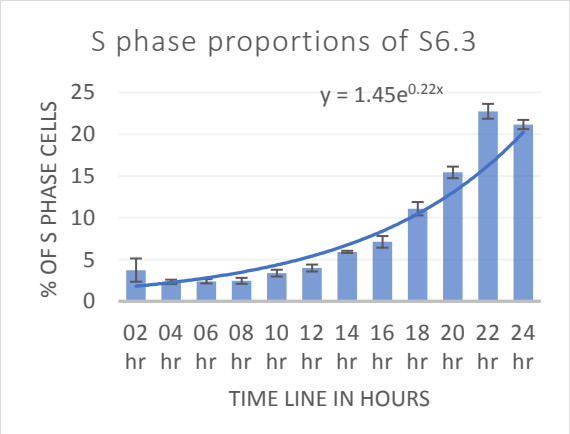

Figure 3.2 Trend line analysis of S phase of S6.3's PHMs following replating.(n=3, r2 = 0.87)

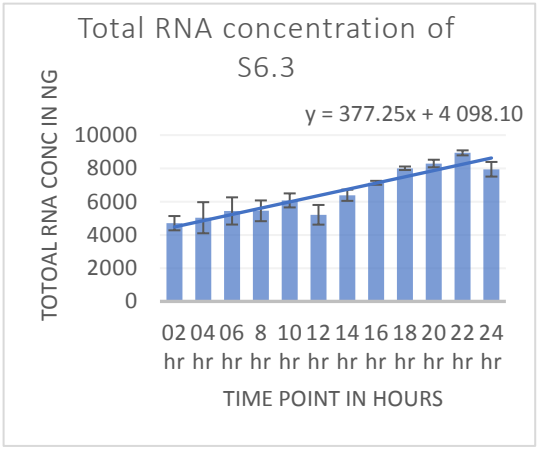

Figure 3.3 Trend line analysis of S6.3's RNA concentration following replating.(n=3, r2 = 0.87)

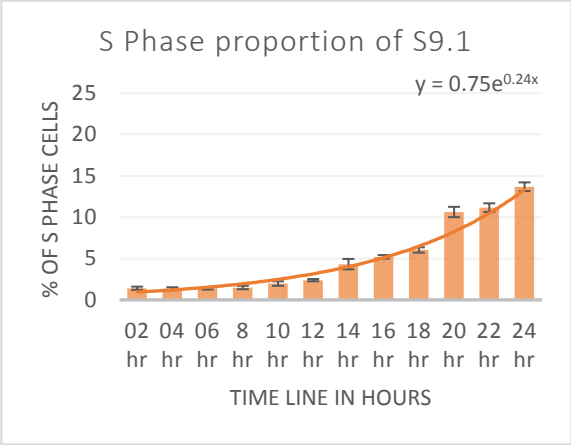

Figure 3.4 Trend line analysis of S phase of S9.1's PHMs following replating. (n=3, r2 = 0.95)

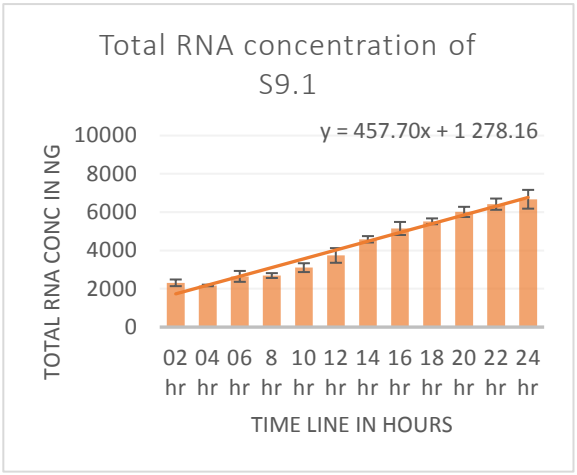

Figure 3.5 Trend line analysis of 9.1's RNA concentration following replating. (n=3, r2 = 0.97)

For statistical analysis comparing data of the two PHMs, see table A3.3 (in appendix) and Figures 3.6 and 3.7. S phase proportion over the 24-hour period indicated that S6.3's PHMs had a higher number of cells in S phase at almost all the time points (04,06,10,12,18,20,22,24) ($p < 0.0005$). Post hoc analysis indicated that, within statistically significantly time points, hour 22 was the most significant with $p < 0.0005$. Timepoints, hour 18 and 24 had the p value of <0.005 and rest of the early time points were seen with $p < 0.05$.

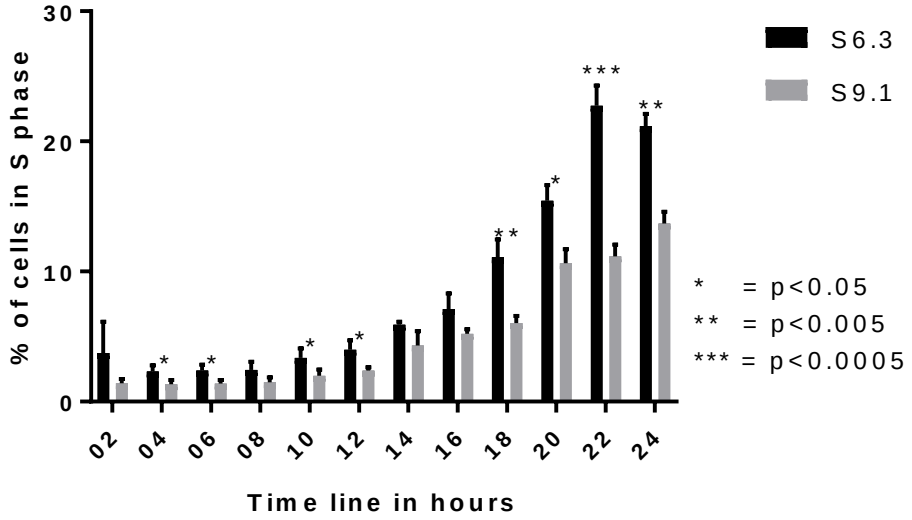

Figure 3.6 Comparison of S phase between S6.3 and S9.1 PHMs stained with PI. Results represent means ± SEM (n=3)

Similar to S phase cells in proportions, total RNA concentrations were consistently different between the two PHM clones over time. At the 02, 04, 06, 08, 10, 14, 16, 18, 20 and the 22-hour timepoints, S6.3's RNA concentrations were higher than S9.1 with p values ranging between $p<0.05$ to $p<0.005$. Here, the 18-hour timepoint was the most significant with $p<0.0005$, whereas hour 02, 10, 20, 22 had p value of <0.005 and the rest of the significant samples were different at the level of $p<0.05$

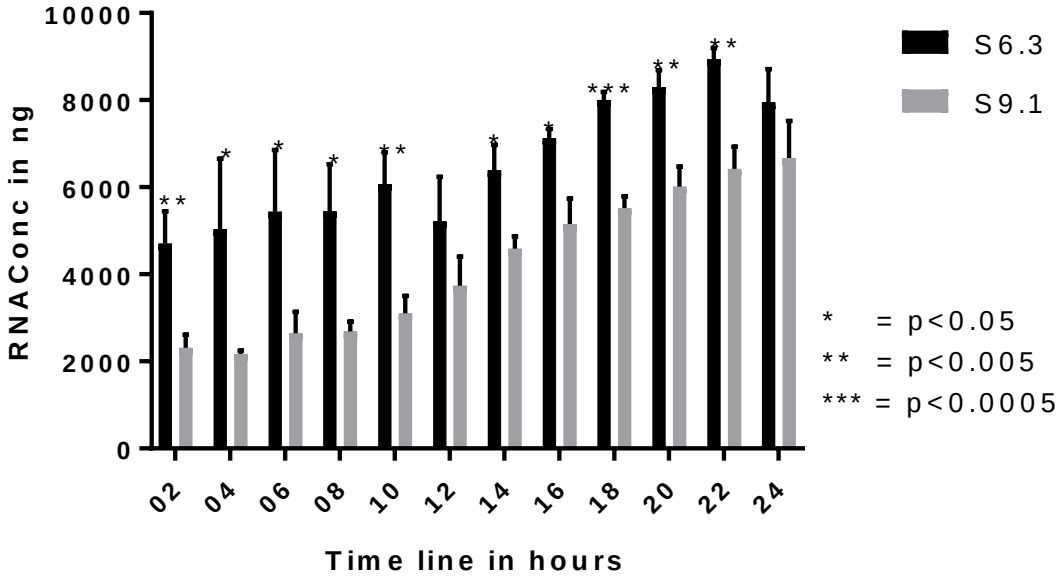

Figure 3.7 Comparison of total RNA concentration between S6.3 .and S9.1 PHMs. RNA was isolated using Phenol-Chloroform method. Results represent means ± SEM (n=3)

Not only quantitative analysis but also phenotypic differences between the PHMs were evident in actively proliferating cells. PHM clones of S6.3's appeared smaller in size compared to S9.1 even though the cells were of the same passage and culture time. While PHMs from S9.1 were larger and had closer interactions with other cells but were visibly fewer (see Fig 3.8, 3.9). However, clone S6.3 PHMs despite their smaller size, were greater in number.

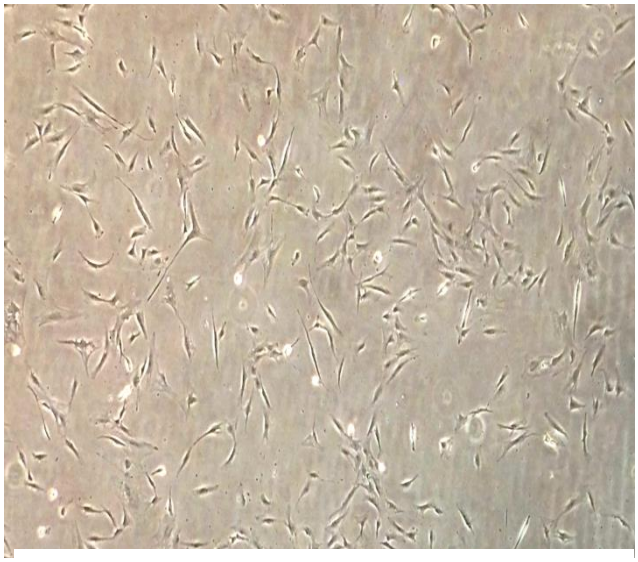

Figure 3.8 20x image of proliferating PHMs S6.3

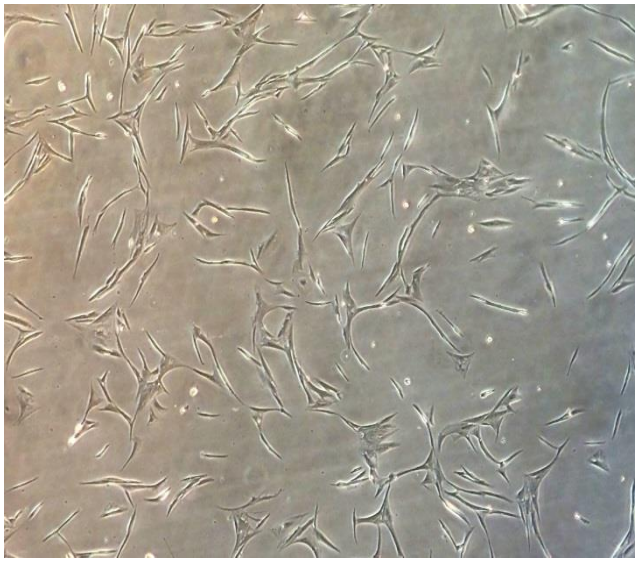

Figure 3.9 20x image of proliferating PHMs S9.1

3.5 Summary of results

This study sought to establish a protocol to use as a comparative index for primary human myoblasts taken from frozen stocks. Specifically, this study aimed to develop a protocol that could be used for quantification of differences in PHMs isolated from different donors.

Cell cycle data for both clones S6.3 and S9.1 illustrated an exponential transition from G1 phase to S phase over time. However, when comparing the rate of transition, it was evident that S9.1 PHMs were slower to transition compared to S6.3. For the majority of timepoints, S6.3's PHMs had a higher rate of entry into S phase

RNA concentration is higher when cells progress from G1 to S phase preparing for the upcoming translation and synthesis of multiple proteins [86]. Total RNA increased with similar linearity reflected by the rate constant in both PHM clones despite the different proportions of cells in S phase reflected by the intercepts. Differences in total RNA concentrations continued throughout the 24-hour time course for the majority of timepoints (10 out of 12), S6.3 PHMs had consistently and significantly higher concentrations of total RNA than S9.1.

Taking the two major findings together, comparison of S phase proportions and total RNA suggests that S9.1 PHMs had a slower rate of proliferation compared to S6.3.

The time course used to establish these differences was important to differentiate clone behaviour.

3.6 Calculating Index

3.6.1 Method 1 A

Since the S phase precedes mitosis and the preparation for mitosis requires more gene transcription and translation than to maintain cells in Go/G1, it was decided to use proportion of cells in S phase at a particular time point within the 24 hr duration of culture and the amount of total RNA present at this time to derive an Index. The data presented therefore includes comparison of both S phase proportion and total RNA at multiple time points by dividing the total RNA (numerator for the equation) by the % of cells (denominator for the equation) in S phase at the particular time point. Thereafter, the next part of this chapter sought to reduce this abundant information into an index.

The index number or the “comparative index” was calculated as the sum of all the calculations made for each time point. Given that in S-phase, mRNA is already being translated and therefore, total RNA would be reduced, the index can be interpreted in this way: higher index number represents slower rate of cell cycle progression with more cells not proceeding with translation, whereas lower index number represents faster translation of mRNA into protein and progression in cell cycle, when comparing the two clones.

Sum of all the S phase time points of clone S6.3 was 101.67 and the sum of total RNA of all time points was 78602.66 yielding the index number 773.12

Sum of all the S phase time points of clone S9.1 was 61.01 and the sum of total RNA of all time points was 51038.68 yielding the index number 836.56

Table 3.2 S phase proportion and total RNA concentration of S6.3 and S9.1 with calculation of comparative index using method 1 A for all the time points

Mean (n=3) S6.3				Mean (n=3)S9.1			
Duration	S phase	Total RNA	Comparative index	Duration	S Phase	Total RNA	Comparative index
	(%)	(ng)			(%)	(ng)	
Time-point (hr)				Time-point (Hr)			
02	3.73	4704.00	1261.13	02	1.41	2312.00	1639.71
04	2.32	5032.00	2168.97	04	1.35	2174.67	1610.87
06	2.39	5440.00	2276.15	06	1.39	2648.00	1905.04
08	2.45	5448.00	2223.67	08	1.49	2690.67	1805.82
10	3.37	6073.33	1802.18	10	1.98	3104.00	1567.68
12	3.98	5209.33	1308.88	12	2.38	3741.33	1571.99
14	5.91	6384.00	1080.20	14	4.32	4585.33	1061.42
16	7.11	7133.33	1003.28	16	5.20	5150.67	990.51
18	11.08	8006.67	722.62	18	6.03	5524.00	916.09
20	15.43	8292.00	537.39	20	10.63	6014.67	565.82
22	22.74	8933.33	392.85	22	11.15	6418.67	575.67
24	21.16	7946.67	375.55	24	13.68	6674.67	487.91
SUM	101.67	78602.66	773.12 (Calculated CI)		61.01	51038.68	836.56 (Calculated CI)

3.6.2 Method 1 B

However, viewing the Figures 3.2, 3.4, one can visualize there is no significant progression from G0/G1 towards S phase until the timepoint of 12 hours. If the 12-hour time point is taken as the base time point for starting to calculate the sum (Σ) 12-hour time point, then the difference between the comparative index calculated for each clone was increased from 63.45 to 119.98. In other words, using all time points (Method 1A) the index difference was 63, but using method 1 B, the difference was 119 suggesting better sensitivity. This in terms of physiological context suggests that initial 12 hours (for both the PHMs) was required to prepare the cells to start progressing through S phase.

Table 3.3 phase proportion and total RNA concentration of S6.3 and S9.1 with calculation of comparative index using method 1 B for the time point starting from 12 hours.

12	3.98	5209.33	1308.88		12	2.38	3741.33	1571.99
14	5.91	6384.00	1080.20		14	4.32	4585.33	1061.42
16	7.11	7133.33	1003.28		16	5.20	5150.67	990.51
18	11.08	8006.67	722.62		18	6.03	5524.00	916.07
20	15.43	8292.00	537.39		20	10.63	6014.67	565.82
22	22.74	8933.33	392.85		22	11.15	6418.67	575.67
24	21.16	7946.67	375.55		24	13.68	6674.67	487.91
SUM	87.41	51905.33	593.82			53.39	38109.34	713.79

3.6.3 Method 2 A

The index number or the “comparative index” for method 2 A was calculated by calculating the area under the curve using the trapezoidal rule, for the total RNA and the % of cells in S phase. The higher index number represents slower rate of cell cycle progression whereas lower index number represents faster rate of cell cycle progression when comparing 2 clones (see appendix table A3.4 for raw data and table A3.5 for calculations).

Area under the curve: using composite trapezoidal rule.

S phase proportion of S6.3 = 178.45

Total RNA concentration of S6.3 = 144554.65

Comparative Index => 144554.65/178.45 = 810.1

S phase proportion of S9.1 = 106.93

Total RNA concentration of S9.1 = 93090.69

Comparative Index =>93090.69/106.93 = 870.58

The comparative index represents S9.1's (870.58) rate of progression to S phase is slower compared to S6.3 (810.1)

Using this method, the difference between the two clones appeared narrower, similar to method 1A

3.6.4 Method 2 B

Applying the similar 12 hour time point rule for the area under the curve method resulted in a similar result to Method 1 B.

Area under the curve: using composite trapezoidal rule.

S phase proportion of S6.3 = 149.68

Total RNA concentration of S6.3 = 90654.66

Comparative Index => 90654.66/149.68 = 605.66

S phase proportion of S9.1 = 90.72

Total RNA concentration of S6.3 = 65802.68

Comparative Index => 65802.68/90.72 = 725.34

The comparative index indicates that S9.1's (725.34) rate of progression to S phase is slower compared to S6.3 (605.66)

3.6.5 Summary of the comparative index values.

Table 3. 1 Summerising the comparative index models.

Method	S 6.3	S phase	Total RNA	CI	S 9.1	S phase	Total RNA	CI	Fold change
1A	SUM	101.67	78602.66	773.12	SUM	61.01	51038.68	836.56	1:1.08
2A	SUM	178.45	144554.65	810.1	SUM	106.93	93090.69	870.58	1:1.08
1B	SUM	87.41	51905.33	593.82	SUM	53.39	38109.34	713.79	1:1.12
2B	SUM	149.68	90654.66	605.66	SUM	90.72	65802.68	725.34	1:1.12

3.6.5.1 Summary for calculation of Comparative Index

All the different methods tested here were options for a comparative index of the tested samples which also indicated differences between the two clones. Although Method 1 A and 2 A were true in mathematical terms, applying it to the physiological context is problematic. Two important reasons persuaded us to recommend Method 1 B and Method 2 B. a) The index values were further apart than 1 A or 2 A, thus possibly improving sensitivity in future comparisons of more clones. b) The physiological context appeared to be more relevant between clones from the 12-hour time. Hence, we propose to use Method 1 B or 2 B for all further calculations of comparative index.

3.7 Conclusion

The experiment was able to distinguish the rate of proliferation between clone S6.3 and S9.1.

Rate of proliferation between clones was calculated using two different methods with a proposal to use method 1B or 2B for further comparisons.

Clones S6.3 and 9.1 have similar lag phase, before the exponential shift from G_0/G_1 to S phase.

Chapter 4: Comparison of two quiescence protocols and development of a novel protocol to induce *in vitro* quiescence in Human Primary Myoblasts.

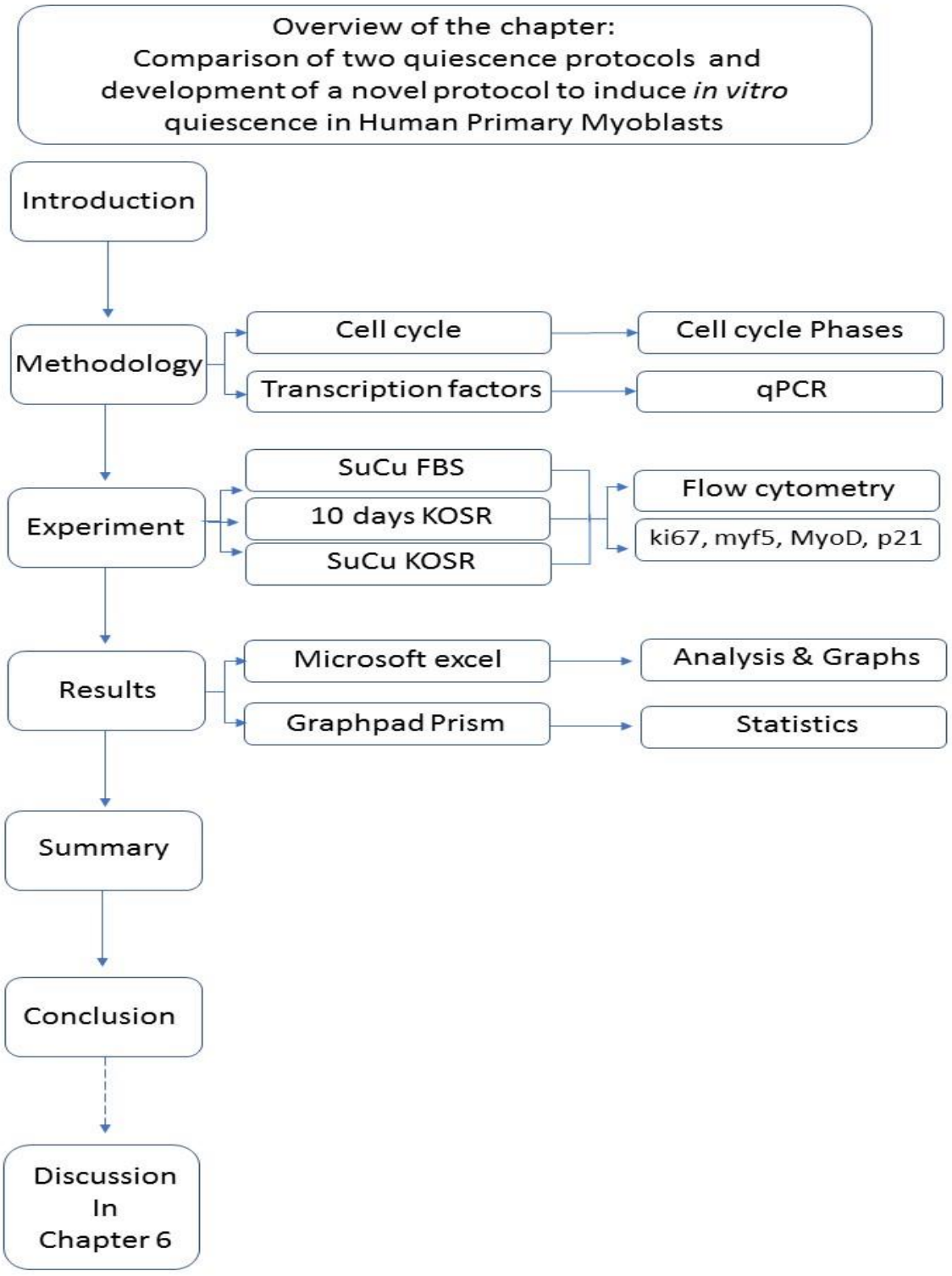

4.1 Introduction

Skeletal muscle has a tremendous ability to regenerate when an injury occurs. The timeline of skeletal muscle regeneration depends on the type and site of injury. The typical regeneration sequence begins within a few hours of injury and is completed in about three to four weeks. However, in the case of severe trauma, the time line could be longer than four weeks [87]. Initiation of regeneration is complex, but many of the responses serve to influence satellite cells [88] in various ways. In severe injuries, continued regeneration is dependent on a pool of satellite cells [89].

In vivo, in healthy uninjured skeletal muscles, satellite cells reside in a state of dormancy (quiescence). Following skeletal muscle injury, satellite cells are activated, proliferate and differentiate to aid the regeneration process. Differentiated satellite cells donate nuclei during fusion with damaged myofibers. A small portion of the active cells return to the G_0 state to restore the quiescent cell pool. To best mimic the *in vivo* environment, it is necessary to simulate reversible *in vitro* quiescence in cultured myoblasts.

"In vitro quiescence" is relatively a new concept [90]. As a result, there are a limited number of experimental protocols available. In this chapter, the first aim was to determine if *in vitro* quiescence could be achieved in the same myoblast clones using two different methods. Thereafter the aspects of the two different *in vitro* quiescence protocols were used for development of a novel "blended protocol".

4.1.1 Suspension culture induction of *in vitro* quiescence.

As mentioned in the introduction (chapter 1.2.1), in order for PHMs to proliferate *in vitro,* cells require cell to surface contact for anchoring and cell-to-cell contact for signalling. The original publication on *in* vitro quiescence induction was performed by depriving PHMs of these two factors using suspension culture (SuCu) for 48 hours [43]. This method showed that reversible cell cycle exit can be achieved using suspension culture containing 2% methyl cellulose that both provided a dense semi-solid medium which deprived the cells from settling to the bottom of the culture well, and kept them suspended in the medium. Uniform mixing of the cells with the suspension media also prevented cell to cell contact. The addition of 20% FBS

provides necessary cell culture growth factors so that quiescent cells can actually remain viable and subsequently re-enter cell cycle. This is the first protocol that will be demonstrated here.

4.1.2 KOSR culture induction of *in vitro* quiescence.

Other studies have induced quiescence in different cell types [91, 92]. In the field of embryonic stem cell biology xeno free media called KOSR has been used [93].

Recently, our research group showed that substitution of FBS with KOSR in the culture media without suspension and without growth factor supplementation induced quiescence in 10 days. That study confirmed that 95.6% of cells were in G_0/G_1 phase after 10 days. That study assessed both Pax7 and MyoD. The current study included additional markers including P21, a controller of quiescence, and Myf5, a promoter of self-renewal.

Whilst both protocols have previously been shown to result in effective quiescence after the intended periods, each one has its own limitations.

4.2 Pros and cons of the two individual protocols.

Firstly, SuCu with FBS is a relatively quick protocol nudging PHMs into the G_0/G_1 phase of the cell cycle within 48 hours. However, with SuCu the PHMs cannot be visualised using microscopy to assess the morphology while suspended in the methyl cellulose. Also, the protocol requires special training to achieve effective quiescence. Most importantly, soon after harvesting the cells from the suspension media, PHMs tend to become active [43].

The KOSR culture method, on the other hand, does not require any special training and morphology can be monitored throughout due to PHMs being adhered to a flask. The main limitations with this method are that 10 days are required to attain effective quiescence and the absence of growth factor supplementation does not effectively simulate *in vivo* conditions, even in the niche where satellite cells are quiescent [94].

Therefore, this chapter aimed to combine the two protocols in a novel “blended protocol” that would use the best features of each. An additional benefit might be that

improved quiescence, with reference to lower expression of cell proliferation gene and myogenic regulatory factors, could be achieved in a briefer time span than using KOSR alone.

4.3 Hypothesis

Considering that both SuCu and KOSR treatment results in quiescence, it was hypothesised that replacing the FBS component of the previously used SuCu method with KOSR, quiescence would be achieved within a relatively short period of time.

4.4 Brief Methodology

PHMs isolated from skeletal muscle biopsies of three young and healthy male subjects were harvested and assessed for myotube formation as previously described (Chapter 2.3.2). Two different types of SuCu media were prepared with either FBS or KOSR (chapter 2.1.4) After 48 hours of SuCu, PHMs were harvested using 1xPBS and 250,000 PHMs were used for total RNA isolation using the phenol-chloroform method (chapter 2.4.4) for qPCR analysis. qPCR was performed using Sybr Green dye (Applied biosystems StepOnePlus™ Thermofisher) to assess the gene expression on selected markers: ki67, myf5, MyoD and p21 (see chapter 2.5 for detailed methods). For cell cycle analysis, first 50,000 events were assessed.

Data reduction and analysis: Cell cycle data are presented as a percentage in a specific phase (%). qPCR data are presented as fold change relative to proliferation sample (n=3).

4.5 Results

Firstly, it was necessary to validate induction of cellular quiescence using the 10 day KOSR protocol. To this end, actively proliferating PHMs were harvested and compared to the KOSR method using flow cytometry and qPCR. Cell cycle analysis indicated that a large proportion (93.13%) of cells were arrested in G_0/G_1 state compared to that seen in the proliferating cells (Fig.4.1) while a significant decrease was noted in the S phase.

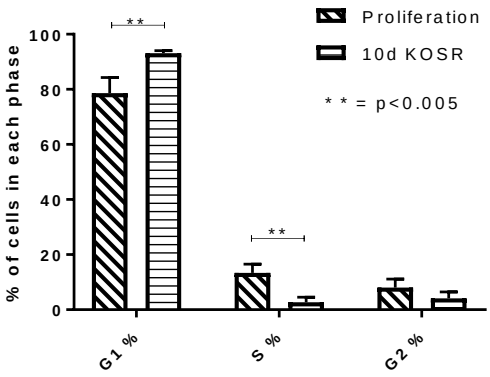

Figure 4.1 Comparison of PHMs (CloneKH3) proliferating vs in quiescence using flow cytometry to assess proportion of cells in G1, S and G2 phases of the cell cycle. The 10 days KOSR protocol was used to induce quiescence.

Due to activation of PHMs with harvesting from SuCu, cell cycle was not assessed in SuCu method. In contrast mRNA has a longer half-life thus able to reflect the pre-harvest conditions.

qPCR analysis on PHMs exposed to either KOSR or SuCu conditions was used to compare the gene expression of ki67, myf5, MyoD and p21. There were no differences in the expression of ki67, MyoD and p21, however myf5 expression was higher in cells cultured in KOSR (Fig 4.2).

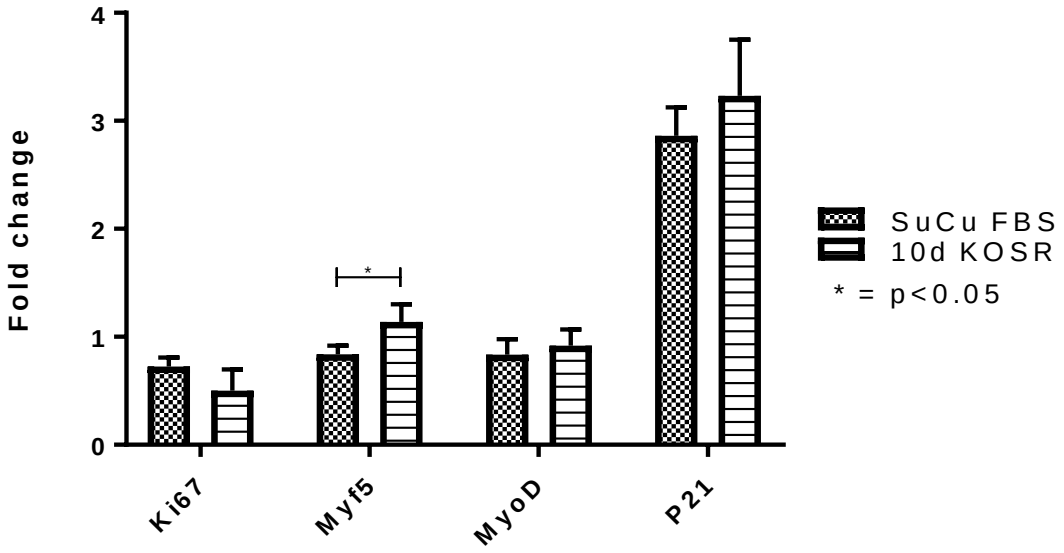

Figure 4.2 Expression of transcription factors influencing proliferation including myogenic regulatory factors in PHMs induced into *in vitro* quiescence with suspension culture (SuCu) and knock-out serum replacement (KOSR). Following induction of quiescence using 48 hour treatment in SuCu or 10 days in KOSR media, cells were harvested and gene expression quantified from isolated RNA. Results represent means ± SEM (n=3)

For the third condition, the expression of ki67, myf5, MyoD and p21 were quantified in PHMs treated with SuCu supplemented with either FBS or KOSR (Figure 4.3). Expression of ki67, myf5 and MyoD were significantly lower in PHMs treated in SuCu KOSR. However, there was no statistical difference in P21 gene expression, although the fold-change from control/non-quiescent cells was high in both groups.

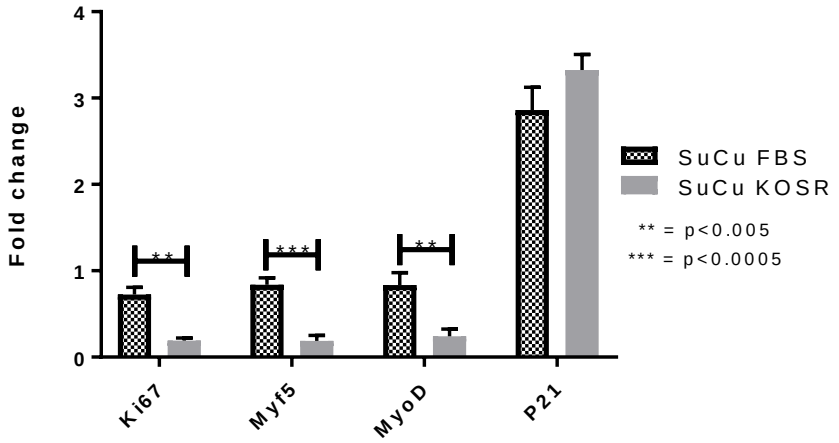

Figure 4.3 Expression of transcription factors influencing proliferation including myogenic regulatory factors in PHMs induced into *in vitro* quiescence with SuCu supplemented with FBS (SuCu FBS) or knock-out serum replacement (SuCu KOSR). Following induction of quiescence using 48 hour treatment in SuCu, cells were harvested and gene expression quantified from isolated RNA. Results represent means ± SEM (n=3)

To compare all three protocols (SuCu FBS, SuCu KOSR and 10d KOSR), the data from Figure 4.2 and 4.3 were merged (Fig 4.4) and suitable statistical test was performed (see legend of Fig 4.4). The novel blended protocol of replacing FBS with KOSR in SuCu (SuCu KOSR), resulted in the lowest relative expression levels of ki67, myf5 and MyoD among all three protocols. ki67 of SuCu KOSR was significantly lower than SuCu FBS (although not different from KOSR alone). myf5 and MyoD were significantly lower compared to both SuCu FBS and KOSR. p21 on the other hand was significantly upregulated in SuCu KOSR compared to SuCu FBS and no significant difference was observed compared to KOSR only.

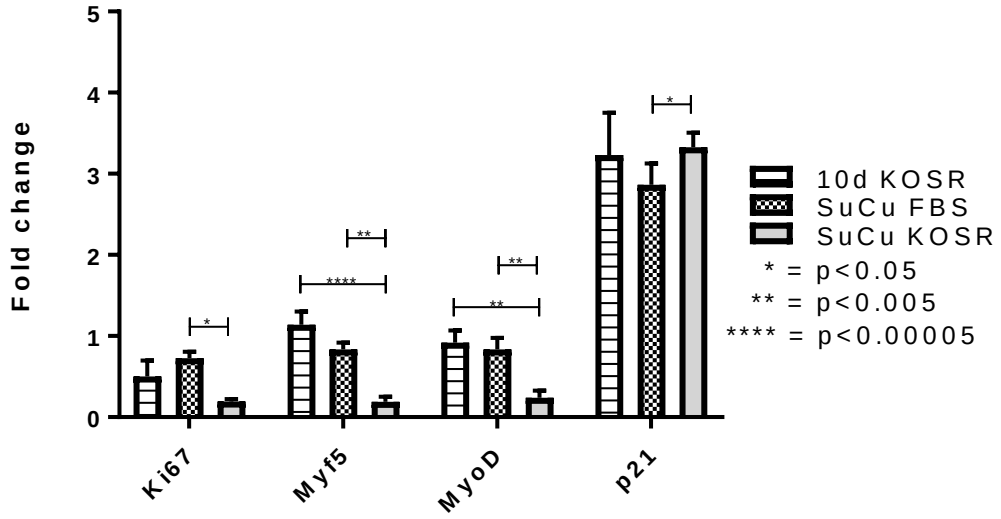

Figure 4.4 Comparison of KOSR, SuCu FBS, SuCu KOSR protocols in KH3. Expression levels of ki67, myf5, MyoD and p21. Results represent means ± SEM (n=3)

4.6 Summary

The 10 day KOSR protocol successfully altered the proportion of cells in the active phases of the cell cycle. When comparing the two individual protocols (SuCu FBS & 10 day KOSR), higher gene expression of myf5 was observed in 10 day KOSR. This may be indicating somewhat greater affinity towards myogenic lineage in 10 day KOSR compared to SuCu.

Expression of ki67 and MyoD were below 1-fold indicating that both protocols are effective in reducing factors that promote proliferation. Quiescence was achieved in a synchronous fashion since very high proportion of PHMs were in G_0/G_1 phase. The presence of methyl cellulose in the harvested cells from SuCu prevented cell cycle analysis in the SuCu sample.

Since p21 had an exceptionally high fold-change, it can be concluded that a major mechanism by which both protocols achieved synchronous quiescence *in vitro was* by inhibition of cell cycle.

The lowest expression of pro-proliferative markers and myogenic regulatory factors was in the blended protocol SuCu KOSR. This supports the hypothesis that substitution of FBS with KOSR in the SuCu protocol achieved quiescence to a greater extent.

4.7 Conclusion

The 10 day KOSR protocol resulted in high proportion of cells in the G_0/G_1 phase thereby inducing cellular quiescence.

The development of the SuCu KOSR method resulted in reduced ki67 expression indicating an improved reversal of proliferation was achieved using this blended quiescence protocol compared to either of the individual protocols.

Chapter 5. Effects of Fibroblast Growth Factors on quiescent PHMs

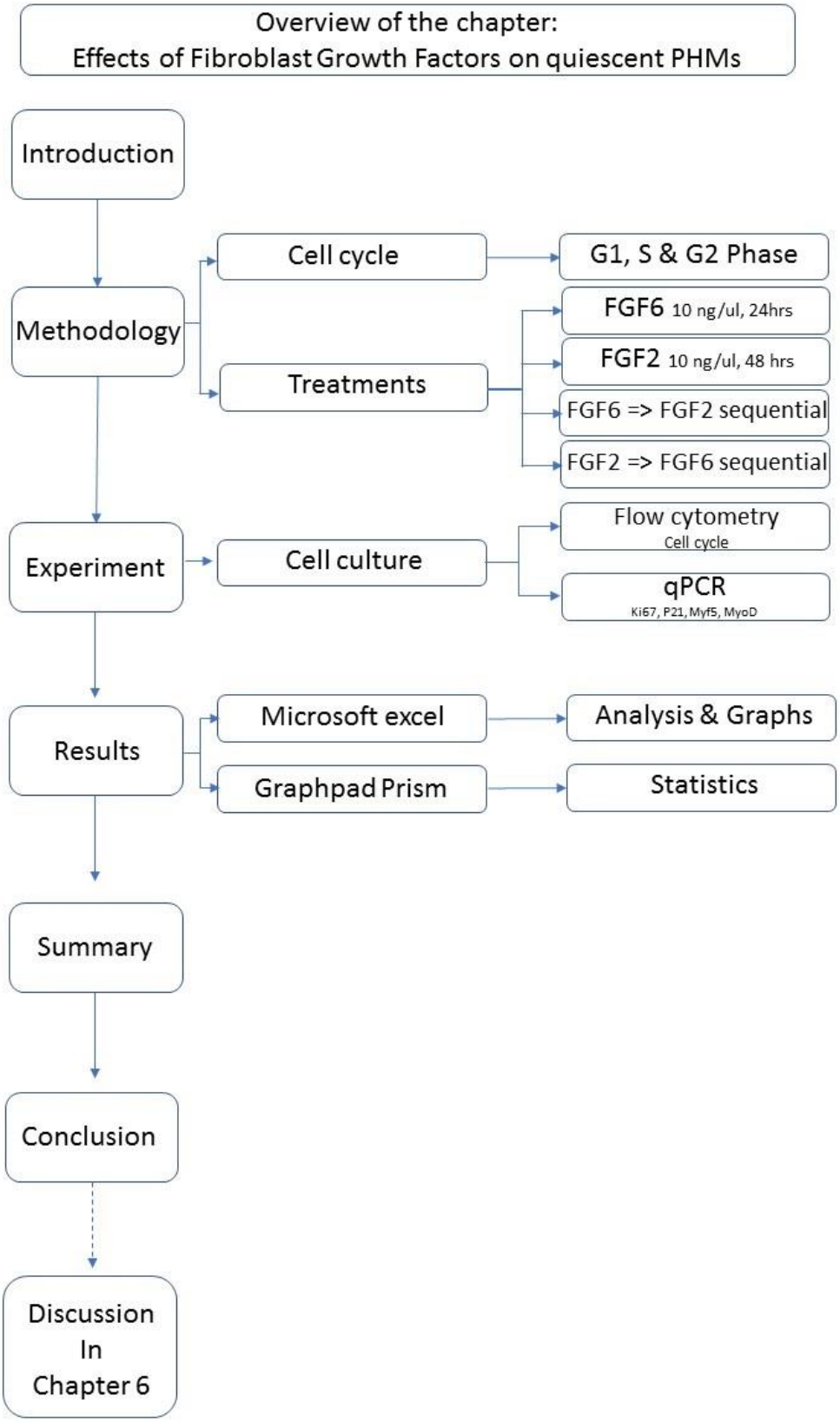

5.1 Introduction to Fibroblast Growth Factors (FGF 2 & 6).

The various FGFs are vital members of the growth factor super family which aid in embryonic and foetal development [95]. In humans, both during the postnatal growth phase and in adult tissue regeneration, the number of satellite cells play equally important roles [26]. FGFs are active in angiogenesis and promote cell proliferation and differentiation in a variety of cell types and are therefore critically important for typical multicellular development. Twenty-two different FGFs have been identified in the human genome [45]. FGFs bind to four receptors (FGFR1-FGFR4) with downstream signalling leading to altered gene expression.

Basic FGF or FGF-β is encoded by the FGF2 gene and hence also called FGF2. FGF2 is an 18 kDa 155 amino acid polypeptide which can bind to different FGF receptors for associated function [96]. It has been shown to be particularly highly expressed during embryonic development contributing to a number of developmental functions. Therefore, FGF2 is a common additive in human embryonic stem cell culture media as a mitogen as well as to maintain stem cells in a proliferative state [53, 97]. Tissue breakdown in the adult is frequently followed by embryonic + foetal programme for healing [98]. This ability of FGF2 to stimulate proliferation has resulted in clinical trials where it has not only been used in skeletal muscle but also in different tissue in relation to regeneration [99]. In myogenesis, FGF2 has been combined with different treatments to achieve effective regeneration resulting in clinical trials [100, 101]. Activation of the satellite cells using FGF6 is still biased [70, 102]. The current study used the application of both FGF2 and 6 to investigate effects on activation and subsequent proliferation of activated PHMs.

FGF6 and its primary function are less well understood compared to FGF2. FGF6 mouse homolog is found to be expressed predominantly in the myogenic lineage [103] and is suggested to be associated with the early stage of regeneration. This was investigated on satellite cells with contradictory evidence regarding FGF6-induced activation [26, 102] It is therefore worth further investigation.

5.1.1 Fibroblast Growth Factor 2 and 6 in adult wound healing context of myogenesis.

Due to the potential role that FGF6 has in cell activation and the involvement of FGF2 in proliferation, utilizing only one type of FGF might not be enough to optimally improve the regeneration process. Up to now, studies use FGF2 to promote proliferation of active cells, but have not specifically used any other agent to activate the quiescent cells. This may be because agents suspected to improve proliferation are added to cells that are already proliferating.

Experiments *in vitro* have used sequential exposure to FGF2, 9, 18 to aid chondrogenic differentiation of hMSCs [99].

Applying FGF6 to potentially activate quiescent myoblasts, followed by FGF2 to promote proliferation could be an attractive means of expanding PHMs in culture. However, the timing of the treatment may hold the key to initiate the particular myogenic events at the right time.

5.2 Hypothesis

Given the current understanding of the FGFs, it was hypothesized that: FGF6 could be used to initiate the activation process of the quiescent PHMs and FGF2 could enhance the proliferation of activated PHMs.

5.3 Aims

Given the current trend of FGF2 use in pre-clinical and clinical trials [55, 104], the first aim was to assess if FGF2 alone can activate the quiescent cells. The second aim was to determine if FGF6, not currently used, could activate the quiescent cells. Given the hypothesis that FGF6 is involved in activation and FGF2 in proliferation, the third aim was to test this sequentially and to compare this in the inverse order. Since data is already more available in the literature on FGF2, it was also decided to try the two FGF treatments in the reverse order, even though the hypothesis was that FGF6 activation followed by FGF2 for proliferation. This could assist in understanding the effect of FGF2 on quiescent cells.

Table 5. 1 Illestration of the proposed treatements with concentration and duration.

	Treatment 1	Treatment 2	Treatment 3	Treatment 4
Treatments	FGF6	FGF2	FGF6 =>FGF2	FGF2 =>FGF6
Concentration	10 ng/ml	10 ng/ml	10 ng/ml =>10 ng/ml	10 ng/ml =>10 ng/ml
Duration	24 hours	48 hours	24 => 48 hours	48 =>24 hours

Recognition of the ideal protocol for inducing quiescence for FGF experiments:

The blended protocol was better at inducing quiescence among the methods tested. However, the blended protocol still is limited by the inability to visualize cells during culture. Secondly, the treatments to be investigated may not have easy access to all the myoblasts in the viscus methyl cellulose solution. It was therefore decided that the 10 day KOSR method was used as the standard method to induce quiescence for the remainder of the thesis.

5.4 Experiment

The experimental design used three different PHM cell populations isolated from healthy donors. Since little is known regarding the myogenic response of PHMs to FGF6, a pilot study was done using 2.5, 5, 7.5, 10, 15 and 20 ng/ml to assess cell cycle proportions. Among these, two different doses of 5 ng/ml and 10 ng/ml were selected for further testing because cell death was observed at the low doses (according to live cell gating) and the higher doses did not appear to have any greater effect on cell cycle proportions than 10 ng/ml. After assessing RNA yield, 10 ng/ml was selected as the optimal treatment dosage, because 5 ng/ml resulted in lower RNA yield. FGF2 dosage was kept constant at 10 ng/ml in line with previous studies (Appendix Table A5.3 and A5.4)

Quiescence was induced in multiple clones of PHMs using the 10 day KOSR method (Chapter 4.5). The duration of the treatment was chosen depending on the type of

anticipated effect. Since FGF6 was a potential activation factor, a 24-hour treatment period was selected while the pro-proliferative FGF2 was administered to cells for 48 hours. For the sequential treatments, FGF6 was administered for 24 hours followed by FGF2 treatment for 48 hours and vice versa.

Analysis included flow cytometry for cell cycle analysis and qPCR gene expression of ki67, myf5, MyoD and p21. For details of the methods, reagents, primers and equipment see chapter 2.5.

Three different PHM clones isolated from three healthy individuals were statistically analysed using Graphphad Prism 7. Results are presented first as n=3 from each individual, thereafter those 3 data were averaged, and a statistical average was performed for PHMs from the three donor subjects (n=3).

5.5 Results

The results will be presented first on Flow cytometry for Cell cycle analysis followed by qPCR for gene expression.

Data reduction and analysis: Cell cycle data are presented as a proportion in a specific phase (%). qPCR data are presented as fold change relative to quiescent sample (n=3).

5.5.1 Flow cytometry

5.5.1.1 Cell cycle analysis of multiple PHM clones with FGF2 treatment.

Quiescent PHMs of three different individuals were treated with FGF2 10 ng/ml for 48 hours. Quiescent cells and FGF2 treated from each donor were compared.

Subject S6.3 did not show changes in cell proportions in any of the cell cycle phases following treatment, whereas PHMs from KH3 had decrease in the proportion of cells in the S phase only following treatment. The proportion of PHMs in the G_0/G_1 phase from KH1 was significantly decreased and G_2 phase significantly increased, with no change in S phase. Due to these inconsistent results, the individual mean and SEM values are provided for scrutiny in appendix (Table A5.1, A5.2)

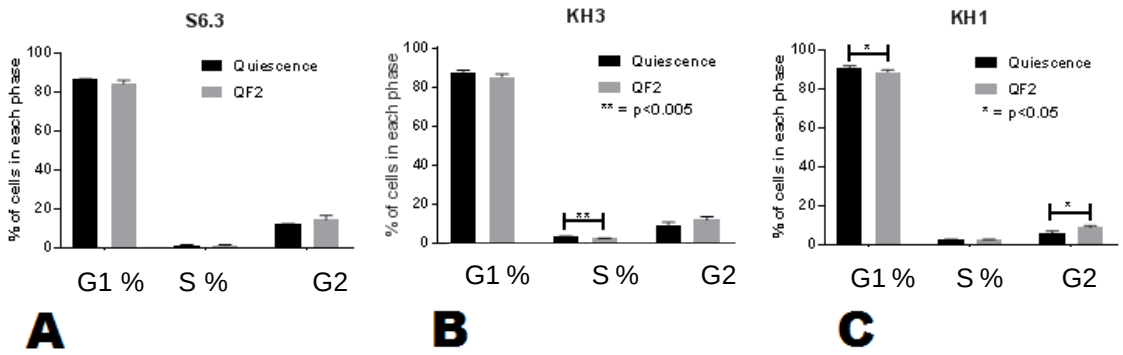

Figure 5.1 Cell cycle analysis of S6.3(A), KH3(B), KH1(C) PHMs, comparision of quiescence vs quiescence with FGF2 (QF2) treatment. PHMs were harvested and cell cycle analysis performed using PI stain. Results represent means ± SEM (n=3)

5.5.1.2 Cell cycle analysis of multiple PHM clones with FGF6 treatment

Next, quiescent PHM clones of the same three different individuals (S6.3, KH3 and KH1) were treated with FGF6 (10 ng/ml) for 24 hours.

Significant decreases in the proportions of cells in G_0/G_1 phase and significant increases in S phase were observed in cells from all donors (Figure 5.1 A, B, C).

A significant decrease in G_2 phase was also noted in subjects S6.3 and KH3. These data are more consistent compared to the responses of FGF2.

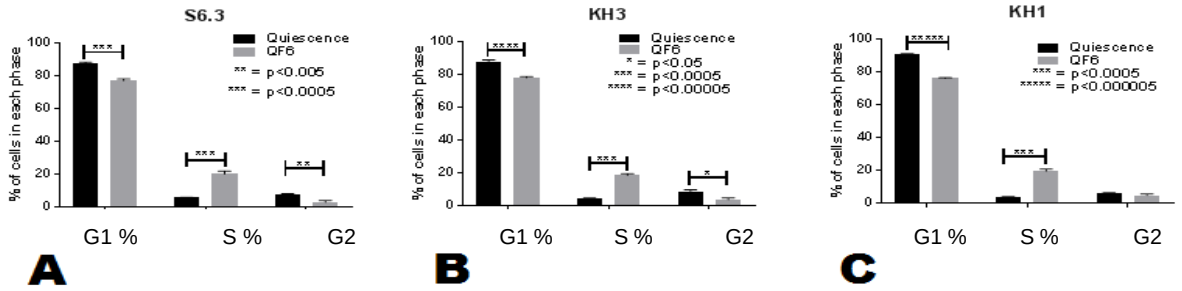

Figure 5.2 Cell cycle analysis of S6.3(A), KH3(B), KH1(C) PHMs, comparision of quiescence vs quiescence with FGF6 (QF6) treatment. PHMs were harvested and cell cycle analysis performed using PI stain. Results represent means ± SEM (n=3)

5.5.1.3 Cell cycle analysis of multiple PHM clones with sequential treatment of FGF6 followed by FGF2.

Comparison of quiescent PHMs with those treated with single FGF6 or sequential treatment of FGF6 and 2 is shown in Figure 5.3. Compared to quiescent cells of donor S6.3, PHMs had lower G_0/G_1 and G_2 phase proportions and a higher proportion in the S phase following treatment with FGF6 alone (Fig 5.3). Sequential treatment with FGF6 followed by FGF2 yielded the same results as FGF6 alone. In the S phase, both FGF6 and the combination treatment showed a significant increase in the proportion of cells compared to quiescence alone although the sequential treatment was less significant.

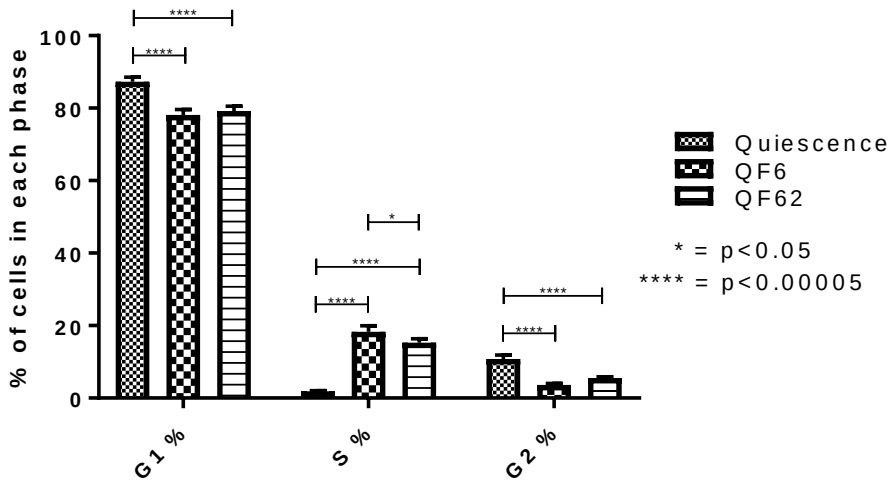

Figure 5.3 Cell cycle analysis of S6.3. Comparision of quiescence vs quiescence with FGF6 (QF6) vs quiescence with FGF6 followed by FGF2 (QF62) treatment. PHMs were harvested and cell cycle analysis performed using PI stain. Results represent means ± SEM (n=3)

Similarly, for clones of KH3 (Fig 5.4), compared to quiescent cells, PHMs had a lower G_0/G_1 phase proportion and was significantly increased in the S phase following treatment with FGF6 alone and sequential treatment. In contrast to S6.3, however, sequential treatment with FGF6 and 2 were different from each other in the G_0/G_1

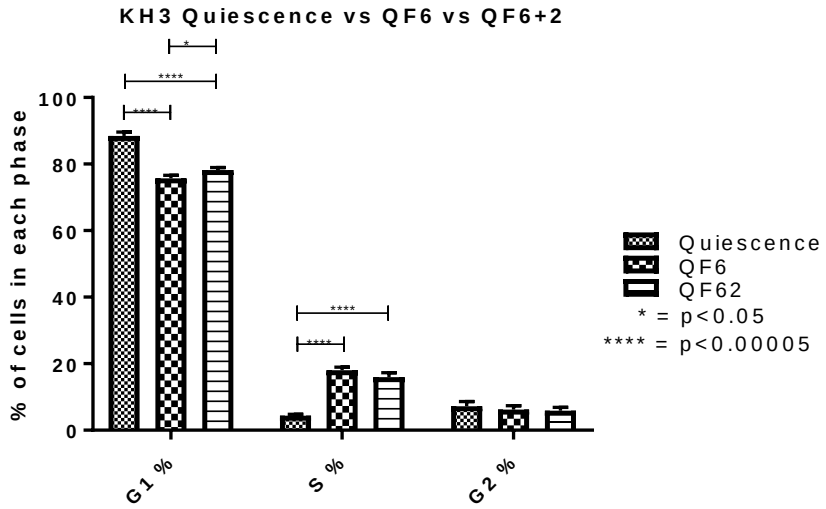

Figure 5.4 Cell cycle analysis of KH1. Comparision of quiescence vs quiescence with FGF6 (QF6) vs quiescence with FGF6 followed by FGF2 (QF62) treatment. PHMs were harvested and cell cycle analysis performed using PI stain. Results represent means ± SEM (n=3)

phase compared to FGF6 alone ($p<0.05$). There was no significant effect in the G_2 phase following either FGF6 treatment alone or sequential treatment (despite the significant difference when comparing only quiescence vs FGF6 Fig 5.2).

Cells from the KH1 clones, (Fig 5.5), when compared to quiescent cells responded similarly to the KH3 interventions. PHMs had a lower G_0/G_1 phase proportion and increases in the S phase following treatment with FGF6 alone and sequential treatment ($p<0.0005$). In contrast to clone S6.3 however, sequential treatment with FGF6 and 2 resulted in significantly higher proportion of cells in the G1 phase compared to FGF6 alone ($p<0.0005$). Similarly, to clone KH3, there was no significant effect on the G_2 phase following treatment with FGF6 alone and sequential treatment.

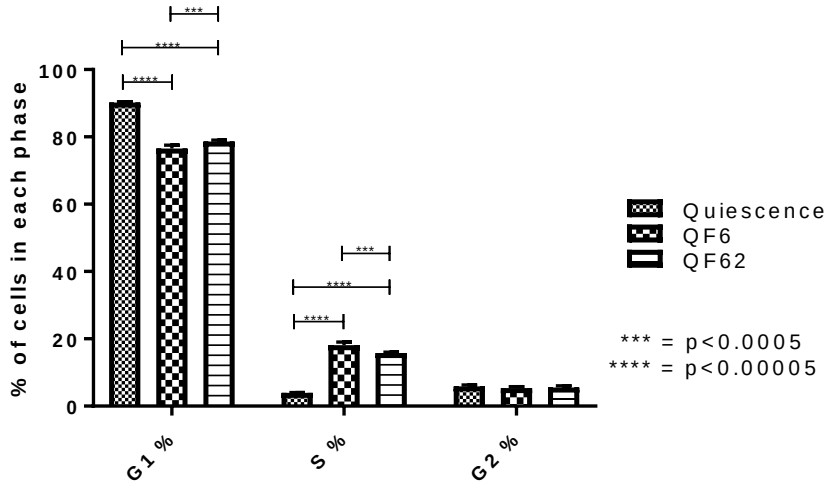

Figure 5.5 Cell cycle analysis of KH3. Comparision of quiescence vs quiescence with FGF6 (QF6) vs quiescence with FGF6 followed by FGF2 (QF62) treatment. PHMs were harvested and cell cycle analysis performed using PI stain. Results represent means ± SEM (n=3)

5.5.1.4 Cell cycle analysis of multiple PHMs with sequential treatment of FGF2 and FGF6.

PHMs from S6.3 treated with FGF2 alone showed no change in the proportion of cells in the G_0/G_1 and S phases compared to quiescent cells. There was however, an increase in the proportion of cells in the G_2 phase ($p<0.05$) (Fig 5.6).

Sequential treatment with FGF2 first and then FGF6, resulted in a decrease of cell proportions in the G_0/G_1 phase and an increase in the G_2 phase proportions compared to quiescent cells. This increase is somewhat more significant than that in PHMs treated with FGF2 alone ($p<0.005$) but only when compared to quiescence and not when compared to each other (Fig 5.6).

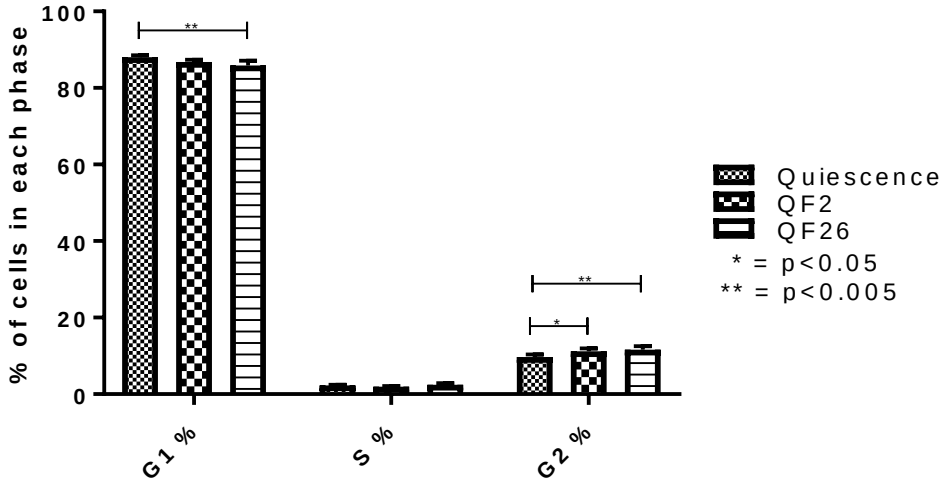

Figure 5.6 Cell cycle analysis of S6.3. Comparision of quiescence vs quiescence with FGF2 (QF2) vs quiescence with FGF2 followed by FGF6 (QF26) treatment. PHMs were harvested and cell cycle analysis performed using PI stain. Results represent means ± SEM (n=3)

PHMs from KH3 (Fig 5.7) responded to FGF2 treatment alone by decreasing the proportion of PHMs in the G_1 phase and increasing PHMs in the G_2 phase, compared to quiescent cells ($p<0.0005$ G_1, $p<0.005$ G_2). Sequential treatment with FGF2 and then FGF6, compared to quiescent cells, resulted in a decrease in cells in the G_1 phase and an increase in the both S and G_2 phase proportions ($p<0.00005$ G_1, $p<0.05$ S, $p<0.0005$ G_2). Sequential treatment resulted in a significantly lower proportion of cells in the G_1 phase only, compared to treatment with FGF2 alone.

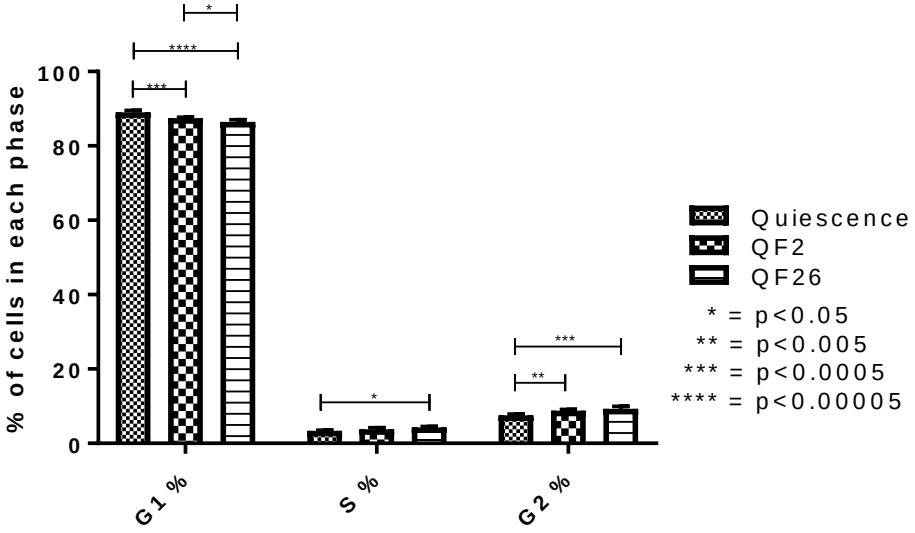

Figure 5.7 Cell cycle analysis of KH1. Comparision of quiescence vs quiescence with FGF2 (QF2) vs quiescence with FGF2 followed by FGF6 (QF26) treatment. PHMs were harvested and cell cycle analysis performed using PI stain. Results represent means ± SEM (n=3)

Essentially, when treated with FGF2 alone or with sequential treatment with FGF2 and FGF6, PHMs from KH1 (Fig 5.8) demonstrated similar changes to those found for KH3, although the levels of significance were slightly less. Compared to quiescent cells, the significant decrease for G_1 phase was subsequently increased in the G_2 phase. However, there were no differences for the S phase even for sequential treatment.

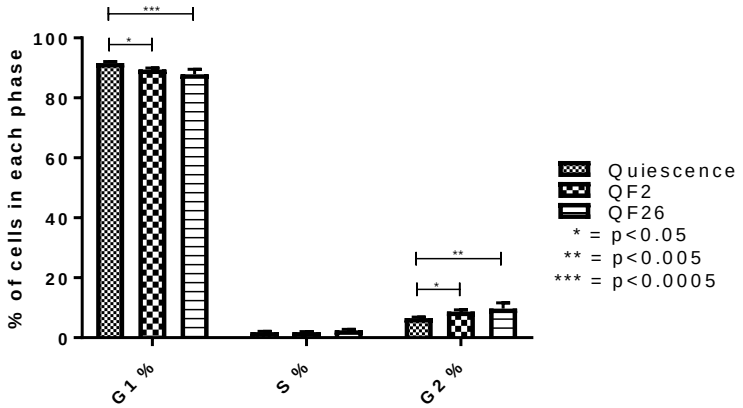

Figure 5.8 Cell cycle analysis of KH3. Comparision of quiescence vs quiescence with FGF2 (QF2) vs quiescence with FGF2 followed by FGF6 (QF26) treatment. PHMs were harvested and cell cycle analysis performed using PI stain. Results represent means ± SEM (n=3)

5.5.2 Gene expression.

Four markers were selected for qPCR analysis to address proliferation (ki67) myogenic regulation (myf5, MyoD) and cell cycle regulation (p21) in response to FGF6 or FGF2 treatments performed individually and in succession. Figure 5.9 to 5.16 are presented in such a way that the responses of the two different clones can be clearly seen. qPCR data is analysed using Δ ΔCT method.

Note: Towards the end of this chapter, in the summary section, a brief overview table and summary are provided with statistical significance of each treatment for easier understanding.

5.5.2.1 Comparison of ki67 expression with individual treatment of FGF6 and FGF2.

Treatment with FGF6 resulted in significant upregulation of the expression of ki67 in PHMs of subjects KH3 and KH1 whereas the smaller increase in S6.3 was not statistically significant compared to quiescent cells.

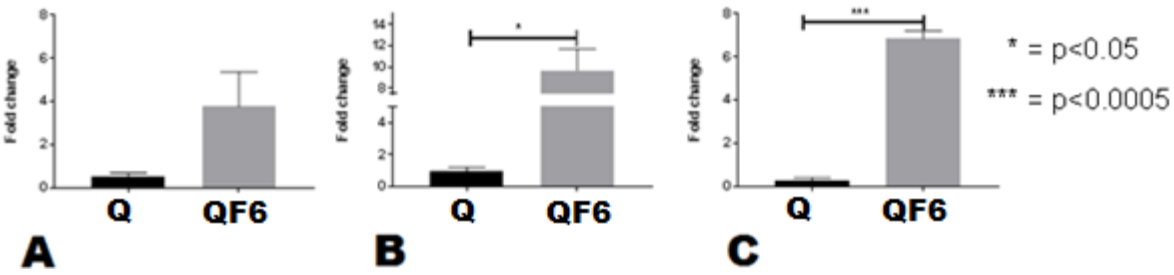

Figure 5.9 Expression of transcription factor ki67 in PHMs, S6.3(A), KH3(B), KH1(C) induced into *in vitro* quiescence with knock-out serum replacement (KOSR). Following induction of quiescence, FGF6 tretment was used for 48 hrs. Cells were harvested and gene expression quantified from isolated RNA. Results represent means ± SEM (n=3)

In contrast, treatment with FGF2 did not alter ki67 expression compared to quiescent cells.

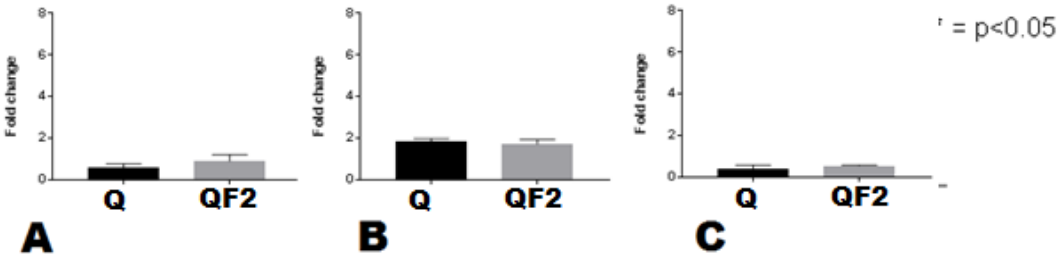

Figure 5.10 Expression of transcription factor ki67 in PHMs, S6.3(A), KH3(B), KH1(C) induced into *in vitro* quiescence with knock-out serum replacement (KOSR). Following induction of quiescence, FGF2 tretment was used for 48 hrs. Cells were harvested and gene expression quantified from isolated RNA. Results represent means ± SEM (n=3)

5.5.2.2 Comparison of p21 expression with individual treatment of FGF6 or FGF2.

Treatment with FGF6 resulted in a significant downregulation in p21 expression in PHMs from KH3 only ($p<0.05$), compared to quiescent cells. This result was the mirror image of the ki67 gene upregulation for KH3, but this was not the case for PHMs from KH1. S6.3 was downregulated however, not statistically significant with p value of 0.06, this can be attributed to the prominent variation levels obtained from the quiescent samples.

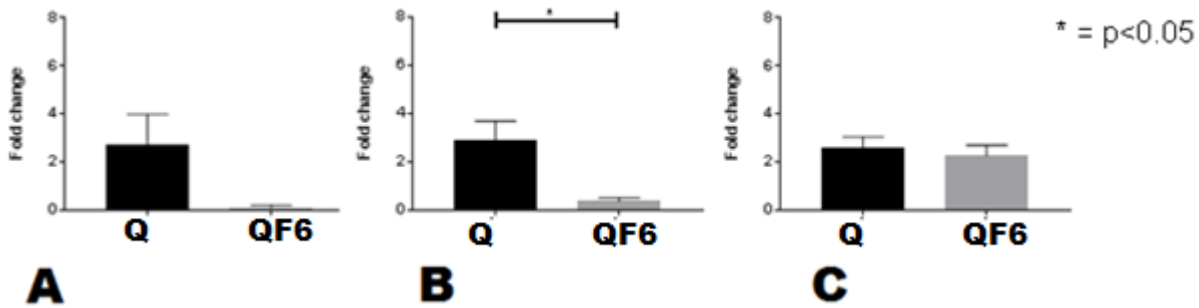

Figure 5.11 Expression of transcription factor p21 in PHMs, S6.3(A), KH3(B), KH1(C) induced into *in vitro* quiescence with knock-out serum replacement (KOSR). Following induction of quiescence, FGF6 tretment was used for 48 hrs. Cells were harvested and gene expression quantified from isolated RNA. Results represent means ± SEM (n=3)

Treatment with FGF2 resulted in downregulation of p21 in PHMs from S6.3 and KH3 ($p<0.05$).

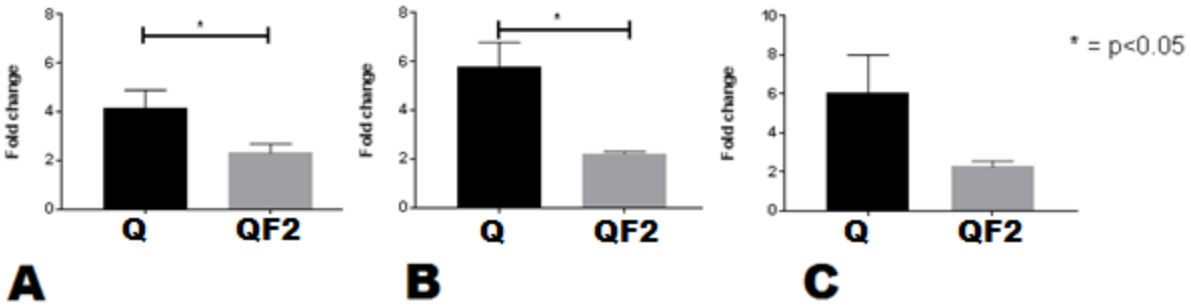

Figure 5.12 Expression of transcription factor p21 in PHMs, S6.3(A), KH3(B), KH1(C) induced into *in vitro* quiescence with knock-out serum replacement (KOSR). Following induction of quiescence, FGF2 tretment was used for 48 hrs. Cells were harvested and gene expression quantified from isolated RNA. Results represent means ± SEM (n=3)

5.5.2.3 Comparison of myf5 expression with individual treatment of FGF6 or FGF2.

Treatment with FGF6 resulted in significant upregulation of myf5 in S6.3 and KH1 PHMs ($p<0.05$) compared to quiescent cells, but this did not reach significance in KH3

Treatment with FGF2, resulted in upregulation in clone S6.3 only ($p<0.05$).

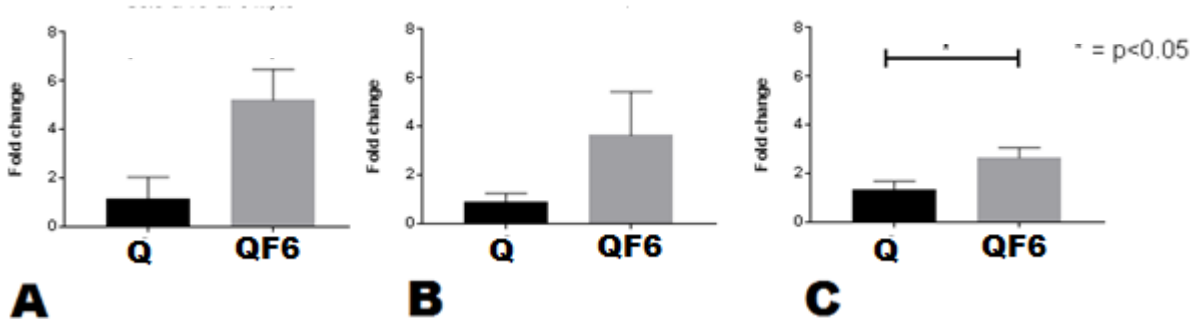

Figure 5.13 Expression of transcription factor myf5 in PHMs, S6.3(A), KH3(B), KH1(C) induced into *in vitro* quiescence with knock-out serum replacement (KOSR). Following induction of quiescence, FGF6 tretment was used for 48 hrs. Cells were harvested and gene expression quantified from isolated RNA. Results represent means ± SEM (n=3)

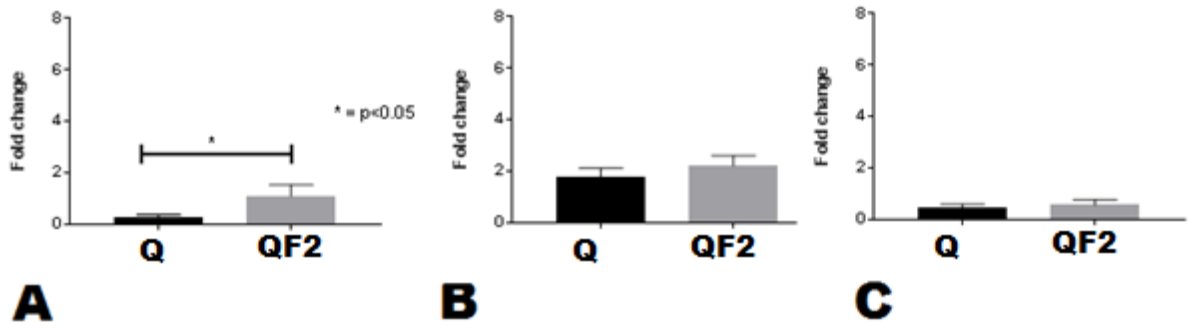

Figure 5.14 Expression of transcription factor myf5 in PHMs, S6.3(A), KH3(B), KH1(C) induced into *in vitro* quiescence with knock-out serum replacement (KOSR). Following induction of quiescence, FGF2 tretment was used for 48 hrs. Cells were harvested and gene expression quantified from isolated RNA. Results represent means ± SEM (n=3)

5.5.2.4 Comparison of MyoD expression with individual treatment of FGF6 or FGF2.

Treatment of FGF6 and FGF2 in all PHMs did not result in any significant changes in MyoD expression, compared to quiescent cells, except for upregulation in response to FGF6 in KH3 ($p<0.05$).

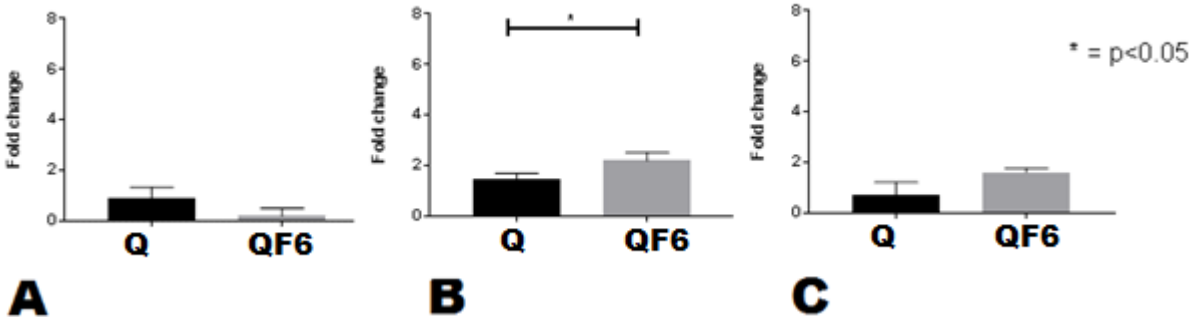

Figure 5.15 Expression of transcription factor MyoD in PHMs, S6.3(A), KH3(B), KH1(C) induced into *in vitro* quiescence with knock-out serum replacement (KOSR). Following induction of quiescence, FGF6 tretment was used for 48 hrs. Cells were harvested and gene expression quantified from isolated RNA. Results represent means ± SEM (n=3)

Treatment with FGF2, resulted in no significant upregulation of MyoD in any of the PHMs.

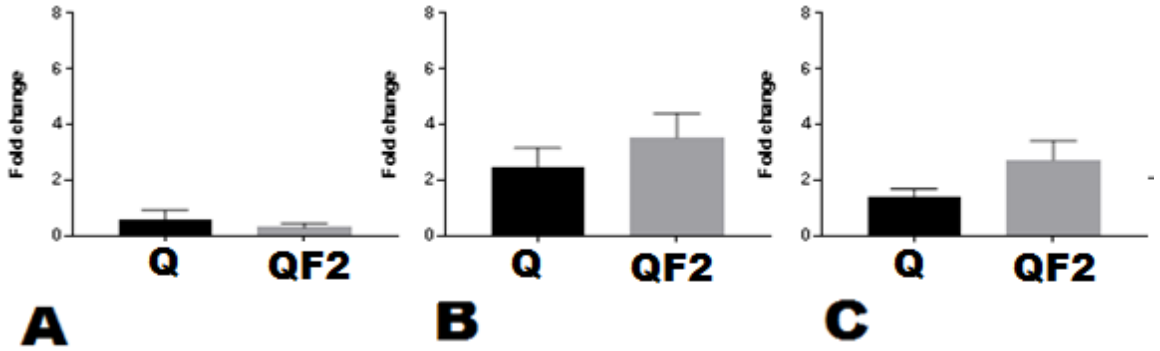

Figure 5.16 Expression of transcription factor MyoD in PHMs, S6.3(A), KH3(B), KH1(C) induced into *in vitro* quiescence with knock-out serum replacement (KOSR). Following induction of quiescence, FGF2 tretment was used for 48 hrs. Cells were harvested and gene expression quantified from isolated RNA. Results represent means ± SEM (n=3)

5.5.2.5 Gene expression of multiple selected markers with FGF6 treatment compared to sequential treatment of FGF6 followed by FGF2.

Next, we compared individual treatments to sequential treatment of FGF6 followed by FGF2. Figures 5.17 to 5.22 are presented so that the responses of each clone are visualised at one time, to facilitate visual comparison between the markers.

In S6.3 PHMs, sequential treatment of FGF6 followed by FGF2 resulted in lower expression of ki67 and myf5, compared to individual treatment of FGF6 where there was significant upregulation. The expression levels of ki67 and myf5 following sequential treatment was similar to that of quiescent cells, however MyoD was significantly upregulated compared to both quiescent cells and those treated with FGF6 alone ($p<0.00005$). The sequential treatment resulted in equivalent p21 expression levels to that of quiescent cells.

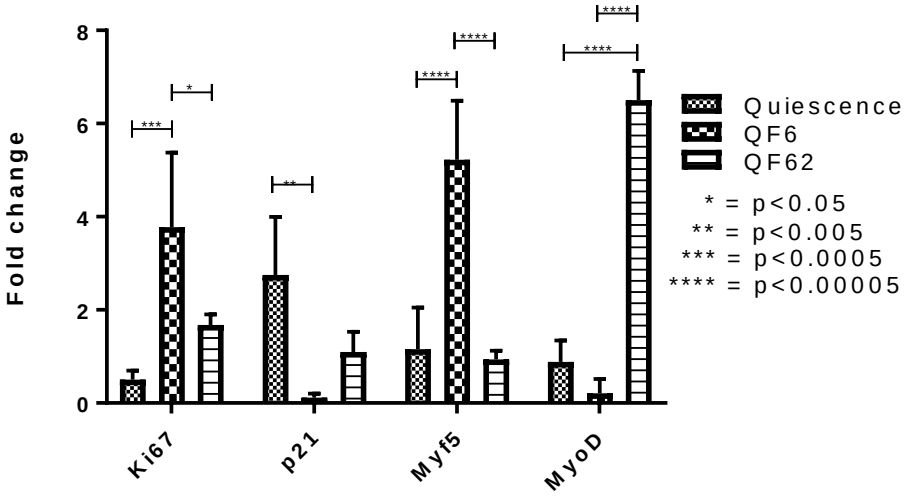

Figure 5.17 Expression of transcription factors influencing proliferation including myogenic regulatory factors in PHM S6.3, induced into *in vitro* quiescence knock-out serum replacement (KOSR). Following induction of quiescence, using 24 hrs treatment of FGF6 followed by 48 hrs of FGF2 in KOSR media, cells were harvested and gene expression quantified from isolated RNA. Results represent means ± SEM (n=3)

Similar to clone S6.3, in KH3 PHMs, ki67 and myf5 expressions for sequential treatments were lower than the FGF6 treatment alone. However, there was no significant effect of sequential treatment on MyoD or p21 expression following sequential treatment of FGF2 and 6 in this PHM clone.

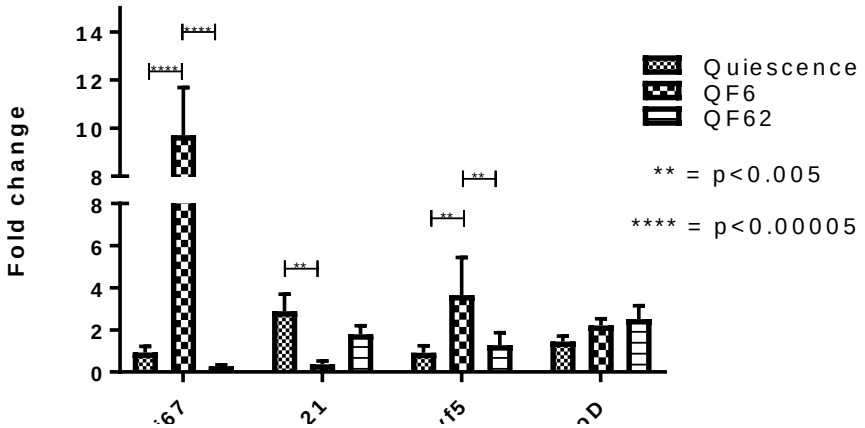

Figure 5.18 qPCR Expression of transcription factors influencing proliferation including myogenic regulatory factors in PHM KH1, induced into *in vitro* quiescence knock-out serum replacement (KOSR). Following induction of quiescence, using 24 hrs treatment of FGF6 followed by 48 hrs of FGF2 in KOSR media, cells were harvested and gene expression quantified from isolated RNA. Results represent means ± SEM (n=3)

Similar to clone S6.3 and KH3, in clone KH1, ki67 and myf5 expressions were lower than the FGF6 treatment alone. Similar to S6.3 but in contrast to KH3 however, MyoD expression was higher following sequential treatment. p21 gene expression was lower following sequential treatment compared to both quiescent cells and those treated with FGF6 alone ($p<0.05$, $p<0.0005$).

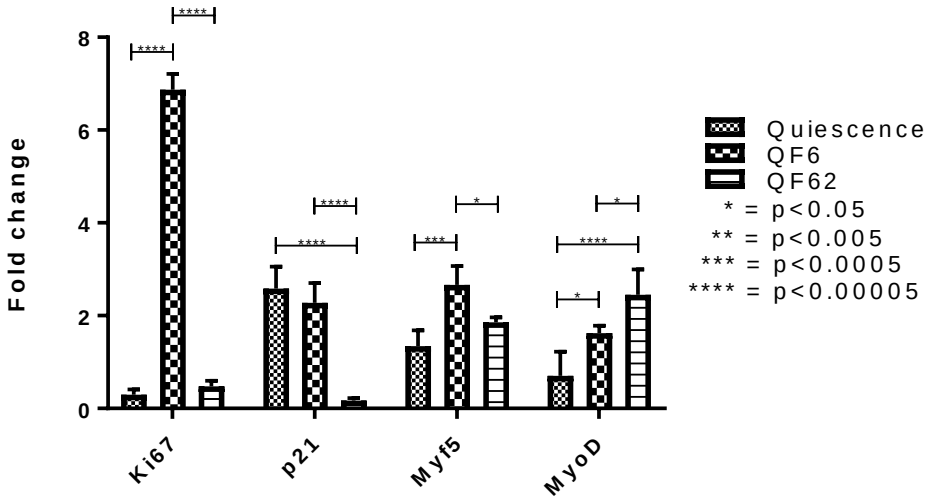

Figure 5.19 Expression of transcription factors influencing proliferation including myogenic regulatory factors in PHM KH3, induced into *in vitro* quiescence knock-out serum replacement (KOSR). Following induction of quiescence, using 24 hrs treatment of FGF6 followed by 48 hrs of FGF2 in KOSR media, cells were harvested and gene expression quantified from isolated RNA. Results represent means ± SEM (n=3)

5.5.2.6 Gene expression of multiple skeletal markers with individual FGF2 compound to sequential treatment FGF2 followed by FGF6

Sequential treatment of FGF2 followed by FGF6 did not result in any significant changes in ki67, myf5 and p21 expression compared to both quiescent cells and those treated with FGF2 alone. However, sequential treatment significantly upregulated MyoD expression compared to FGF2 treatment alone and quiescent cells (numbers and p values).

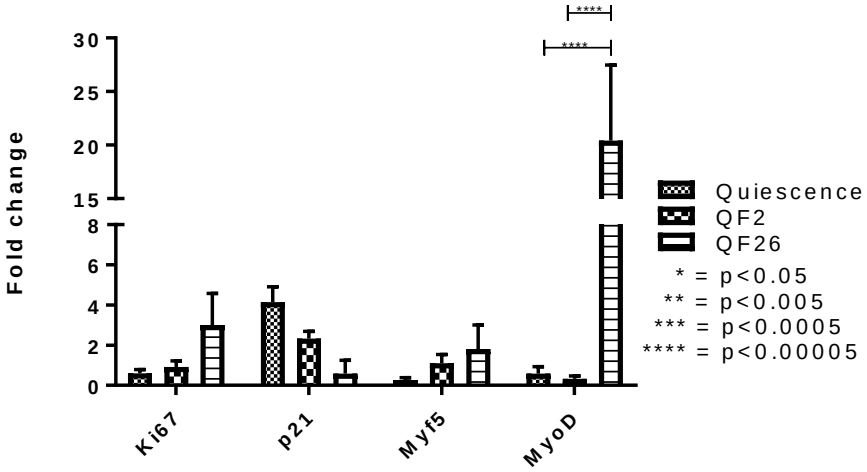

Figure 5.20 Expression of transcription factors influencing proliferation including myogenic regulatory factors in PHM S6.3, induced into *in vitro* quiescence knock-out serum replacement (KOSR). Following induction of quiescence, using 48 hrs treatment of FGF2 followed by 24 hrs of FGF6 in KOSR media, cells were harvested and gene expression quantified from isolated RNA. Results represent means ± SEM (n=3)

5.5.2.7 Comparison of multiple gene expression with individual and sequential treatment of FGF2 followed by FGF6

Similarly, to clone S6.3, in KH3 PHMs, sequential treatment did not have an effect on ki67 and myf5 expression with respect to quiescent cells and those treated with FGF2 individually. MyoD expression was again upregulated with sequential treatment and was significantly higher than quiescent cells and cells treated with FGF2 alone ($p<0.0005$). In contrast to clone S6.3, sequential treatment resulted in lower expression of p21 compared to individual treatment as well as quiescent cells ($p<0.0005$)

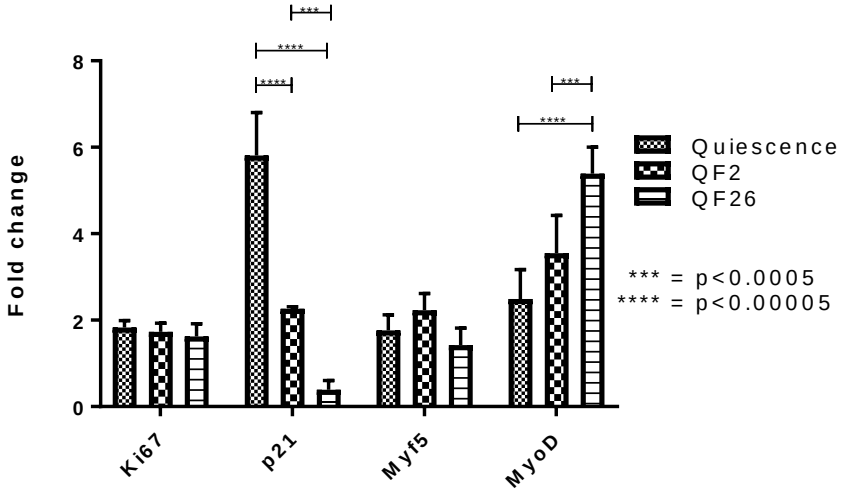

Figure 5.21 Expression of transcription factors influencing proliferation including myogenic regulatory factors in PHM KH3, induced into *in vitro* quiescence knock-out serum replacement (KOSR). Following induction of quiescence, using 48 hrs treatment of FGF2 followed by 24 hrs of FGF6 in KOSR media, cells were harvested and gene expression quantified from isolated RNA. Results represent means ± SEM (n=3)

5.5.2.8 Comparison of multiple gene expression with individual and sequential treatment of FGF2 followed by FGF6

In KH1 PHMs, sequential treatment of FGF2 followed by FGF6 upregulated ki67, myf5 and MyoD expression compared to quiescent cells ($p<0.0005$ ki67, myf5 and MyoD). Similar to KH3 PHMs, p21 expression was reduced following sequential treatment compared to quiescent cells ($p<0.0005$).

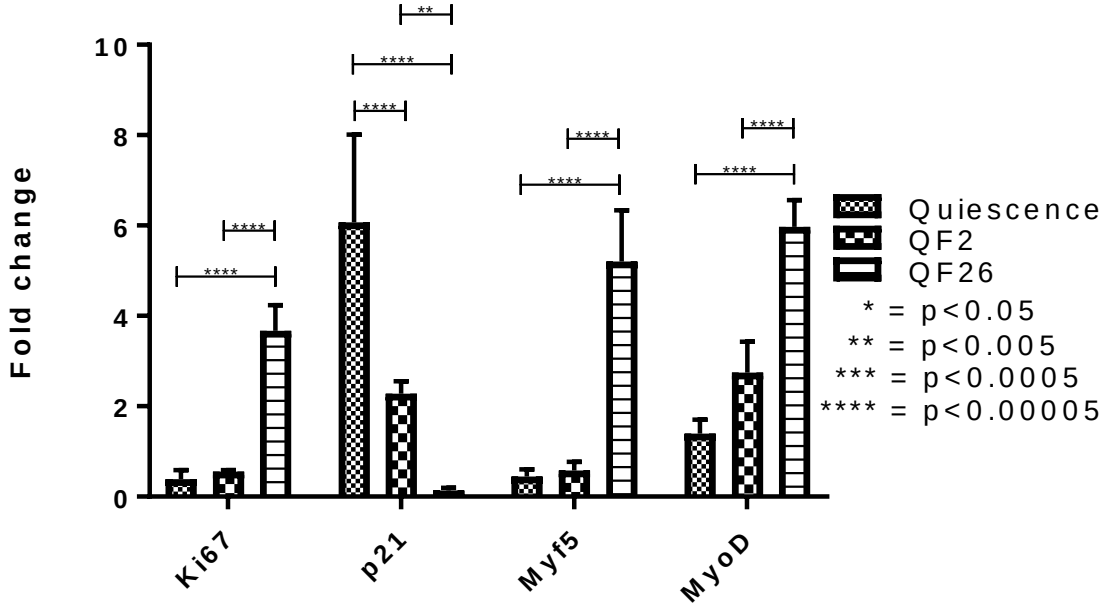

Figure 5.22 Expression of transcription factors influencing proliferation including myogenic regulatory factors in PHM KH1, induced into *in vitro* quiescence knock-out serum replacement (KOSR). Following induction of quiescence, using 48 hrs treatment of FGF2 followed by 24 hrs of FGF6 in KOSR media, cells were harvested and gene expression quantified from isolated RNA. Results represent means ± SEM (n=3)

5.6 Summary

Table 5.1 Gene expression of 2 cell cycle markers in response to FGF2 or FGF6 in relation each other,

FGF6 treatment						
	S6.3		KH3		KH1	
ki67	↑ns	(p=0.068)	↑ *	(p=0.01)	↑ ***	(p=0.0003)
p21	↓ns	(p=0.066)	↓*	(p=0.02)	~ns	(p=0.44)
FGF2 treatment						
	S6.3		KH3		KH1	
ki67	↑ns	(p=0.13)	~ns	(p=0.56)	~ns	(p=0.27)
p21	↓*	(p=0.01)	↓*	(p=0.02)	↓ns	(p=0.07)

Table 5.2 Gene expression of 2 markers related to myogenesis in response to FGF2 or FGF6 in relation each other,

FGF6 treatment							
	S6.3		KH3		KH1		
myf5	↑*	(p=0.01)	ns	(p=0.11)	↑*	(p=0.01)	
MyoD	↓ns	(p=0.11)	↑*	(p=0.03)	↑ns	(p=0.08)	
FGF2 treatment							
	S6.3		KH3		KH1		
myf5	↑*	(p=0.02)	↑ns	(p=0.20)	~ns	(p=0.41)	
MyoD	~ns	(p=0.24)	↑ns	(p=0.17)	↑ns	(p=0.058)	

Legend: ↑ = Significant upregulation or trend towards significant upregulation
↓ = Significant downregulation or trend towards significant downregulation
~ = No significance or trend towards deviation from the mean
ns = No statistical significance
(p) = Actual p value

Treatment with FGF6 seems to activate the quiescent PHMs to allow them to re-enter the cell cycle in all 3 clones, although to a different statistical extent as seen with the ki67 proliferation marker. Individual treatment using FGF2 alone did not have a pro-proliferative effect on the quiescent PHMs, except in one clone which demonstrated a trend for increased proliferation. However, viewing the ki67 and p21 data together, it appears that FGF2 treatment does not directly promote proliferation but indirectly aids in reducing inhibitory mechanisms including the downregulation of p21 when applied to the quiescent PHMs. This was the case for all the three clones (Fig 5.12).

MyoD is a dominant and master myogenesis marker of which neither FGF2 nor FGF6 regulated MyoD expression consistently: only one clone responded to FGF6 by increasing MyoD expression significantly (KH3). FGF6 is proposed to contribute to PHM's activation and this may explain the lack of response in MyoD expression. Therefore, FGF6 may potentially be involved only in the early stages of activation and proliferation with no significant influence on differentiation. Relative to GAPDH, the differential expression of MyoD across all three PHM clones suggests that MyoD might have its own internal feedback mechanism. In other words, when it starts low, it is unlikely to respond, but when there is some presence it might respond slightly better (KH3, KH1).

When considering the ki67 and myf5 expression, the majority of the response occurs together where they were similarly changed or remained unchanged for FGF6 and FGF2 following the treatments. myf5 is associated with quiescent satellite cells and as an early proliferation marker for myoblasts, therefore upregulation suggests promotion of activation of the PHMs. This promotor of activation seemed to proceed further in the myogenic pathway for clones KH3 and KH1. In contrast, clone S6.3 clearly had a much larger myf5 response and no MyoD response. This suggests an alternate role for myf5, perhaps favouring self-renewal.

With regards to sequential treatments using FGF6 followed by FGF2, data suggests that the timing of the treatment would need to be optimised for effective proliferation after activation. The 24-hour time period of FGF6 treatment did not seem sufficient for completion of the activation sequence of the PHMs in order to facilitate the significant effect of subsequent treatment of FGF2. By providing sufficient time after the initial treatment, PHMs proliferation could be improved.

These data suggest that timing and choice of treatment with respect to the state of cells is crucial for enhancing activation, proliferation and myogenic function.

5.7 Conclusion

The effects of FGF6 or FGF2 alone and sequential combinations of both are highly dependent on the source of PHMs.

FGF6 treatment alone was able to activate and aid in the re-entry of PHMs into the cell cycle in quiescent PHM clones of all three subjects.

FGF2 treatment alone did not promote the activation and re-entry in the cell cycle. However, it did inhibit the inhibition factors of proliferation, like p21, which could indirectly influence proliferation. This was the case for all three subjects.

Sequential treatment of FGF6 followed by FGF2 showed promise for significantly influencing proliferation, however, did not effectively achieve the hypothesis. This is possibly due to the timing of sequential treatment.

Sequential treatment of FGF2 followed by FGF6 did not seem to have profound effects on the activation or proliferation of the quiescent cells. This also indicates the sequence of the treatment is crucial to obtain effective activation and improved proliferation of the PHMs.

Chapter 6: Discussion

The main rationale leading to all the chapters in this thesis was: given that FGF6 is found predominantly in muscle lineage and early stages of development, it could be utilised to activate the quiescent PHMs. Furthermore, sequential treatment with FGF2 after FGF6 treatment could improve the proliferation rate of PHMs. In order to properly investigate the effects of these FGFs, two distinct *in vitro* quiescence protocols were compared. To consider the differences between the PHMs harvested and expanded from the different donors, this thesis also set out to establish comparative index to compare the PHMs *in vitro* to each other in order to understand the variability of PHMs and the possible variability in response to the treatment with FGFs.

6.1.1 Variability between different PHM populations and rate of proliferation.

Rate of proliferation has been studied for a long period of time in cancer studies [105-108]. When the first studies defined the four phases of the cell cycle using radioactive labelling techniques, it was discovered that not all cells in the population proliferate at a similar rate [109]. This causes variability, not only in similar cell types, but also in primary cells where the adaption to the environment of the origin of cells could have altered the rate at which the cells divide. In the study performed here establishing the comparative index, it was proposed that even though the PHMs were obtained for volunteers with similar age and physical activity habits, this index would be able to assess the PHMs to determine a basal proliferation characteristic. Depending on this index, the PHMs might or might not respond differently after specific FGF treatment application *in vitro*.

The study design was aimed at assessing the rate of proliferation from G_1 to S phase and the amount of total RNA synthesised. These two variables provided the baseline to compare multiple PHMs to each other.

The comparative index study showed that up to 10 hours after plating cells from the expanded stocks of S6.3 and S9.1, there was no significant transition from G_1 to S phase (Figure 3.2, 3.4). This could be due to the time required for anchoring and re-initiating cell metabolism after trypsinisation. Depending on the type of cell, the timeline could differ from the one seen in the current study [84, 110-113]. Although the study

was performed on asynchronized PHMs, the initial lag phase in both the PHMs showed exponential increase in transition. However, with the 24 hrs assessed, the S phase proportion for S6.3 peaked at 22% at the 22-hour time point and subsequently seemed to decrease. S9.1 had not reached the peak proportion at the same time point and the S phase proportion was still rising at the 24-hour timepoint. Therefore, this experiment identified the differential rate of cell cycle progression between the two PHM populations. This testing environment could be used in future for different applications, including the application of different treatments to a slower clone to increase the rate of proliferation to match that of the faster clones.

However, RNA concentrations did not require the long lag phase after plating the cells. This can be explained as RNA is continually generated even before the initiation of the S phase [114]. RNA was seen to increase from the 4 to 6 hour time points and increased linearly until the 22-hour time point for S6.3 where it subsequently started to decrease. S9.1 however, coincided with the S phase data and kept increasing even up to the 24 hour time point.

The differences between the two clones could indicate that the cells could have had adapted according to the niche environment of origin leading to downstream consequences on their *in vitro* culture characteristics. Within each clone, there were similar observations when comparing S phase proportion and RNA.

6.1.2 Advantages of establishing a baseline for comparison of cell proliferation.

Rate of proliferation is the speed at which the cell progresses from one phase to the next until cell division. With establishment of a baseline rate of proliferation, populations of healthier, actively proliferating cells may be identified. Since the characteristics of cells change with higher passage, the baseline can assist in identifying more active and younger batches of cells.

Although the study focussed on PHMs and the transition from G_1 to S phase, the same concept can be applied to other proliferating cells (for example, C2C12 cells transiting from G_1 to S, S to G_2 or even G_2 to M phase). It may be necessary not only to look at G_1 but all phases during the process of cell division. Although assessment of proliferation index was useful, the in-depth view of other phases may influence

downstream applications. The phase at which the cells are positioned may also assist in choosing the right delivery time point for a particular intervention. Here, two examples will be given. Firstly, in order for cells to progress through mitosis and create two daughter cells, protein synthesis is essential. This step (protein synthesis) initiates, typically in the late S phase and G_2 phase [115]. Therefore, a treatment aimed at promoting this process should not be added earlier. Secondly, myoblasts are cells with a high requirement for protein synthesis so the divided cells can prepare adequately for subsequent fusion by synthesising not only MRFs but also early sarcomere proteins and fusion proteins. In this case treatment could best be applied in G_2 phase.

Rate of proliferation can be assessed using variety of methods. For example, Some of these established method include the MTT (3-(4,5-dimethylthiazol-2-yl)-2,5-diphenyl tetrazolium bromide) [12] assay which measures the overall metabolic activity of the cell using a permeable dye; the intensity of the coloured end product is easily detected and measured using a calorimeter. Similarly, WST-1 also is a dye used to measure cellular activity which can be used to assess the rate of proliferation. Again, this is an indirect method based on intensity of the reaction and colour produced. The WST-1 assay works by cleaving tetrazolium salt, MTS (3-(4,5-dimethylthiazol-2-yl)-5-(3-carboxymethoxyphenyl)-2-(4-sulfophenyl)-2H-tetrazolium), in the cell by mitochondrial dehydrogenase to produce formazan product (artificial chromogenic product) which can further be detected by colorimeter. Higher the number of metabolically active cells, higher the formazan product. Fluorescent dyes are also used to measure the rate of cellular proliferation providing greater sensitivity and precision e.g. eFluor 670 proliferation dye [116], Cell Biolabs' CytoSelect™ [117-119]. The CytoSelect™ works on the principle of incorporating (^{3}H)thymidine into the DNA which can further be detected using fluorometric measurements.

Not all cells during proliferation multiply at the same rate [12]. Assessing the cell count over time is the most direct method for estimating rate of proliferation [12]. Cell count alone, however, does not provide the sufficient level of details attained from cell cycle behaviour. Estimating the proportion of cells in different phases of the cell cycle provides an in depth understanding of the proliferation cycle of the cell clones.

6.1.3 Effects of Rate of proliferation.

Rate of proliferation is an important part of cell cycle. The rate at which cell divides greatly influences the viability of the cell. Cells are constantly replenished in the body although at different rates for different tissues [12]. In the regeneration scenario, the quicker the cells proliferate the better it is to restore the damaged tissue [12]. However, this also can lead to mutations in the genomic content due to restricted time for repairing DNA damage before undergoing DNA replication [64]. With repeated accumulation of mutations, the cell could become cancerous in nature [120]. Further, cells exposed to these different conditions may exhibit variable rates of proliferation.

6.1.4 Downstream applications of a proliferative/comparative index (CI)

In the area of regenerative medicine, transplantation of cells is moving towards becoming a more common practice in personalised treatments than a decade ago [12]. A comparative index could assist in choosing the best batch of cells possible for the treatment. With autologous transplantation, help of proliferative agents such as FGF2 can also be incorporated to enhance the proliferative capacity of the cells to multiply faster *in vitro* before transplanting, resulting in quicker turnaround to help regeneration. Also, identifying the ideal delivery time point according to synchronization and cell cycle phase may prove to be important in future.

In the field of cancer studies, some of the chemotherapeutic drugs act according to the rate of proliferation rather than the mutation. The rate of cell division is targeted, and cell cycle phase is recognised by the drug. This creates a "*proliferation rate paradox*" [120]. In future, the comparative index such as described in this thesis could help identify cells that have acquired mutations and proliferate at a different rates. Either reprograming or applying a treatment to such cells to improve their proliferation rate, could then be checked for efficacy using CI. Reprogrammed ultimately the drug may need to act on specific cells with different rate of proliferation.

In contrast, slower dividing cells could be used further for *in vitro* studies in order to provide prolonged time to elucidate factors influencing the process of cell division.

6.1.5 Achieving effective quiescence in vitro.

Initiating induction of quiescence from a state of activation one can study the feedback mechanisms utilised to induce quiescence. Achieving effective *in vitro* quiescence in a limited amount of time could assist in understanding specific early aspects of skeletal muscle regeneration such as activation. Here effective quiescence was considered to be achieved when the expression of ki67 was lower compared to the proliferating cells. PHM re-entry into the cell cycle following activation is crucial for assessing effective quiescence induction, because it would indicate that no permanent negative effects were caused, such as senescence.

In chapter 4, PHMs were subjected to SuCu KOSR for 48 hours, the levels of cyclin genes' expression were down regulated significantly, more importantly, cell cycle shift was observed towards reduced proliferation resulting in achievement of cellular quiescence. A similar protocol was used by Sellathurai *et al,* (2013) wherein ki67 and p21 mRNA expression in PHMs treated with SuCu FBS were assessed. Similar to the current study, ki67 was downregulated while p21 was upregulated in suspension media [43].

6.1.6 State of quiescence

Understanding of the G_0 phase which can sometimes be viewed either as an extension of G_1 phase or an individual state outside of the repetitive cell division cycle, plays an important role in understanding cell cycle. With the timeline of G_1 phase being diverse, even within the same tissue but different cells [121, 122] understanding the transition from G_0-G_1 is essential. Transcriptomes of various types of stem cells which reside in quiescent states exhibit downregulation of important cell cycle genes such as cyclin A2, B1 and E2 [90, 123]. However, even during the quiescent state some of the genes relating to stem cell fate are upregulated e.g. FOXO3 and EZH1 [90]. In Chapter 4, where multiple *in vitro* quiescence protocols were tested, the induction of quiescence was seen with the downregulation of cell cycle genes. Although the expression of genes such as ki67 and myf5 were significantly downregulated, it still does not mean complete arrest of the molecular function. This was confirmed by continued expression of total RNA. *In vitro* the duration of quiescence poses more questions to be probed. For example, which functions remain active, even though

quiescence has halted cell cycle progression? Additionally, does the state of quiescence differ in PHM clones from different donors?

6.1.7 Mechanism of G_0 exit.

Cyclin C and retinoblastoma(Rb) protein have been shown to be involved in the G_0 exit and G_1-S phase re-entry by hyperphosphorylation of Rb [124-126]. In mammalian cells, cyclin C mRNA is found to be at elevated levels at the time of cell cycle re-entry suggesting their involvement in Rb phosphorylation [127, 128]. Furthermore, the activity of Rb was found to be lower during the G_1-S phase transition compared to early G1 phase. This suggests that the involvement of Rb is more important during G_0-G_1 transition. The E2F family, playing a major role in G_1/S phase transition, is involved in the coding of multiple transcription factors [129-132] and has been shown to be active resulting in the activation of the necessary genes such as CCNA1,2 CCND1,2 by recruiting histone acetyltransferase, essential for the G_1 entry [128]. In a study performed by Armand *et al* (2003) [133] it was demonstrated that, the injection of recombinant FGF6 in the *soleus* muscle for regeneration in a FGF6(-/-) mice, cyclin D1 was upregulated with downregulation of calcineurin [64]. In future *in vitro* studies, these additional regulators could be assessed at different time points after FGF6 treatment in quiescent cells. For example, the effect of cyclin C can further be confirmed by *in vitro* experiments such as knockdown and over expression in the state of quiescence and early activation.

6.1.7.1 The importance of restriction point in exit from G_0

Restriction point or R-point in the cell cycle is referred to the point of commitment towards DNA synthesis and cell division (before S phase). During the exit from quiescence the cell requires extracellular stimulation to initiate the progression, during the third subphase of G_1, the cell commits to the DNA replication process after which the stimulation is not required. The withdrawal of the stimulants before the commitment could result in cell's revision to quiescence. Under reversal conditions the cell might need additional time to restart the re-entry process known as withdrawal time which can be about 8 hours which can be clearly seen in the figure 3.2 and 3.4. The trend line analysis demonstrates no significant progression from G0/G1 to S

phase during the first 10-12 hours due to trypsinisation which resets the withdrawal time.

6.1.8 FGFs: A family performing individual tasks.

FGFs with four FGF receptors act on various aspects of tissue synthesis [45, 134, 135]. Although the 22-member family is critically involved in embryonic growth as shown by knockout studies [136, 137], the role involving each FGF in the adult tissue needs to be probed.

With respect to myoblasts in the adult process of myogenesis, various FGFs play a crucial role in specific aspects of the process. The data presented here indicate that FGF6 is involved in activation of the quiescent satellite cells initiating the cascade of events which when followed with FGF2 helped in proliferation of the activated PHMs. Other FGFs may also assist in the differentiation of the cells promoting fusion [138, 139].

The current study using PHMs found that FGF6 and FGF2 both promoted activation and proliferation of quiescent PHMs but do so by adapting different regulating factors. This included a greater increase in ki67 expression with FGF6 than FGF2. This could be explained by the activation of the Cdk complex, which could be investigated in future studies. To determine if specific FGF receptors may play a role, receptor blockade could prove to be informative.

A second regulatory effect was reduction in the expression of p21. Specifically, FGF2 downregulated the inhibitory checkpoint of p21 which could indirectly allow PHM's activation. FGF2 is known to be an upstream initiator of the MAPK pathway [140, 141]. By releasing Cks1, FGFR substrate 2 [142] recruits downstream molecules for signalling and is ultimately associated with downregulation of p27. During the late mitosis phases, M-Cdk is inactivated by Cdc20-APC (tumour suppressor protein). However, Cdc20-APC is also stimulated by M-Cdk. The loss of M-cyclin in the late mitosis phase inactivates all APC activity. Completion of cell division, the cell starts accumulating M-cyclin for the next cycle in G_1, which assists in G_1-S phase transition during cell cycle [85]. Activation of the Cdk complex is achieved when the cyclin-dependent kinase binds to the cyclin and phosphorylates it. The formed complex

regulates the transcription factors and production of mRNA [143, 144]. In future studies, the observed changes in total RNA should be analysed in more detail, possibly using microarray.

In the case of muscle regeneration, without a considerable number of proliferative myoblasts in the injured muscle niche, treatment with FGF2 might not be ideal for regeneration. Since the rate of proliferation increases with active cells and FGF6 induces activation of quiescent PHMs, a combination treatment could therefore provide effective support for the sequence of regeneration. With the rapid increase in the S phase with the treatment of FGF6 in all three PHMs clones assessed in this thesis, the data suggest that FGF6 should be used first in the sequence as an activation agent (Figure 5.2). Also, FGF2 induced progression from S phase to G_2 phase and this suggests that it should be applied second in the sequence.

The cell cycle data were supported by the qPCR analysis of the PHMs. FGF6 treatment increased ki67 and decreased p21 expression (Figure 5.9, 5.11). In contrast,FGF2 treatment had no effect on ki67 (Fig 5.10) but similarly decreased p21 expression. These results collectively suggest that the treatment with FGF6 and FGF2 could also be beneficial together and not just sequentially. Future studies should test this sequence in an *in vivo* model of injury regeneration.

6.1.9 Using FGF6 along with FGF2 could enhance regeneration of skeletal muscle.

Activation of satellite cells *in vivo* is a tightly orchestrated process after injury. Upon injury, activation signals are released which in turn activate the quiescent satellite cells. In a study mentioned in the introduction, FGF6 was upregulated when skeletal muscle tissue was damaged [69]. The data of this thesis indicated under controlled conditions that FGF6 activated the quiescent PHMs (chapter 5). However, FGF6 could also have an effect on proliferation mediated by ERK, MAPK [61] as it has been shown in a recent study how cells, such as osteoblasts and osteoclasts, both respond by proliferating [65]. We propose that the same mechanism of action in osteoblasts could also be applicable in satellite cells. Hence, treatment with FGF6 with FGF2 could potentially enhance regeneration initiating from activation by FGF6 and proliferation by FGF2 with a brief overlap.

6.1.10 Implementing comparative index (CI) after interventions with FGFs.

CI could be used widely to compare different kinds of cells, different treatments or even the same cells prior to and post intervention. Establishing an index reference bank can help in different ways. Primarily, this thesis suggests its usefulness to assess the functionality of PHM explants from different individuals so that they could be compared to a CI in a reference data bank from known robust stocks. CI could also be used to distinguish between fast and slow proliferating cells in process other than myogenesis, such as cancer studies where the rate of proliferation is an important part of diagnosis.

Once CI is established for G_0/G_1 to S phase, one could also similarly develop an index to compare the rate of cell cycle through other phase transitions. FGF2 is ineffective when the majority of cells are in G_0/G_1 phase(Chapter 5.10), however when the cells progress through to S / G_2 phase, FGF2 treatment could have a significant effect on the rate of proliferation and on a calculated CI based specifically in this phase transition.

6.2 Limitations:

These studies were performed on PHMs. As discussed earlier, PHMs may have different behaviour that might produce different results for similar experiments when performed on PHMs harvested from different donors.

CI was established and tested on two different PHM explants. This needs to be tested on a larger number of samples to verify and to create the proposed “reference bank”. Limited number of PHMs might be providing narrow range of outcomes. Increasing the number of different PHMs could help attain a better understanding and the variance between PHM clones could be estimated. CI could also be used on an immortalised cell line such as C2C12, where the proliferation rate should remain stable with relatively low passage numbers, in order to verify repeatability.

The treatments of FGFs were performed *in vitro* which follows a linear path, these experiments need to be performed *in vivo* to confirm the results. *In vivo* the cascade

of other events that might affect the treatments could alter the outcome. Animal model tests would provide better indication of the *in vivo* effects.

6.3 Future recommendations:

6.3.1 Establishing an improved bridged protocol.

The SuCu achieved quiescence in 48 hours. However, soon after harvesting the PHMs get activated. Nevertheless, with the establishment of the bridged protocol, this thesis opened up a new avenue that could be taken further. For example, combining SuCu-KOSR and the KOSR techniques could establish a stable protocol to induce quiescence *in vitro*. A combined and improved bridged protocol could have the SuCu for the first 48 hours and upon harvesting, the PHMs could be plated in KOSR medium potentially attaining quiescence shortly after replating in KOSR media. The proposed improvement of using the SuCu protocol followed by KOSR is that, the whole 10 days required to initiate quiescence with KOSR alone, would be shortened significantly. This provides all the benefits of KOSR protocol without the disadvantages of SuCu.

6.3.2 Comparative index

CI could use the comparison not only between different PHMs but also between different cell lines providing an insight on the ratio of rate of proliferation between different cell types in tissue. However, it needs to be assessed in detail how different cells respond to the 24hr protocol. Also comparing an immortalised cell line (C2C12) to PHMs could provide a better insight on how similar they are to PHMs of healthy donors.

6.3.3 *In vivo* treatment with FGF6 and or FGF2

With the effects of FGF6 and FGF2 now established *in vitro*, applied to a quiescence state, a similar protocol can be constructed to be assessed in animal models. The effect of the treatment once administered *in vivo* can be tracked over days by harvesting the tissue over 3,7,14,21 days by assessing the rate of activation

/ proliferation. Staining markers such as pax7, PCNA, myf5, MyoD and myogenin can be included in the assessment.

In vitro studies follow a linear pathway of assessment, such as the effect of the only treatment administered. In the *in vivo* environment there is cascade of events occurring which might intervene/influence with the administered treatment. The whole response might still be a positive influence even if slightly different.

The mechanisms involved in pro-activation and anti-inhibition of cell cycle progression need to be probed in PHMs in more detail. This could give a vital understanding of the role of two different FGFs for combination or sequential treatments.

6.3.4 Overview of incorporating comparative index and FGF treatments

The comparative index provides the different rate of progression in various phases of the cell cycle. With sufficient samples processed for different clones and testing the dose response with FGF could help plot a curve with rate of progression and dosage of FGF. This can be utilized in determining the dose response as a treatment to influence the rate of proliferation before transplanting the cells *in vivo*.

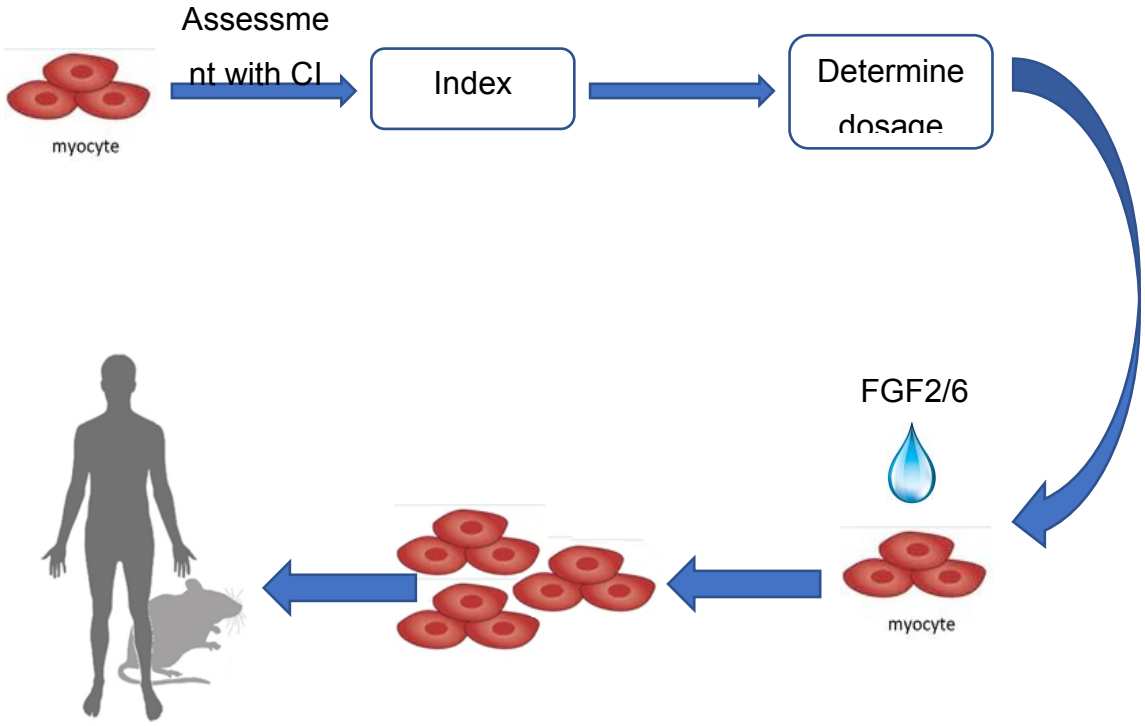

References

1. Riddle, D., T. Blumenthal, and B. Meyer, *The organization, structure, and function of muscle*. 1997: Cold Spring Harbor (NY): Cold Spring Harbor Laboratory Press; 1997.
2. Gillies, A.R. and R.L. Lieber, *Structure and function of the skeletal muscle extracellular matrix.* Muscle Nerve, 2011. **44**(3): p. 318-31.
3. Grosberg, A., P.L. Kuo, C.L. Guo, N.A. Geisse, M.A. Bray, W.J. Adams, S.P. Sheehy, and K.K. Parker, *Self-organization of muscle cell structure and function.* PLoS Comput Biol, 2011. **7**(2): p. e1001088.
4. Hinds, S., W. Bian, R.G. Dennis, and N. Bursac, *The role of extracellular matrix composition in structure and function of bioengineered skeletal muscle.* Biomaterials, 2011. **32**(14): p. 3575-83.
5. *Muscle cell growth and development*. Designing foods: Animal product options in the marketplace. 1988: National Research Council (US) Committee on Technological Options to Improve the Nutritional Attributes of Animal Products.
6. Noto, R.E. and M.A. Edens, *Physiology, muscle*. 2018: Treasure Island (FL): StatPearls Publishing; 2019.
7. U. S. National Institutes of Health, N.C.I.S.T.m. *Seer training modules, anatomy and physiology*. [Training module] 14/08/2019; Available from: https://training.seer.cancer.gov/anatomy/muscular/structure.html.
8. Mauro, A., *Satellite cell of skeletal muscle fibers.* J Biophys Biochem Cytol, 1961. **9**: p. 493-5.
9. Allbrook, D.B., M.F. Han, and A.E. Hellmuth, *Population of muscle satellite cells in relation to age and mitotic activity.* Pathology, 1971. **3**(3): p. 223-43.
10. Schmalbruch, H. and U. Hellhammer, *The number of satellite cells in normal human muscle.* Anat Rec, 1976. **185**(3): p. 279-87.
11. Lindstrom, M. and L.E. Thornell, *New multiple labelling method for improved satellite cell identification in human muscle: Application to a cohort of power-lifters and sedentary men.* Histochem Cell Biol, 2009. **132**(2): p. 141-57.

12. Sajko, S., L. Kubinova, E. Cvetko, M. Kreft, A. Wernig, and I. Erzen, *Frequency of m-cadherin-stained satellite cells declines in human muscles during aging.* J Histochem Cytochem, 2004. **52**(2): p. 179-85.
13. Bareja, A. and A.N. Billin, *Satellite cell therapy - from mice to men.* Skelet Muscle, 2013. **3**(1): p. 2.
14. Schultz, E., *Satellite cell proliferative compartments in growing skeletal muscles.* Dev Biol, 1996. **175**(1): p. 84-94.
15. Campion, D.R., R.L. Richardson, J.O. Reagan, and R.R. Kraeling, *Changes in the satellite cell population during postnatal growth of pig skeletal muscle.* J Anim Sci, 1981. **52**(5): p. 1014-8.
16. Mesires, N.T. and M.E. Doumit, *Satellite cell proliferation and differentiation during postnatal growth of porcine skeletal muscle.* Am J Physiol Cell Physiol, 2002. **282**(4): p. C899-906.
17. Forcina, L., C. Miano, L. Pelosi, and A. Musaro, *An overview about the biology of skeletal muscle satellite cells.* Curr Genomics, 2019. **20**(1): p. 24-37.
18. Kuang, S., S.B. Charge, P. Seale, M. Huh, and M.A. Rudnicki, *Distinct roles for pax7 and pax3 in adult regenerative myogenesis.* J Cell Biol, 2006. **172**(1): p. 103-13.
19. Seale, P., L.A. Sabourin, A. Girgis-Gabardo, A. Mansouri, P. Gruss, and M.A. Rudnicki, *Pax7 is required for the specification of myogenic satellite cells.* Cell, 2000. **102**(6): p. 777-86.
20. Alfaro, L.A., S.A. Dick, A.L. Siegel, A.S. Anonuevo, K.M. McNagny, L.A. Megeney, D.D. Cornelison, and F.M. Rossi, *Cd34 promotes satellite cell motility and entry into proliferation to facilitate efficient skeletal muscle regeneration.* Stem Cells, 2011. **29**(12): p. 2030-41.
21. Ceafalan, L.C., B.O. Popescu, and M.E. Hinescu, *Cellular players in skeletal muscle regeneration.* Biomed Res Int, 2014. **2014**: p. 957014.
22. Deyhle, M.R. and R.D. Hyldahl, *The role of t lymphocytes in skeletal muscle repair from traumatic and contraction-induced injury.* Front Physiol, 2018. **9**: p. 768.
23. Ten Broek, R.W., S. Grefte, and J.W. Von den Hoff, *Regulatory factors and cell populations involved in skeletal muscle regeneration.* J Cell Physiol, 2010. **224**(1): p. 7-16.

24. Yang, W. and P. Hu, *Skeletal muscle regeneration is modulated by inflammation.* J Orthop Translat, 2018. **13**: p. 25-32.
25. Almeida, C.F., S.A. Fernandes, A.F. Ribeiro Junior, O. Keith Okamoto, and M. Vainzof, *Muscle satellite cells: Exploring the basic biology to rule them.* Stem Cells Int, 2016. **2016**: p. 1078686.
26. Yin, H., F. Price, and M.A. Rudnicki, *Satellite cells and the muscle stem cell niche.* Physiol Rev, 2013. **93**(1): p. 23-67.
27. Collins, C.A., I. Olsen, P.S. Zammit, L. Heslop, A. Petrie, T.A. Partridge, and J.E. Morgan, *Stem cell function, self-renewal, and behavioral heterogeneity of cells from the adult muscle satellite cell niche.* Cell, 2005. **122**(2): p. 289-301.
28. Lepper, C., S.J. Conway, and C.M. Fan, *Adult satellite cells and embryonic muscle progenitors have distinct genetic requirements.* Nature, 2009. **460**(7255): p. 627-31.
29. Lepper, C., T.A. Partridge, and C.M. Fan, *An absolute requirement for pax7-positive satellite cells in acute injury-induced skeletal muscle regeneration.* Development, 2011. **138**(17): p. 3639-46.
30. McCarthy, J.J., J. Mula, M. Miyazaki, R. Erfani, K. Garrison, A.B. Farooqui, R. Srikuea, B.A. Lawson, B. Grimes, C. Keller, G. Van Zant, K.S. Campbell, K.A. Esser, E.E. Dupont-Versteegden, and C.A. Peterson, *Effective fiber hypertrophy in satellite cell-depleted skeletal muscle.* Development, 2011. **138**(17): p. 3657-66.
31. Murphy, M.M., J.A. Lawson, S.J. Mathew, D.A. Hutcheson, and G. Kardon, *Satellite cells, connective tissue fibroblasts and their interactions are crucial for muscle regeneration.* Development, 2011. **138**(17): p. 3625-37.
32. Sacco, A., R. Doyonnas, P. Kraft, S. Vitorovic, and H.M. Blau, *Self-renewal and expansion of single transplanted muscle stem cells.* Nature, 2008. **456**(7221): p. 502-6.
33. Sambasivan, R., R. Yao, A. Kissenpfennig, L. Van Wittenberghe, A. Paldi, B. Gayraud-Morel, H. Guenou, B. Malissen, S. Tajbakhsh, and A. Galy, *Pax7-expressing satellite cells are indispensable for adult skeletal muscle regeneration.* Development, 2011. **138**(17): p. 3647-56.
34. Dayanidhi, S. and R.L. Lieber, *Skeletal muscle satellite cells: Mediators of muscle growth during development and implications for developmental disorders.* Muscle Nerve, 2014. **50**(5): p. 723-32.

35. Dai, L., J. Trillo-Tinoco, Y. Cao, K. Bonstaff, L. Doyle, L. Del Valle, D. Whitby, C. Parsons, K. Reiss, J. Zabaleta, and Z. Qin, *Targeting hgf/c-met induces cell cycle arrest, DNA damage, and apoptosis for primary effusion lymphoma.* Blood, 2015. **126**(26): p. 2821-31.
36. Jarrin, M., T. Pandit, and L. Gunhaga, *A balance of fgf and bmp signals regulates cell cycle exit and equarin expression in lens cells.* Mol Biol Cell, 2012. **23**(16): p. 3266-74.
37. Kimura, I., H. Tsuneki, M. Okabe, and M. Ogasawara, *Platelet-derived growth factor blocks the cell-cycle transition from the g0 to g1 phase in subcultured angiogenic endothelial cells in rat thoracic aorta.* Jpn J Pharmacol, 1997. **74**(4): p. 303-11.
38. Larson, R.C., G.G. Ignotz, and W.B. Currie, *Platelet derived growth factor (pdgf) stimulates development of bovine embryos during the fourth cell cycle.* Development, 1992. **115**(3): p. 821-6.
39. Zhang, K., J. Sha, and M.L. Harter, *Activation of cdc6 by myod is associated with the expansion of quiescent myogenic satellite cells.* J Cell Biol, 2010. **188**(1): p. 39-48.
40. Kondoh, K., K. Sunadome, and E. Nishida, *Notch signaling suppresses p38 mapk activity via induction of mkp-1 in myogenesis.* J Biol Chem, 2007. **282**(5): p. 3058-65.
41. Jones, N.C., K.J. Tyner, L. Nibarger, H.M. Stanley, D.D. Cornelison, Y.V. Fedorov, and B.B. Olwin, *The p38alpha/beta mapk functions as a molecular switch to activate the quiescent satellite cell.* J Cell Biol, 2005. **169**(1): p. 105-16.
42. Kadi, F., P. Schjerling, L.L. Andersen, N. Charifi, J.L. Madsen, L.R. Christensen, and J.L. Andersen, *The effects of heavy resistance training and detraining on satellite cells in human skeletal muscles.* J Physiol, 2004. **558**(Pt 3): p. 1005-12.
43. Sellathurai, J., S. Cheedipudi, J. Dhawan, and H.D. Schroder, *A novel in vitro model for studying quiescence and activation of primary isolated human myoblasts.* PLoS One, 2013. **8**(5): p. e64067.
44. Passerin-d'Entreves., N., *The dose and time dependent effects of hgf, myf5, myod and mir31 expression in quiescent primary human myoblasts.*, in *M.Sc in Physiological Sciences*. 2017, Stellenbosch University: Stellenbosch.

45. Yun, Y.R., J.E. Won, E. Jeon, S. Lee, W. Kang, H. Jo, J.H. Jang, U.S. Shin, and H.W. Kim, *Fibroblast growth factors: Biology, function, and application for tissue regeneration.* J Tissue Eng, 2010. **2010**: p. 218142.
46. Blaber, M., J. DiSalvo, and K.A. Thomas, *X-ray crystal structure of human acidic fibroblast growth factor.* Biochemistry, 1996. **35**(7): p. 2086-94.
47. Ornitz, D.M. and N. Itoh, *Fibroblast growth factors.* Genome Biol, 2001. **2**(3): p. Reviews3005.
48. Lim, W., H. Bae, F.W. Bazer, and G. Song, *Fibroblast growth factor 2 induces proliferation and distribution of g2 /m phase of bovine endometrial cells involving activation of pi3k/akt and mapk cell signaling and prevention of effects of er stress.* 2018. **233**(4): p. 3295-3305.
49. Ornitz, D.M. and N. Itoh, *The fibroblast growth factor signaling pathway.* Wiley Interdiscip Rev Dev Biol, 2015. **4**(3): p. 215-66.
50. Crisona, N.J., K.D. Allen, and R.C. Strohman, *Muscle satellite cells from dystrophic (mdx) mice have elevated levels of heparan sulphate proteoglycan receptors for fibroblast growth factor.* J Muscle Res Cell Motil, 1998. **19**(1): p. 43-51.
51. Casar, J.C., C. Cabello-Verrugio, H. Olguin, R. Aldunate, N.C. Inestrosa, and E. Brandan, *Heparan sulfate proteoglycans are increased during skeletal muscle regeneration: Requirement of syndecan-3 for successful fiber formation.* J Cell Sci, 2004. **117**(Pt 1): p. 73-84.
52. Florkiewicz, R.Z., F. Shibata, T. Barankiewicz, A. Baird, A.M. Gonzalez, E. Florkiewicz, and N. Shah, *Basic fibroblast growth factor gene expression.* Ann N Y Acad Sci, 1991. **638**: p. 109-26.
53. Lotz, S., S. Goderie, N. Tokas, S.E. Hirsch, F. Ahmad, B. Corneo, S. Le, A. Banerjee, R.S. Kane, J.H. Stern, S. Temple, and C.A. Fasano, *Sustained levels of fgf2 maintain undifferentiated stem cell cultures with biweekly feeding.* PLoS One, 2013. **8**(2): p. e56289.
54. Li, X., Y. Chen, S. Scheele, E. Arman, R. Haffner-Krausz, P. Ekblom, and P. Lonai, *Fibroblast growth factor signaling and basement membrane assembly are connected during epithelial morphogenesis of the embryoid body.* J Cell Biol, 2001. **153**(4): p. 811-22.

55. Nunes, Q.M., Y. Li, C. Sun, T.K. Kinnunen, and D.G. Fernig, *Fibroblast growth factors as tissue repair and regeneration therapeutics.* PeerJ, 2016. **4**: p. e1535.
56. Feng, Y., L.L. Niu, W. Wei, W.Y. Zhang, X.Y. Li, J.H. Cao, and S.H. Zhao, *A feedback circuit between mir-133 and the erk1/2 pathway involving an exquisite mechanism for regulating myoblast proliferation and differentiation.* Cell Death Dis, 2013. **4**: p. e934.
57. Zhang, D., X. Li, C. Chen, Y. Li, L. Zhao, Y. Jing, W. Liu, X. Wang, Y. Zhang, H. Xia, Y. Chang, X. Gao, J. Yan, and H. Ying, *Attenuation of p38-mediated mir-1/133 expression facilitates myoblast proliferation during the early stage of muscle regeneration.* PLoS One, 2012. **7**(7): p. e41478.
58. Ling, L., S. Gu, Y. Cheng, and L. Ding, *Bfgf promotes sca1+ cardiac stem cell migration through activation of the pi3k/akt pathway.* Mol Med Rep, 2018. **17**(2): p. 2349-2356.
59. Hagiwara, K., G. Chen, N. Kawazoe, Y. Tabata, and H. Komuro, *Promotion of muscle regeneration by myoblast transplantation combined with the controlled and sustained release of bfgfcpr.* J Tissue Eng Regen Med, 2016. **10**(4): p. 325-33.
60. Jump, S.S., T.E. Childs, K.A. Zwetsloot, F.W. Booth, and S.J. Lees, *Fibroblast growth factor 2-stimulated proliferation is lower in muscle precursor cells from old rats.* Exp Physiol, 2009. **94**(6): p. 739-48.
61. Pawlikowski, B., T.O. Vogler, K. Gadek, and B.B. Olwin, *Regulation of skeletal muscle stem cells by fibroblast growth factors.* J Cell Physiol, 2017. **246**(5): p. 359-67.
62. Harthan, L.B., D.C. McFarland, and S.G. Velleman, *Changes in proliferation, differentiation, fibroblast growth factor 2 responsiveness and expression of syndecan-4 and glypican-1 with turkey satellite cell age.* Dev Growth Differ, 2013. **55**(5): p. 622-34.
63. Hosoyama, T., M.G. Meyer, D. Krakora, and M. Suzuki, *Isolation and in vitro propagation of human skeletal muscle progenitor cells from fetal muscle.* Cell Biol Int, 2013. **37**(2): p. 191-6.
64. Armand, A.S., C. Pariset, I. Laziz, T. Launay, F. Fiore, B. Della Gaspera, D. Birnbaum, F. Charbonnier, and C. Chanoine, *Fgf6 regulates muscle*

differentiation through a calcineurin-dependent pathway in regenerating soleus of adult mice. J Cell Physiol, 2005. **204**(1): p. 297-308.

65. Bosetti, M., M. Leigheb, R.A. Brooks, F. Boccafoschi, and M.F. Cannas, *Regulation of osteoblast and osteoclast functions by fgf-6.* J Cell Physiol, 2010. **225**(2): p. 466-71.
66. Armand, A.S., I. Laziz, and C. Chanoine, *Fgf6 in myogenesis.* Biochim Biophys Acta, 2006. **1763**(8): p. 773-8.
67. Zhao, P. and E.P. Hoffman, *Embryonic myogenesis pathways in muscle regeneration.* Dev Dyn, 2004. **229**(2): p. 380-92.
68. Neuhaus, P., S. Oustanina, T. Loch, M. Kruger, E. Bober, R. Dono, R. Zeller, and T. Braun, *Reduced mobility of fibroblast growth factor (fgf)-deficient myoblasts might contribute to dystrophic changes in the musculature of fgf2/fgf6/mdx triple-mutant mice.* Mol Cell Biol, 2003. **23**(17): p. 6037-48.
69. Floss, T., H.H. Arnold, and T. Braun, *A role for fgf-6 in skeletal muscle regeneration.* Genes Dev, 1997. **11**(16): p. 2040-51.
70. Fiore, F., A. Sebille, and D. Birnbaum, *Skeletal muscle regeneration is not impaired in fgf6 -/- mutant mice.* Biochem Biophys Res Commun, 2000. **272**(1): p. 138-43.
71. Gorin, C., G.Y. Rochefort, R. Bascetin, H. Ying, J. Lesieur, J. Sadoine, N. Beckouche, S. Berndt, A. Novais, M. Lesage, B. Hosten, L. Vercellino, P. Merlet, D. Le-Denmat, C. Marchiol, D. Letourneur, A. Nicoletti, S.O. Vital, A. Poliard, B. Salmon, L. Muller, C. Chaussain, and S. Germain, *Priming dental pulp stem cells with fibroblast growth factor-2 increases angiogenesis of implanted tissue-engineered constructs through hepatocyte growth factor and vascular endothelial growth factor secretion.* Stem Cells Transl Med, 2016. **5**(3): p. 392-404.
72. Liu, Y. and M.F. Schneider, *Fgf2 activates trpc and ca(2+) signaling leading to satellite cell activation.* Front Physiol, 2014. **5**: p. 38.
73. U.S.National Library of Medicine, *Clinical trials involving fgf2*. 2019; Available from: https://clinicaltrials.gov/.
74. *Mki67 marker of proliferation ki-67 [homo sapiens (human)]*, in *NCBI*. 2019, Database Resources of the National Center for Biotechnology Information: NCBI Gene report.

75. Scholzen, T. and J. Gerdes, *The ki-67 protein: From the known and the unknown.* J Cell Physiol, 2000. **182**(3): p. 311-22.
76. *Cdkn1a cyclin dependent kinase inhibitor 1a [homo sapiens (human)]*, in *NCBI*. 2019, Database Resources of the National Center for Biotechnology Information: NCBI Gene report.
77. Gartel, A.L. and S.K. Radhakrishnan, *Lost in transcription: P21 repression, mechanisms, and consequences.* Cancer Res, 2005. **65**(10): p. 3980-5.
78. Spencer, S.L., S.D. Cappell, F.C. Tsai, K.W. Overton, C.L. Wang, and T. Meyer, *The proliferation-quiescence decision is controlled by a bifurcation in cdk2 activity at mitotic exit.* Cell, 2013. **155**(2): p. 369-83.
79. Yamamoto, M., N.P. Legendre, A.A. Biswas, A. Lawton, S. Yamamoto, S. Tajbakhsh, G. Kardon, and D.J. Goldhamer, *Loss of myod and myf5 in skeletal muscle stem cells results in altered myogenic programming and failed regeneration.* Stem Cell Reports, 2018. **10**(3): p. 956-969.
80. Biressi, S., C.R. Bjornson, P.M. Carlig, K. Nishijo, C. Keller, and T.A. Rando, *Myf5 expression during fetal myogenesis defines the developmental progenitors of adult satellite cells.* Dev Biol, 2013. **379**(2): p. 195-207.
81. Lassar, A.B., B.M. Paterson, and H. Weintraub, *Transfection of a DNA locus that mediates the conversion of 10t1/2 fibroblasts to myoblasts.* Cell, 1986. **47**(5): p. 649-56.
82. Tapscott, S.J., R.L. Davis, M.J. Thayer, P.F. Cheng, H. Weintraub, and A.B. Lassar, *Myod1: A nuclear phosphoprotein requiring a myc homology region to convert fibroblasts to myoblasts.* Science, 1988. **242**(4877): p. 405-11.
83. Fuchtbauer, E.M. and H. Westphal, *Myod and myogenin are coexpressed in regenerating skeletal muscle of the mouse.* Dev Dyn, 1992. **193**(1): p. 34-9.
84. Cooper, G.M., *The cell: A molecular approach.* . 2nd edition. ed. 2000: Sunderland (MA): Sinauer Associates.
85. B, A., J. A, and L. J, *Molecular biology of the cell. 4th edition.* 2002: New York: Garland Science; 2002.
86. Lodish, H., A. Berk, S.L. Zipursky, P. Matsudaira, D. Baltimore, and J. Darnell., *Molecular cell biology, 4th edition.* New York: W. H. Freeman, 2000.
87. Winkler, T., P. von Roth, G. Matziolis, M.R. Schumann, S. Hahn, P. Strube, G. Stoltenburg-Didinger, C. Perka, G.N. Duda, and S.V. Tohtz, *Time course of*

skeletal muscle regeneration after severe trauma. Acta Orthop, 2011. **82**(1): p. 102-11.

88. Smith, C., M.J. Kruger, R.M. Smith, and K.H. Myburgh, *The inflammatory response to skeletal muscle injury: Illuminating complexities.* Sports Med, 2008. **38**(11): p. 947-69.
89. Tidball, J.G., *Mechanisms of muscle injury, repair, and regeneration.* Compr Physiol, 2011. **1**(4): p. 2029-62.
90. Cheung, T.H. and T.A. Rando, *Molecular regulation of stem cell quiescence.* Nat Rev Mol Cell Biol, 2013. **14**(6): p. 329-40.
91. Mitra, M., L.D. Ho, and H.A. Coller, *An in vitro model of cellular quiescence in primary human dermal fibroblasts.* Methods Mol Biol, 2018. **1686**: p. 27-47.
92. Rumman, M., A. Majumder, L. Harkness, B. Venugopal, M.B. Vinay, M.S. Pillai, M. Kassem, and J. Dhawan, *Induction of quiescence (g0) in bone marrow stromal stem cells enhances their stem cell characteristics.* Stem Cell Res, 2018. **30**: p. 69-80.
93. Martin Gonzalez, J., S.M. Morgani, R.A. Bone, K. Bonderup, S. Abelchian, C. Brakebusch, and J.M. Brickman, *Embryonic stem cell culture conditions support distinct states associated with different developmental stages and potency.* Stem Cell Reports, 2016. **7**(2): p. 177-91.
94. Syverud, B.C., K.W. VanDusen, and L.M. Larkin, *Growth factors for skeletal muscle tissue engineering.* Dev Dyn, 2016. **202**(3-4): p. 169-179.
95. Dorey, K. and E. Amaya, *Fgf signalling: Diverse roles during early vertebrate embryogenesis.* Development, 2010. **137**(22): p. 3731-42.
96. Nayak, S., M.M. Goel, A. Makker, V. Bhatia, S. Chandra, S. Kumar, and S.P. Agarwal, *Fibroblast growth factor (fgf-2) and its receptors fgfr-2 and fgfr-3 may be putative biomarkers of malignant transformation of potentially malignant oral lesions into oral squamous cell carcinoma.* PLoS One, 2015. **10**(10): p. e0138801.
97. Sugimoto, K., Y. Miyata, T. Nakayama, S. Saito, R. Suzuki, F. Hayakawa, S. Nishiwaki, H. Mizuno, K. Takeshita, H. Kato, R. Ueda, A. Takami, and T. Naoe, *Fibroblast growth factor-2 facilitates the growth and chemo-resistance of leukemia cells in the bone marrow by modulating osteoblast functions.* Sci Rep, 2016. **6**: p. 30779.

98. Tanaka, E. and B. Galliot, *Triggering the regeneration and tissue repair programs.* Development, 2009. **136**(3): p. 349-53.

99. Correa, D., R.A. Somoza, P. Lin, S. Greenberg, E. Rom, L. Duesler, J.F. Welter, A. Yayon, and A.I. Caplan, *Sequential exposure to fibroblast growth factors (fgf) 2, 9 and 18 enhances hmsc chondrogenic differentiation.* Osteoarthritis Cartilage, 2015. **23**(3): p. 443-53.

100. Doukas, J., K. Blease, D. Craig, C. Ma, L.A. Chandler, B.A. Sosnowski, and G.F. Pierce, *Delivery of fgf genes to wound repair cells enhances arteriogenesis and myogenesis in skeletal muscle.* Mol Ther, 2002. **5**(5 Pt 1): p. 517-27.

101. Aviles, R.J., B.H. Annex, and R.J. Lederman, *Testing clinical therapeutic angiogenesis using basic fibroblast growth factor (fgf-2).* Br J Pharmacol, 2003. **140**(4): p. 637-46.

102. Fu, X., H. Wang, and P. Hu, *Stem cell activation in skeletal muscle regeneration.* Cell Mol Life Sci, 2015. **72**(9): p. 1663-77.

103. *Fgf6 fibroblast growth factor 6 [homo sapiens (human)]*, in *NCBI*. 2019, Database Resources of the National Center for Biotechnology Information: NCBI Gene report.

104. Swierczek, B., M.A. Ciemerych, and K. Archacka, *From pluripotency to myogenesis: A multistep process in the dish.* J Muscle Res Cell Motil, 2015. **36**(6): p. 363-75.

105. Olsson, H., B. Baldetorp, M. Ferno, and R. Perfekt, *Relation between the rate of tumour cell proliferation and latency time in radiation associated breast cancer.* BMC Cancer, 2003. **3**: p. 11.

106. Tubiana, M., *Tumor cell proliferation kinetics and tumor growth rate.* Acta Oncol, 1989. **28**(1): p. 113-21.

107. Kerr, K.M. and D. Lamb, *Actual growth rate and tumour cell proliferation in human pulmonary neoplasms.* Br J Cancer, 1984. **50**(3): p. 343-9.

108. Beresford, M.J., G.D. Wilson, and A. Makris, *Measuring proliferation in breast cancer: Practicalities and applications.* Breast Cancer Res, 2006. **8**(6): p. 216.

109. Howard, A. and S.R. Pelc, *Synthesis of desoxyribonucleic acid in normal and irradiated cells and its relation to chromosome breakage.* International Journal of Radiation Biology and Related Studies in Physics, Chemistry and Medicine, 1986. **49**(2): p. 207-218.

110. Su, T.T. and P.H. O'Farrell, *Size control: Cell proliferation does not equal growth.* Curr Biol, 1998. **8**(19): p. R687-9.
111. Morten, B.C., R.J. Scott, and K.A. Avery-Kiejda, *Comparison of three different methods for determining cell proliferation in breast cancer cell lines.* J Vis Exp, 2016(115).
112. Moxnes, J.F., J. Haux, and K. Hausken, *The dynamics of cell proliferation.* Med Hypotheses, 2004. **62**(4): p. 556-63.
113. Holstein, T.W. and C.N. David, *Cell cycle length, cell size, and proliferation rate in hydra stem cells.* Dev Biol, 1990. **142**(2): p. 392-400.
114. Darzynkiewicz, Z., D.P. Evenson, L. Staiano-Coico, T.K. Sharpless, and M.L. Melamed, *Correlation between cell cycle duration and rna content.* J Cell Physiol, 1979. **100**(3): p. 425-38.
115. Kronja, I. and T.L. Orr-Weaver, *Translational regulation of the cell cycle: When, where, how and why?* Philos Trans R Soc Lond B Biol Sci, 2011. **366**(1584): p. 3638-52.
116. Begum, J., W. Day, C. Henderson, S. Purewal, J. Cerveira, H. Summers, P. Rees, D. Davies, and A. Filby, *A method for evaluating the use of fluorescent dyes to track proliferation in cell lines by dye dilution.* Cytometry A, 2013. **83**(12): p. 1085-95.
117. Latifi-Pupovci, H., Z. Kuci, S. Wehner, H. Bonig, R. Lieberz, T. Klingebiel, P. Bader, and S. Kuci, *In vitro migration and proliferation ("wound healing") potential of mesenchymal stromal cells generated from human cd271(+) bone marrow mononuclear cells.* J Transl Med, 2015. **13**: p. 315.
118. Yoneura, N., S. Takano, H. Yoshitomi, Y. Nakata, R. Shimazaki, S. Kagawa, K. Furukawa, T. Takayashiki, S. Kuboki, M. Miyazaki, and M. Ohtsuka, *Expression of annexin ii and stromal tenascin c promotes epithelial to mesenchymal transition and correlates with distant metastasis in pancreatic cancer.* Int J Mol Med, 2018. **42**(2): p. 821-830.
119. Zhao, Y., M. Jiang, D. Chen, X. Zhao, C. Xue, R. Hao, W. Yue, J. Wang, and J. Chen, *Single-cell electrical phenotyping enabling the classification of mouse tumor samples.* Sci Rep, 2016. **6**: p. 19487.
120. Bielas, J.H. and J.A. Heddle, *Proliferation is necessary for both repair and mutation in transgenic mouse cells.* Proc Natl Acad Sci U S A, 2000. **97**(21): p. 11391-6.

121. Stacey, D.W., *Three observations that have changed our understanding of cyclin d1 and p27 in cell cycle control.* Genes Cancer, 2010. **1**(12): p. 1189-99.
122. Audibert, A., F. Simon, and M. Gho, *Cell cycle diversity involves differential regulation of cyclin e activity in the drosophila bristle cell lineage.* Development, 2005. **132**(10): p. 2287-97.
123. Coller, H.A., L. Sang, and J.M. Roberts, *A new description of cellular quiescence.* PLoS Biol, 2006. **4**(3): p. e83.
124. Bertoli, C., J.M. Skotheim, and R.A. de Bruin, *Control of cell cycle transcription during g1 and s phases.* Nat Rev Mol Cell Biol, 2013. **14**(8): p. 518-28.
125. Henley, S.A. and F.A. Dick, *The retinoblastoma family of proteins and their regulatory functions in the mammalian cell division cycle.* Cell Div, 2012. **7**(1): p. 10.
126. Weinberg, R.A., *The retinoblastoma protein and cell cycle control.* Cell, 1995. **81**(3): p. 323-30.
127. Sage, J., *Cyclin c makes an entry into the cell cycle.* Dev Cell, 2004. **6**(5): p. 607-8.
128. Ren, S. and B.J. Rollins, *Cyclin c/cdk3 promotes rb-dependent g0 exit.* Cell, 2004. **117**(2): p. 239-51.
129. DeGregori, J., *The genetics of the e2f family of transcription factors: Shared functions and unique roles.* Biochim Biophys Acta, 2002. **1602**(2): p. 131-50.
130. Lukas, J., B.O. Petersen, K. Holm, J. Bartek, and K. Helin, *Deregulated expression of e2f family members induces s-phase entry and overcomes p16ink4a-mediated growth suppression.* Mol Cell Biol, 1996. **16**(3): p. 1047-57.
131. Johnson, D.G., J.K. Schwarz, W.D. Cress, and J.R. Nevins, *Expression of transcription factor e2f1 induces quiescent cells to enter s phase.* Nature, 1993. **365**(6444): p. 349-52.
132. Wu, L., C. Timmers, B. Maiti, H.I. Saavedra, L. Sang, G.T. Chong, F. Nuckolls, P. Giangrande, F.A. Wright, S.J. Field, M.E. Greenberg, S. Orkin, J.R. Nevins, M.L. Robinson, and G. Leone, *The e2f1-3 transcription factors are essential for cellular proliferation.* Nature, 2001. **414**(6862): p. 457-62.
133. Armand, A.S., T. Launay, C. Pariset, B. Della Gaspera, F. Charbonnier, and C. Chanoine, *Injection of fgf6 accelerates regeneration of the soleus muscle in adult mice.* Biochim Biophys Acta, 2003. **1642**(1-2): p. 97-105.

134. Teven, C.M., E.M. Farina, J. Rivas, and R.R. Reid, *Fibroblast growth factor (fgf) signaling in development and skeletal diseases.* Genes Dis, 2014. **1**(2): p. 199-213.

135. Flanagan-Steet, H., K. Hannon, M.J. McAvoy, R. Hullinger, and B.B. Olwin, *Loss of fgf receptor 1 signaling reduces skeletal muscle mass and disrupts myofiber organization in the developing limb.* Dev Biol, 2000. **218**(1): p. 21-37.

136. Itoh, N., *The fgf families in humans, mice, and zebrafish: Their evolutional processes and roles in development, metabolism, and disease.* Biol Pharm Bull, 2007. **30**(10): p. 1819-25.

137. Haffter, P., M. Granato, M. Brand, M.C. Mullins, M. Hammerschmidt, D.A. Kane, J. Odenthal, F.J. van Eeden, Y.J. Jiang, C.P. Heisenberg, R.N. Kelsh, M. Furutani-Seiki, E. Vogelsang, D. Beuchle, U. Schach, C. Fabian, and C. Nusslein-Volhard, *The identification of genes with unique and essential functions in the development of the zebrafish, danio rerio.* Development, 1996. **123**: p. 1-36.

138. Pownall ME and I. HV., *Fgf signalling in vertebrate development.* 2010: San Rafael (CA): Morgan & Claypool Life Sciences; 2010.

139. Templeton, T.J. and S.D. Hauschka, *Fgf-mediated aspects of skeletal muscle growth and differentiation are controlled by a high affinity receptor, fgfr1.* Dev Biol, 1992. **154**(1): p. 169-81.

140. Katz, M., I. Amit, and Y. Yarden, *Regulation of mapks by growth factors and receptor tyrosine kinases.* Biochim Biophys Acta, 2007. **1773**(8): p. 1161-76.

141. Park, O.J., H.J. Kim, K.M. Woo, J.H. Baek, and H.M. Ryoo, *Fgf2-activated erk mitogen-activated protein kinase enhances runx2 acetylation and stabilization.* J Biol Chem, 2010. **285**(6): p. 3568-74.

142. Zhang, Y., Y. Lin, C. Bowles, and F. Wang, *Direct cell cycle regulation by the fibroblast growth factor receptor (fgfr) kinase through phosphorylation-dependent release of cks1 from fgfr substrate 2.* J Biol Chem, 2004. **279**(53): p. 55348-54.

143. Liu, Y., C. Kung, J. Fishburn, A.Z. Ansari, K.M. Shokat, and S. Hahn, *Two cyclin-dependent kinases promote rna polymerase ii transcription and formation of the scaffold complex.* Mol Cell Biol, 2004. **24**(4): p. 1721-35.

144. Kelso, T.W., K. Baumgart, J. Eickhoff, T. Albert, C. Antrecht, S. Lemcke, B. Klebl, and M. Meisterernst, *Cyclin-dependent kinase 7 controls mrna synthesis*

by affecting stability of preinitiation complexes, leading to altered gene expression, cell cycle progression, and survival of tumor cells. Mol Cell Biol, 2014. **34**(19): p. 3675-88.

Appendix

Table A3.3 Mean data of S phase and total RNA between S6.3 and S9.1

Mean (N=3) S6.3				**Mean (N=3) S9.1**		
Duration	S phase (%)	Total RNA (ng)		Duration	S Phase (%)	Total RNA (ng)
Timepoints (hr)				Timepoints (Hr)		
02	3.73	4704.00		02	1.41	2312.00
04	2.32	5032.00		04	1.35	2174.67
06	2.39	5440.00		06	1.39	2648.00
08	2.45	5448.00		08	1.49	2690.67
10	3.37	6073.33		10	1.98	3104.00
12	3.98	5209.33		12	2.38	3741.33
14	5.91	6384.00		14	4.32	4585.33
16	7.11	7133.33		16	5.20	5150.67
18	11.08	8006.67		18	6.03	5524.00
20	15.43	8292.00		20	10.63	6014.67
22	22.74	8933.33		22	11.15	6418.67
24	21.16	7946.67		24	13.68	6674.67

Table A3.4 Raw data for method 2 B for calculating comparative index

Mean (n=3) S6.3			**Mean (n=3) S9.1**		
Duration	S phase (%)	Total RNA (ng)	Duration	S Phase (%)	Total RNA (ng)
Timepoints (hr)			Timepoints (Hr)		
12	3.98	5209.33	12.00	2.38	3741.33
14	5.91	6384.00	14.00	4.32	4585.33
16	7.11	7133.33	16.00	5.20	5150.67
18	11.08	8006.67	18.00	6.03	5524.00
20	15.43	8292.00	20.00	10.63	6014.67
22	22.74	8933.33	22.00	11.15	6418.67
24	21.16	7946.67	24.00	13.68	6674.67

Table A3.5 calculations of comparative index using method 2B

S6.3		S9.1	

Trepezoid Areas for S phase	Trepezoid Areas for total RNA	Trepezoid Areas for S	Trepezoid Areas for RNA
9.89	11593.33	6.70	8326.66
13.02	13517.33	9.52	9736.00
18.19	15140.00	11.23	10674.67
26.51	16298.67	16.66	11538.67
38.17	17225.33	21.78	12433.34
43.90	16880.00	24.83	13093.34
149.68	90654.66	90.72	65802.68

Table A5.1 Cell cycle analysis data of Subject S6.3, KH 3 and KH 1, Quiescence vs Quiescence + FGF2

Q vs FGF2							
S6.3	Quiescence				QF2		
	G1%	S %	G2 %		G1%	S %	G2 %
N1	86.46	1.13	12.41		86.06	1.68	12.26
N2	86.73	1.36	11.92		83.70	0.96	15.33
N3	86.22	1.70	12.08		82.75	1.21	16.06
KH 3 cells	Quiescence				QF2		
	G1%	S %	G2 %		G1%	S %	G2 %
N1	87.28	3.31	9.41		85.95	2.68	11.37
N2	88.68	3.59	7.73		86.41	2.59	11.01
N3	85.54	3.69	10.77		83.69	2.58	13.73
KH 1 cells	Quiescence				QF2		
	G1%	S %	G2 %		G1%	S %	G2 %
N1	91.48	2.89	5.63		89.73	2.15	8.12
N2	90.16	2.77	7.07		88.47	2.44	9.10
N3	91.44	2.88	5.68		87.58	2.77	9.65

Table A5.2 Cell cycle analysis data of Subject S6.3, KH 3 and KH 1, Quiescence vs Quiescence + FGF6

Quiescence vs Quiescence + FGF6							
S6.3	Quiescence				QF6		
	G1%	S %	G2 %		G1%	S %	G2 %
N=1	87.15	5.54	7.31		76.12	21.1	2.78
N=2	86.2	5.84	7.96		77.95	18.12	3.93
N=3	88.16	5.17	6.68		77.17	20.95	1.89
KH 3 cells	Quiescence				QF6		
	G1%	S %	G2 %		G1%	S %	G2 %
N=1	86.45	3.94	9.61		77.42	17.68	4.9
N=2	88.94	4.13	6.93		77.72	19.48	2.8
N=3	87.19	4.57	8.24		78.65	18.17	3.18
KH 1 cells	Quiescence				QF6		
	G1%	S %	G2 %		G1%	S %	G2 %
N=1	90.19	3.79	6.02		76.11	18.43	5.46
N=2	91.01	3.84	5.15		75.49	20.55	3.96
N=3	90.6	3.57	5.83		76.11	19.4	4.49

Table A5.3 Cell cycle data with FGF6 treatment of 5 ng/ml

	FGF6 5 ng					
N=1	Quiescent			Quiescent + FGF6		
	G1 %	86.99		G1 %	85.23	
	S phase %	4.3		S phase %	7.28	
	G2 %	8.71		G2 %	7.5	
N=2	Quiescent			Quiescent + FGF6		
	G1 %	88.63		G1 %	84.57	
	S phase %	4.01		S phase %	9.47	
	G2 %	7.35		G2 %	5.96	
N=3	Quiescent			Quiescent + FGF6		
	G1 %	87.68		G1 %	84.88	
	S phase %	4.3		S phase %	8.49	
	G2 %	8.02		G2 %	6.63	

		Quiescent Mean	SE			Quiescent + FGF6 Mean	SE	% difference
Stats	G1 %	87.77	0.78		G1 %	84.89	-0.34	-3.27
	S phase %	4.20	-0.10		S phase %	8.41	1.13	100.16
	G2 %	8.03	-0.68		G2 %	6.70	-0.80	-16.57

Table A5.4 Cell cycle data with FGF6 treatment of 10 ng/ml

	FGF6 10 ng						
N=1	Quiescent			Quiescent + FGF6			
	G1 %	87.15		G1 %	76.12		
	S phase %	5.54		S phase %	21.1		
	G2 %	7.31		G2 %	2.78		
N=2	Quiescent			Quiescent + FGF6			
	G1 %	86.2		G1 %	77.95		
	S phase %	5.84		S phase %	18.12		
	G2 %	7.96		G2 %	3.93		
N=3	Quiescent			Quiescent + FGF6			
	G1 %	86.56		G1 %	76.53		
	S phase %	5.96		S phase %	20.6		
	G2 %	7.48		G2 %	2.87		
		Quiescent Mean	SE		Quiescent + FGF6 Mean	SE	% difference
Stats	G1 %	86.64	-0.51	G1 %	76.87	0.75	-11.28
	S phase %	5.78	0.24	S phase %	19.94	-1.16	244.98
	G2 %	7.58	0.27	G2 %	3.19	0.41	-57.89